Dissertation

Persistence of the inner limiting membrane after epiretinal membrane peeling

submitted by

Dr.med.univ.

Gerald SEIDEL

for the Academic Degree of

Doctor of Medical Science

(Dr. scient. med.)

at the

Medical University of Graz

Department of Ophthalmology

under the Supervision of

Prof. Dr. Anton HAAS

2016

Declaration

I hereby declare that this thesis is my own original work and that I have fully acknowledged by name all of those individuals and organisations that have contributed to the research for this thesis. Due acknowledgement has been made in the text to all other material used. Throughout this thesis and in all related publications I followed the “Standards of Good Scientific Practice and Ombuds Committee at the Medical University of Graz“.
Date 10.05.2016

Acknowledgements

I want to dedicate this thesis to all the people who have inspired me on my journey so far, which especially includes my friends and my family.
Thank you.

Table of contents

Abbreviations and Definitions

A2E	N-retinyl-N-retinylidene ethanolamine
A2PE	N-retinyl-phosphatidylethanolamine
am	amacrine cell
ATP	adenosine triphosphate
ABCA4	ATP-binding cassette transporter, subfamily A, member 4
BBG	Brilliant Blue G
BCVA	best corrected visual acuity
BIOM	binocular indirect ophthalmomicroscope
CFT	central foveal thickness
ELOVL4	elongation of very long chain fatty acids protein 4
ERM	epiretinal membrane
ERM-Th	epiretinal membrane thickness
FDA	Food and Drug Administration
gc	ganglion cell
ICG	indocyanine green
ILM	inner limiting membrane
IPL	inner plexiform layer
IS/OS	inner segment/outer segment junction
RPE	retinal pigment epithelium
OCT	optical coherence tomography
OPL	outer plexiform layer
SD-OCT	spectral domain optical coherence tomography
SLD	super luminescent diode
TB	Trypan Blue

Abstract

Purpose: To identify preoperative markers on spectral domain optical coherence tomography (SD-OCT) for residual inner limiting membrane (ILM) in epiretinal membrane (ERM) peeling.
Methods: In this retrospective case series the preoperative SD-OCTs from 119 eyes of 119 consecutive patients who underwent surgery for idiopathic ERM by a single surgeon were evaluated for markers predisposing for ILM persistence after ERM removal. ILM persistence was determined via intraoperative indocyanine green staining. The main outcome measures were correlation of central foveal thickness (CFT), ERM thickness, extent of elevated ERM and retinal folding, intraretinal cysts, and discontinuation of the ERM, with ILM persistence after ERM peeling.
Results: The persistence of the ILM was found in 50.4% (n = 60). After Bonferroni correction for multiple testing, a greater extent of elevated ERM and thicker ERMs were associated with persistence of the ILM ($p < 0.005$). The other parameters showed no statistically significant correlations with the persistence of the ILM ($p \geq 0.005$).
Conclusion: Residual ILM can be found in nearly half of the eyes after ERM peeling. A loose connection between the ERM and the retinal surface predisposes for ILM persistence. Preoperative SD-OCT is helpful in identifying risk markers for the persistence of the ILM in ERM surgery.

Abstrakt

Ziel: Die Identifizierung präoperativer Marker in der spectral domain optischen Kohärenztomographie (SD-OCT) für ein Verbleiben residualer Membrana limitans interior (ILM) nach dem operative Abziehen einer epiretinalen Membran (ERM),
Methoden: Es wurde eine retrospektive Fallserie durchgeführt. Die präoperativen SD-OCT Bilder von 119 Augen von 119 konsekutiver Patienten bei welchen ein Abziehen der ERM durchgeführt wurde, wurden eingeschlossen. Diese Bilder wurden auf

präoperative Marker die zu einer persistierenden ILM Anhaftung nach dem Abziehen der ERM untersucht. Diese Persistenz der ILM wurde mittels Indozyaningrün ermittelt. Die Hauptzielgrößen waren die Korrelation zwischen der Persistenz der ILM nach dem Abziehen der ERM mit folgenden OCT Parametern: zentraler Foveadicke, ERM-Dicke, Ausmaß der ERM-Elevation, Ausmaß an Netzhautfalten, intraretinalen zystoiden Spalten und Unterbrechungen in der ERM.
Ergebnisse: Eine Persistenz der ILM trat in 50.4% (n = 60) auf. Nach der Bonferroni Korrektur für multiples Testen zeigte sich eine signifikante Korrelation zwischen der Persistenz der ILM nach ERM Anziehung und einem größeren Ausmaß an ERM Elevation so wie einer dickeren ERM ($p < 0.005$). Alle anderen Parameter zeigten keine statistisch signifikante Korrelation zur ILM Persistenz ($p \geq 0.005$).
Schlussfolgerungen: Eine residuale ILM findet sich in etwa der Hälfte der Fälle nach dem Abziehen der ERM. Eine lose Verbindung zwischen der ERM und der Netzhautoberfläche prädisponiert zu einem solchen Verbleib der ILM. Die präoperative SD-OCT ermöglicht eine Identifikation von Risikomarkern für eine Persistenz der ILM nach dem Abziehen der ERM.

1.1 Epiretinal Membranes

1.1.1 Definition

Epiretinal Membranes (ERM) are sheets of fibrotic tissue on the inner surface of the retina. These membranes comprise to varying degree type IV collagen, retinal pigment epithelial cells, and fibroblast-like cells [1] [2] [3] The latter most probably represent transdifferntiated retinal Müller cells, which have been transformed under cytokinetic stress such as by TGF-ß1. [1]

These avascular membranes vary in thickness and size from 4 to 70 micrometers measured by spectral domain optical coherence tomography (OCT; unpublished data by Seidel G. et al) and might contract to a varying degree. This

contraction leads to a distortion of the retinal tissue that in turn causes the visual symptoms.

The patients complain from a plethora of visual disturbances such as loss of visual acuity, metamorphopsia (distorted vision), diplopia, and anisoconia (dissimilar image size between the two eyes).

Many patients with epiretinal membranes do not experience a drop in visual acuity, but are rather asymptomatic in this regard. However, with increasing distortion of the retinal architecture the visual acuity decreases and can reach levels as low as counting fingers. Still, some patients with normal or good visual acuity can be severely bothered by other visual disturbances that might warrant an intervention.

Metamorphopsia, that is distorted vision, is one of the hallmark signs of ERMs. It often is the symptom of most concern to the patient and has a higher correlation with visual quality of life than visual acuity in ERM patients. [4] [5] What is more is that the metamorphopsia often persist even after best-corrected visual acuity already has improved after an ERM peeling surgery. [6]

The incidence of reported anisoconia in ERM patients ranges from 78 to 100%. [7] [8] [9] [10] [11] In almost all cases the anisoconia is a macropsia and is horizontal as well as vertical. [11]

The subjective overall visual impairment ranges from none to severe and patients might loose their capability to read or to drive a car even if only one eye is affected because the altered visual impression on the affected eye may impede the simultaneous use of both eyes. [12] [13] This might seriously affect the vision related quality of life, which should be an indication for treatment. [4]

ERMs have been graded according to various classification symstems. The ones most relevant today include at least partially OCT findings. The clinical relevance of these systems remains to be elucidated. Konidaris et al. proposed an elaborate solemnly OCT based system as shown in Table 1. On this classification system by Stevenson et al tried to improve witth his classification (Table 2). Another classification by Hwang et al. is mainly based on the foveal appearance (Table 3; further OCT examples of this classification in the chapter on the inner retina)

Table 1. OCT based morphologic of ERMs by Konidaris et al.

Group A: with posterior vitreous detachment	
A1	No contraction
A2	Contraction
A2.1	with retinal folding
A2.2	with edema
A2.3	with cystoid macular edema
A2.4	with lamellar macular hole
Group B: with vitreous attachment	
B1	No traction
B2	vitreomacular traction
B2.1	with edema
B2.2	with retinal detachment
B2.3	with schisis

1.1.2 The epidemiology of ERMs

The prevalence of ERMs increases with age, ranging from around 0.5% at the age of 40 to 49 to a prevalence of over 10% at the age of over 70 years. [14] [15]Apart from age, the development of ERMs increases in a plethora of subpopulations. These include patients with diabetes, retinal vein occlusions, retinal tears, retinal detachment,

Table 2. ERM classification scheme that takes into account pathogenesis and clinically relevant SD-OCT findings by Stevenson et al.[16]

Definition		
A highly reflective membranous structure at the vitreomacular interface		
Classification		
Idiopathic	No identifiable etiology	
Primary	Secondary to posterior vitreous detachment	
Secondary	Secondary to another disorder known to cause epiretinal membrane formation	
Central foveal thickness		
	Stratus OCT (µm)	**Spectralis OCT (µm)**
Normal	< 250	< 320
Thickened	≥ 250	≥320
Inner segment ellipsoid band integrity		
Intact	Clear and consistent	
Disrupted	Blurred, interrupted, or absent	

previous retinal laser photo coagulation, previous ocular trauma or surgery, uveitis, and ocular tumors. [17] [14] In these cases the term secondary ERM is applied, contrasting primary ERMs where no triggering agent is known. A certain role is attributed to a possible incomplete posterior vitreous detachment, which is found consistently in a higher percentage of patients with ERMs than in those without. [18] [19] [20] [21]

Table 3. OCT-based morphologic classification of idiopathic ERMs by Hwang et al. [22]

Group 1: fovea-involving ERM	
1 A	Outer retinal thickening and minimal inner retinal change
1 B	Outer retinal inward projection and inner retinal thickening
1 C	Prominent thickening of the inner retinal layer
Group 2: fovea-sparing ERM	
2 A	Formation of a macular pseudohole
2 B	Schisis-like intraretinal splitting

A significant variance in prevalence rates has been reported for various ethnicities.

The Beaver Dam Eye study, a population based cross sectional study in the US, reported a prevalence of 34.1% with spectral domain OCT and 29.2% with fundus photography in a mostly Caucasian population of 1540 subjects with a mean age of 74.1 ± 7.1 years (range 63 to 102 years) in 2015. [23] [24]

Twenty years earlier the prevalence of ERMs in the Beaver Dam Eye study's population of 4926 people older than 43 years was 11.8% and 2.4% for bilateral ERMs detected by fundus photography only. The reason for the lower prevalence rates 20 years earlier, even when comparing the photographical assessment only, is not entirely clear, but might be influenced by the shift towards older participants in the later evaluation. [15]

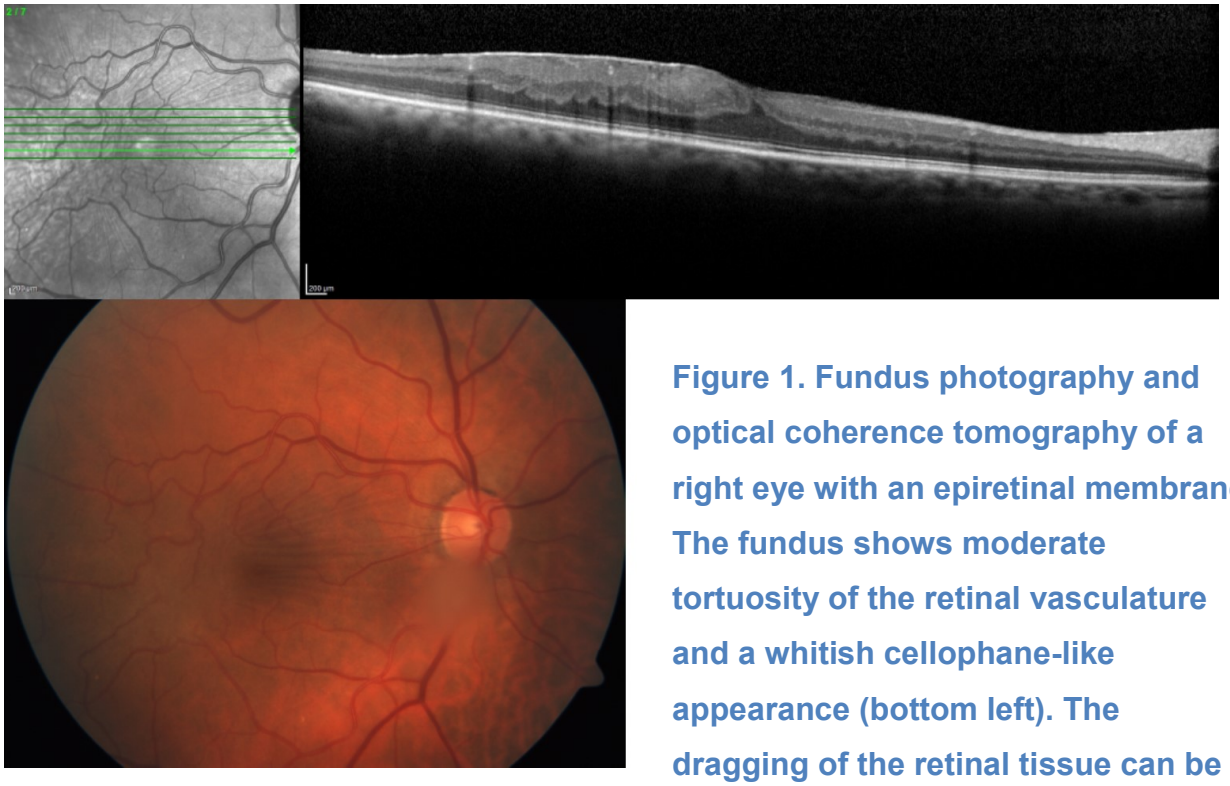

Figure 1. Fundus photography and optical coherence tomography of a right eye with an epiretinal membrane. The fundus shows moderate tortuosity of the retinal vasculature and a whitish cellophane-like appearance (bottom left). The dragging of the retinal tissue can be higher contrast on the infrared image (top left). The thin hyperreflective topmost layer on the optical coherence tomogram and the loss of the foveal contour are hallmarks of an ERM and such eyes are prone to be symptomatic. This eye had a visual acuity of 0.3 and the patient noted some metamorphopsia.

The Blue Mountain Eye Study, the Australian pendant to the Beaver Dam study, found in a population older than 50 a prevalence of 7.0% in its 3490 subjects based on fundus photography. [25] A large population based analysis in a European cohort is missing so far.

Compared to Caucasians the reported rates for Asian populations have been somewhat lower. A recent Japanese OCT study including 500 subjects drawn from a pool of patients scheduled for cataract surgery reported a prevalence of 8.6%. Most cases were idiopathic (72%) of which interestingly only 4.8% were symptomatic. [26] Similar results were reported in a Chinese study with 2005 participants of 50 years and older. 8.4% of the participants presented with an ERM, which would translate after standardization for the age distribution of the Chinese population into an overall

prevalence of 7.3% of Chinese aged 50 plus. [27] This was confirmed in a second Chinese study. [14]

The most reliable data on Hispanics originates from the Los Angeles Latino Eye Study, which reported in 5982 patients with an average age of 54.7 ± 10.7 a prevalence of 18.5% (of those were 19.9% bilateral). [17]

Despite the significant variation in prevalence rates for various ethnicities, there is limited comparability between most studies. Discrepancies in the reported prevalence rates for different populations might partially be due to variation in measurement techniques. While some studies used fundus photography, others used optical coherence tomography. ERMs are sometimes hard to identify on fundus photography and as such it is not surprising that that studies using OCT like the Beaver Dam Eye Study reported higher prevalence rates of 34.1% in its population, as compared to around 7% in similar populations evaluated by fundus photography. [23] Similar differences were found in a Chinese study with a relative increase in ERM detection of 15% when evaluating the spectral domain OCTs instead of the fundus photography. [27] In summary, the evidence for a variation of ERM prevalence according to ethnicity remains inconclusive to this point.

1.1.3 Complications of ERMs

Besides the metamorphopsia caused by the tangential traction and subsequent distortion of the retinal tissue ERMs can cause visual deterioration via other mechanisms. A plethora of structural complications associated ERMs have been described. One is leakage of the retinal vasculature with development of a cystoid macular edema. The differentiation between a tractional cystoid macular edema and a cystoid macular edema secondary to other diseases can sometimes prove difficult. Some common diseases regularly cause cystoid macular edema, but also predispose for a secondary ERM development. Prime examples of such diseases are maculopathy and retinal vein occlusions.

The therapeutic approach to a secondary ERM must address the accompanying disease as well and often surgery would not be considered the initial

therapy. The leakage in patients with cystoid macular edema secondary due to retinal vein occlusions or diabetes often respond very well to intravitreal medication, while a purely tractional edema is often hardly responsive to anti-VEGF or corticosteroid therapy and often requires vitreoretinal surgery to resolve. [28] Mixed forms of the two might certainly be present in patients, in which case a surgery with ERM peeling in a persisting edema after intravitreal edema might prove successful. Besides the clinical implications, research data regarding ERMs need differentiation between primary and secondary ERMs. In the latter case multiple parameters such as postoperative visual acuity, surgical complications, and natural history of the disease can differ tremendously from primary ERMs. While some general principles apply to both types of ERMs, the author wants to point out that the present thesis focuses on primary ERMs specifically.

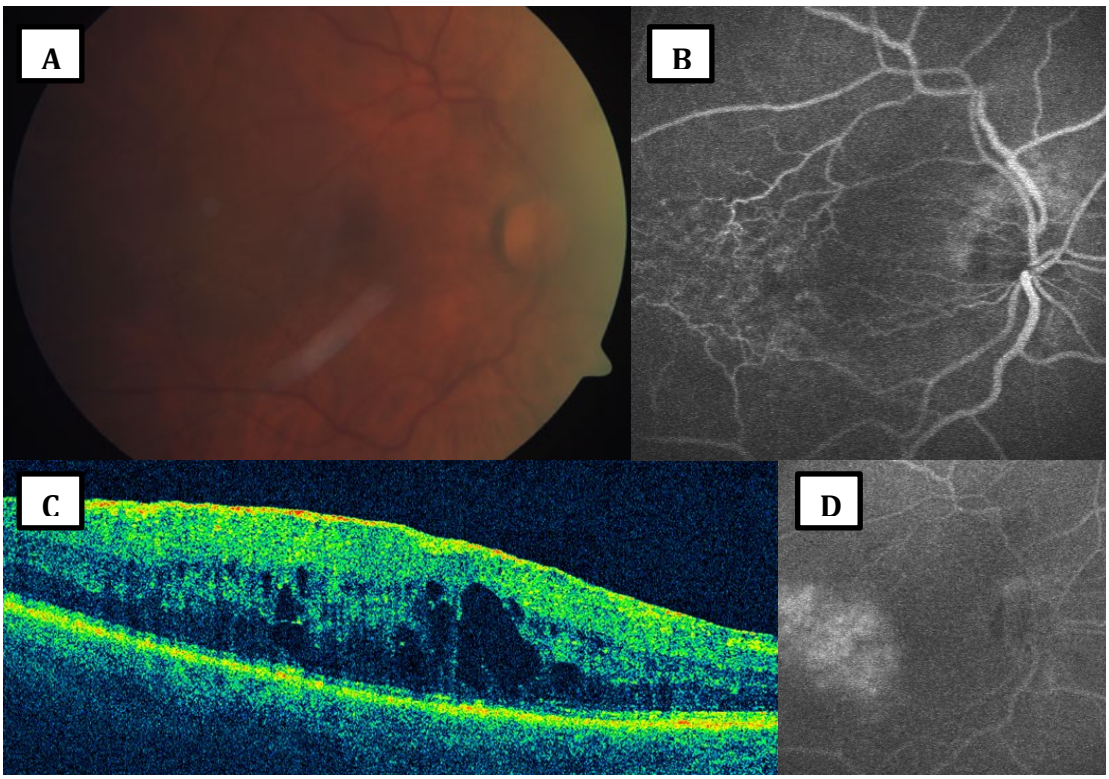

Figure 1. Long standing epiretinal membrane with cystoid macular edema. On the fundus image (A) a faint gray reflex can be identified. On the early phase of the fluorescein angiography (B) the vascular dragging and the teleangiectatic

alteration of the retinal vasculature becomes apparent. These vessels leak in the late phase of the angiogram (D) causing the cystoid macular edema as shown on optical coherence tomography (C).

Besides the concentric contraction which leads to the loss of the foveal contour, ERMs can also contract in a centripetal fashion causing the central retinal tissue to tear. This typically results in a schisis in the outer layers of the retina and to the formation of a macular lamellar hole (Figure 2.). These holes represent a completely different entity from full thickness macular holes. The latter are caused by vertical traction by the vitreous and are usually an indication for vitreoretinal surgery.

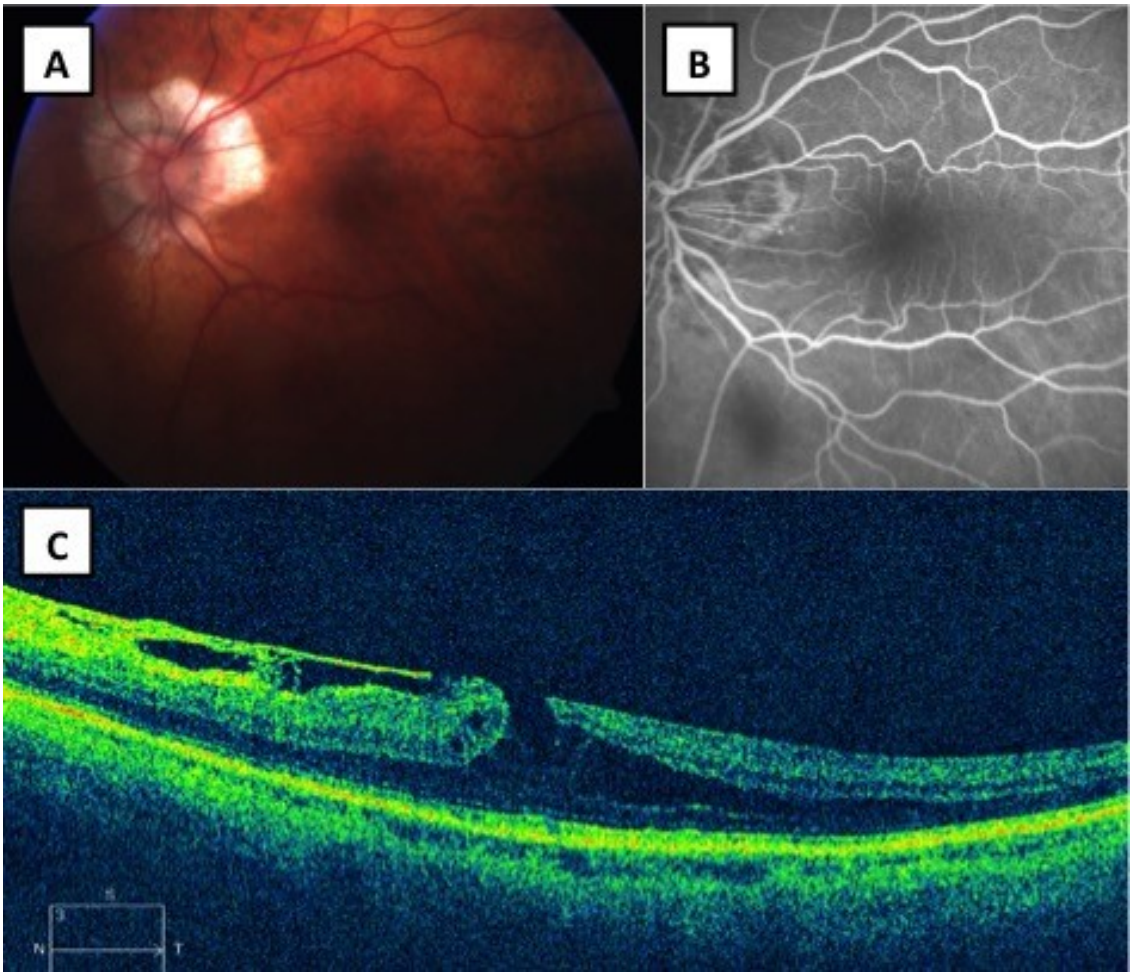

Figure 2 Macular lamellar hole due to an epiretinal membrane. A moderate epiretinal membrane with traction on the retinal tissue can be observed on both

the fundus photo (A) and the early phase of a fluorescein angiogram (B). On optical coherence tomography the traction of the membrane nasally form the fovea causes the outer nuclear and Hennle's layer to split (C). While the pathology is prominent on optical coherence tomography the fundus appearance (A) is relatively unremarkable. An similarly fluorescein angiography (B) does not show any leakage as it would be seen in cystoid formation in patient with retinal vein occlusions or diabetics, who can present with secondary epiretinal membrane formation.

The term macular pseudo-hole id often used interchangingly with macular lamellar-hole, but represents a distinct entity in that it lacks any schitic component and only shows an accentuated foveal dent. It is caused by a concentric horizontal traction without elevating the fovea and usually does not require an intervention. Figure 3 shows two exemplary cases for a true macular hole and a macular pseudo-hole. It is important to note that due to the difference in pathophysiology neither the macular pseudo-hole nor the macular lamellar-hole will ever evolve into a true macular hole. Macular holes are generally not a complication of epiretinal membranes, but result from a vertical traction of the vitreoretinal interface (so called vitreoretinal traction syndrome) that failed to spontaneously detach, but tore the foveal retinal tissue. As most patients with an ERM already have a detached vitreous the encounter of both pathologies, an ERM and a vitreoretinal traction syndrome , in a single eye is exceedingly rare. The progression from a macular traction syndrome to a true hole formation is depicted in Figure 4. However, there have been reports of the development of atypical full thickness macular-holes in patients with ERMs. [29]

While classical macular holes have a wide base and an narrow isthmus on the top with cystoid spaces on the edge of the hole, ERM induced holes are inverted, meaning they usually are narrow on the bottom and wide at the top without cystoid spaces. Such atypical full thickness holes seem to occur more frequently in younger highly myopic patients with a previous lamellar macular hole. The also tend to be relatively small and spontaneously close and reopen more often than regular macular

holes do. Also, compared to the regular macular holes, they often fail to show the same extend of visual improvement after surgery.[29]

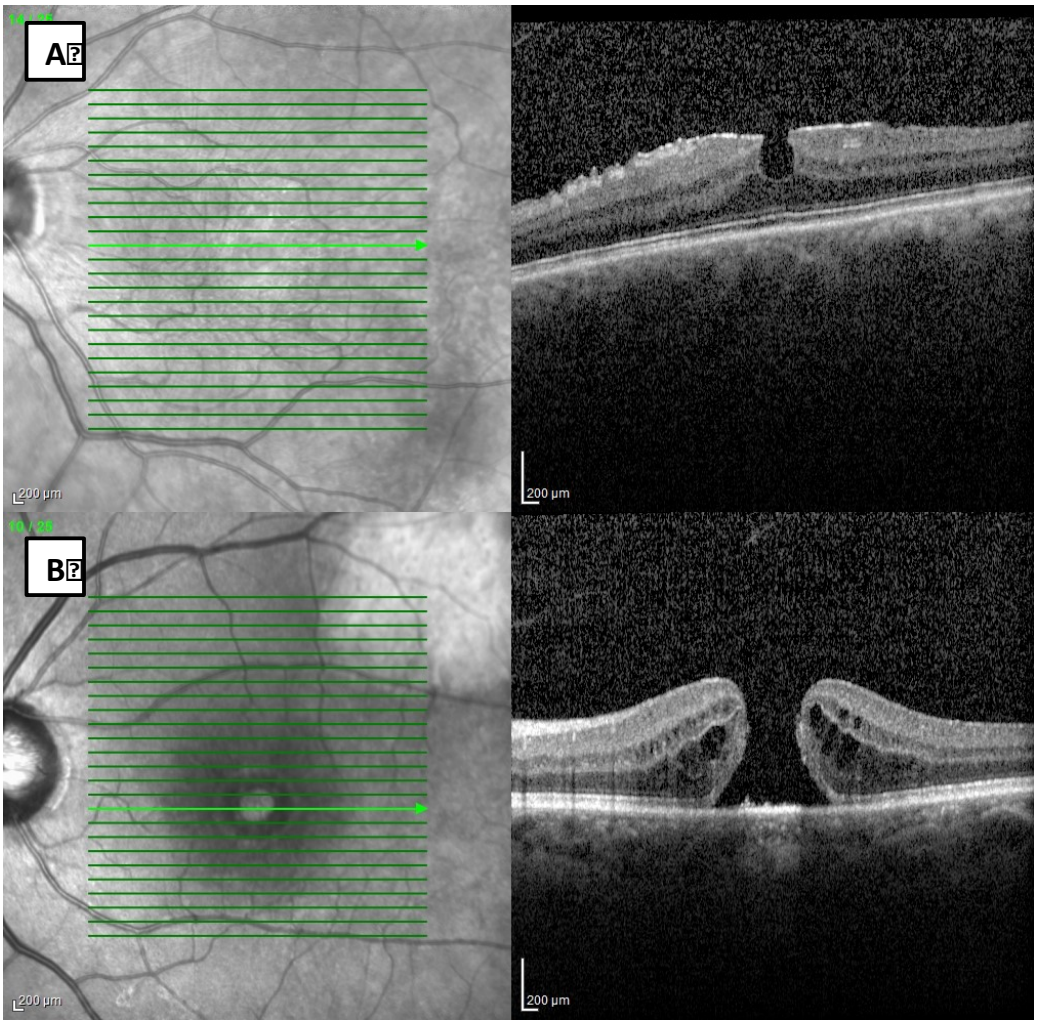

Figure 3. A macular pseudo-hole versus a true macular hole. (A) shows the for a pseudo-hole characteristic hole like pit at the level of the fovea. This result from a horizontal centripetal traction on the retinal tissue with sparing of the fovea. Notably this contrasts with the formation of a lamellar hole where the contraction is centrifugal (As seen in the previous figure). (B) shows an optical coherence tomogram of a true macular hole. In this pathology all retinal layers down to the retinal pigment epithelium are interrupted. Notably there is some hyperreflective debris at the bottom of the hole, which clinically represents yellow deposit giving the fundus image a salami like appearance. These

changes are associated with a longer persistence of the pathology. In the presented case the vitreoretinal interface has detached (the original pathophysiologic cause of the hole formation) and remnants of the vitreal cortex can be appreciated on the top left aspect of the optical coherence tomogram. This case would be classified as stage 4 according to Gass

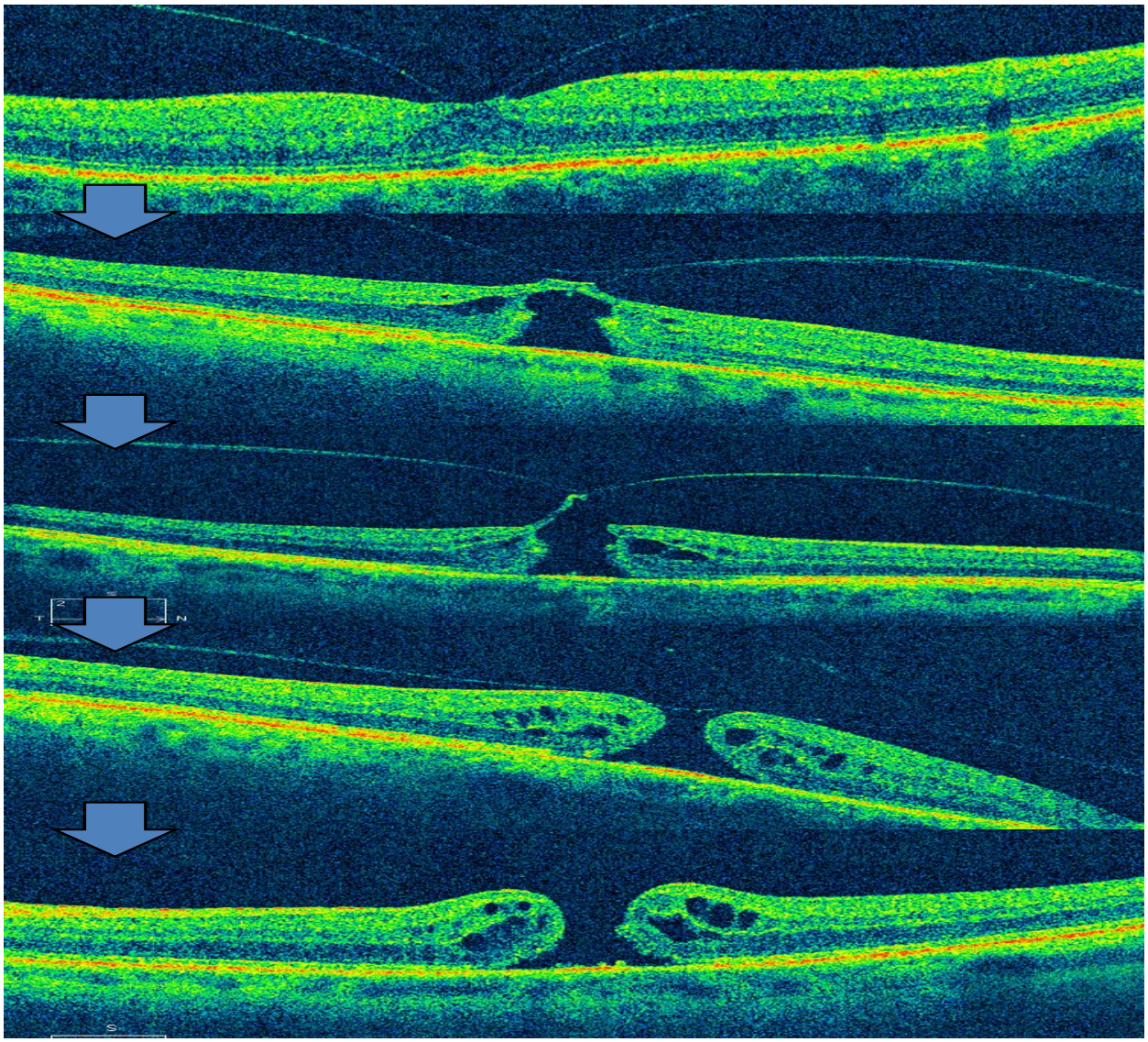

Figure 4. The progression of a macular hole formation. The vitreous cortex is in many people physiologically firmer attached ad the area of the fovea. In case of a partial detachment an adherence to the fovea might persist (as can be seen

on the top most image). In case a spontaneous detachment fails to occur, traction with subsequent cystoid changes of the underlying retina might occur. At this stage the patient starts to be symptomatic. Still a spontaneous resolution can occur at this stage, but a tear in the thin sheet covering the cystoid space underneath takes place in 40% of patients. The process is followed by a further retraction of the vitreous form the hole leading to the later stages at the bottom of the figure.

1.2 The Inner Limiting Membrane

The Inner limiting membrane (ILM) is a thin sheet of tissue at the most inner surface of the retina. Its thickness varies depending on the location in the eye from 70nm in the periphery and 200 to 400µm at the posterior pole. [30] [31] Further the ILM thickness increases with age. [32]It is formed by small feet of the retinal Müller cells for which it constitutes the basement membrane. Besides its role as a barrier between the retina and the vitreous, it is believed to serve as a scaffold for the fibrous growth in patients with ERMs. This supported by reduced recurrence rates of ERMs after removing the ILM during ERM surgery as compared to patients where the ILM was left in place. Recurrence rates and the ILM of up to 56% have been reported in patients with the ILM left on the retina compared to 9% after additional ILM removal.[33, 34, 35, 36]

In addition to its role as a scaffold for ERM growth, the ILM most likely can exhibit a tractional force on the retinal tissue itself. From histologic surgery specimens it has been proposed that the ILM might itself be pathologically thickened in ERM patients.

Another indication for a potential tractional role of the ILM is that there is ample evidence mounting that a peeling of the ILM reduces the reopening rates of full thickness macular holes after surgery. The reported reduction of the reopening rate in a recent meta-analysis that had included 5480 eyes was from 7.12% without an ILM peeling to only 1.18% with an ILM peeling. The mechanism behind this effect might

be a centripedal traction of the ILM even after removal of any vitreoretinal adhesion. [37]

Removal of the ILM has also been implicated to have a beneficial effect in cases of retinal detachment with proliferative vitreoretinopathy. In such cases the peeling of the ILM seems to prevent the occurrence of secondary membranes and might reduce the stress on the retina. Further it is the most definite way to ensure that the vitreous is completely removed in retinal detachment cases. A thin reminiscent layer of vitreous is sometimes hard to identify intraoperatively and also might proof difficult to remove. [38] [39]

1.3 Epiretinal Membrane Treatment

Most cases of epiretinal membranes do not require treatment as many patients are asymptomatic (see the epidemiology section). When however the patient experiences symptoms due to a distortion of the retinal architecture a surgical removal of the ERM is indicated. A spontaneous peeling of ERMs due to a posterior vitreous detachment is seldom the case. Whilst this might elevate the traction on the retinal surface, rendering a surgical intervention unnecessary, ERMs due not resolve by themselves.

1.3.1 The Surgery of epiretinal membranes

ERM peeling is together with macular hole surgery the most common macular surgery performed today and ranks as the third most common indication for pars plana vitrectomy. [40] As surgical techniques are constantly improving, not least because of newly available technologies, the indications for surgery start to encompass an increasing number of cases.

ERM surgery comprises 2 basic steps: first, the removal of the vitreous gel via a pars plana vitrectomy and second, the peeling of the ERM from the retinal surface. Often times these steps are combined with a anteceding cataract surgery, the use of dies to stain the ERM or ILM, and a peeling of the ILM afterwards. Most uncomplicated cases do not require a postoperative tamponade with gases, but for

the clinical practice surprisingly high rates of gas tamponade have been reported for the surgery of idiopathic ERMs (38.5% in a UK based study) [41]

The most common approach to pars plana vitrectomy today is via a 3 port 23 gauge trocar system. For the insertion of the trocars the conjunctive is displaced and the trocars are inserted 3.5 mm from the limbus at the temporal- or sometimes nasal inferior, the temporal superior, and the nasal superior quadrant of the bulbus. To facilitate correct estimation of the distance of the insertion to the limbus a plate of 7mm in diameter is pressed on the bulbus through its central opening the trocars are inserted in a 25° angle. (Figure 5) The later creates a valve like sealing of the wound after the removal of the trocars at the end of the surgery, which renders suturing usually unnecessary.

After the insertion of the trocars an infusion is plugged into the inferior trocar leaving the superior two trocars for the illumination probe and the tools for manipulation such as a vitreous cutter or an end gripping forceps. Some surgeons prefer to use an additional chandelier light, which is basically a stationary light probe that one inserts through the pars plana at the 12 o'clock position. This is less often necessary for ERM surgery, but it is helpful when a bimanual manipulation is advantageous such as cases with severe fibrovascular membrane formation.
The placement of the trocar system is followed by the visualization of the fundus.

1.3.1.1 Biom versus contact lens.

The early vitrectomies were conducted under fundus visualization with a contact lens. While these lenses are still in use today, in the past few decades the fundus with a non-contact binocular indirect ophthalmomicroscope (BIOM) has gained increasing popularity amongst vitreoretinal surgeons.

The setup with a contact lens has multiple drawbacks. First, the contact lens by definition sits directly on the cornea with the risk of corneal damage. Second, due to the curvature of the bulbus the contact lens tends to slip from the corneal center to the sides. To prevent delocalization of the contact lens a trained assistant is required to hold the lens in place during the surgery. Third, the contact lens only permits a

limited view of the peripheral retina. Current biconcave lenses do outperform their ancestors, but still limit the angle of view to 35° at most.

Still some surgeons prefer the contact lens system over the non-contact systems for macular surgeries like the ERM peeling, because of a they felt that the image was sharper.

The BIOM gives a wider view of the retina, up to 130° and modern systems allow for high resolution visualization of the fundus which is comparable to the contact lens based systems. As such most surgeon today tend to use a BIOM for vitreoretinal surgeries including ERM peelings.

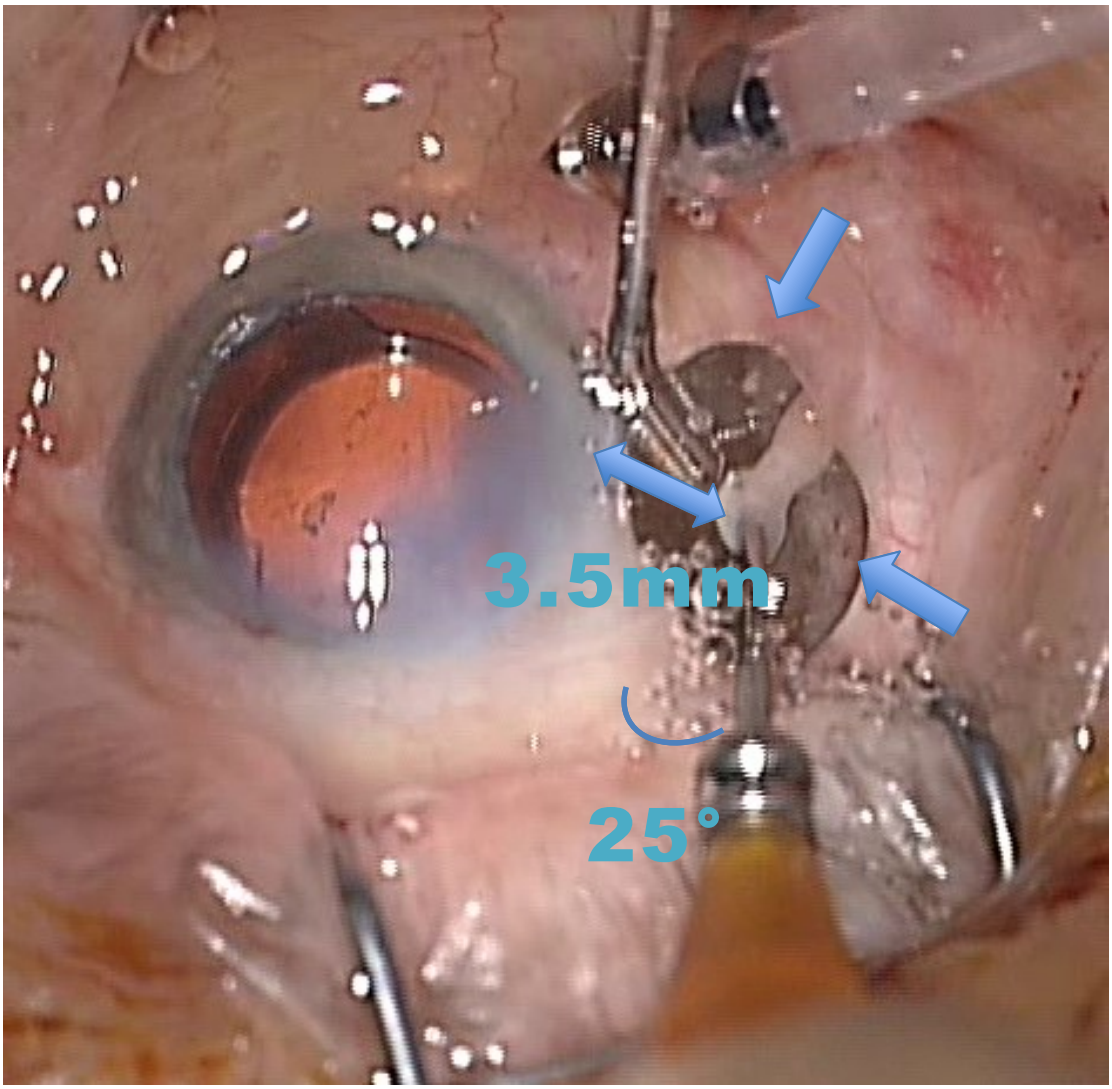

Figure 5. Trocar insertion during 23 gauge pars plana vitrectomy. A 7mm diameter plate (arrows) is pressed on the globe to 1.) dislocate the conjunctiva to create a discontinuation in the wound channel after removal 2.) to measure the distance from the limbus (3.5,mm) 3.) to flatten the sclera for an improved convex valve formation after trocar removal and 4.) to angle the insertion to 25° by sliding the trocar touching the inner edge from the plate towards the center.

Once the trocars are inserted and the fundus is sharply visualized the surgery proceeds to the removal of the vitreous core including varying amounts of peripheral vitreous. As most cases of ERM already present with a detached vitreous an

intraoperative vitreous detachment is seldom necessary. If this step is needed, a staining of the vitreous strands with intravitreal triamcinolone might be considered [42]

After the removal of the vitreous gel a dye might be applied onto the macular area to improve the visualization of the ERM. This additional staining procedure for a pars plana vitrectomy is also called chromovitrectomy. Some surgeons advocate staining in an air-filled eye to enhance the contrast of the staining and prevent dispersion of the dye within the vitreous cavity. [43] This, however, comes at the cost of at least one additional step during surgery (fluid air exchange) and risks a clouding of the posterior lens capsule, which in turn can make the peeling process exceedingly difficult. As such it might jeopardize a safe ERM surgery or even force the surgeon to perform an air-fluid exchange increasing the duration of the surgery once again.
To improve the staining capabilities the modern staining agents are usually mixed with a 5-10% glucose to increase their density over the density of balanced salt solution in the eye, which effectively makes them heavier than water and the dye sinks due to gravity to the posterior pole. This gives good staining properties confined to the area of interest, namely the macula and reduces the dispersion of the dy in the vitreous cavity which would make a save visualization difficult. The staining agents currently used are Indocyanine Green (ICG), Trypan Blue, and Brilliant Blue. These will be discussed in further detail in the following section.

1.3.1.2 Chromovitrectomy

1.3.1.2.1 Indocyanine Green

The initial attempts to stain transparent intraocular tissues were with fluorescein in 1978 [44], but it was really the advance of ICG in 2000 that sparked the routine use of intraocular staining agents. [45] ICG had been originally developed for the use in photography in the first have of the 20ieth century, but got early attention after the second world war as a measurement tool for hepatic function since it is exclusively metabolized in the liver. In ophthalmology ICG struggled to overcome some technical

difficulties as a fluorescing agent in fundus angiography, but eventually, with technological advances in the camera systems, it became a standard for functional imaging of the choroidal vasculature. [46]

ICG belongs to the group of polymethine dyes, which are characterized by a single or multiple methine groups in their molecular structure. Its amphiphilic behavior results in staining of cellular and acellular tissue components, which gives it good staining properties for both the ILM and the ERM.[47]

The use of ICG as an intraoperative staining agent significantly increased the ease of ERM and ILM removal, however, the addition of a chemical intraocular compound raised the question of retinal toxicity. Indeed, ICG has been shown in vitro to significantly reduce the viability of human RPE cells and photoreceptors. [48] In addition to the in vitro studies in vivo observations both in animal models and in humans have shown RPE changes in concentrations used in routine practice. [49]

Another point that might play a significant role in improving the intraoperative behavior of the ILM is that in increase in ILM stiffness after the application of staining agents such as ICG and Brilliant Blue has been observed. This effect is most pronounced in ICG treated ILMs and is further enhanced after illumination of the stained tissue. This indicates a photoreactivity similar to the one implicated in the toxicological analyses. [50]

Out of concern about the retinotoxic effect of ICG many European clinics have abandoned ICG as an intraoperative staining agent and have switched to ether Brilliant blue or Trypan blue. In the United States ICG is still in widespread use since other dies have not yet been FDA approved.

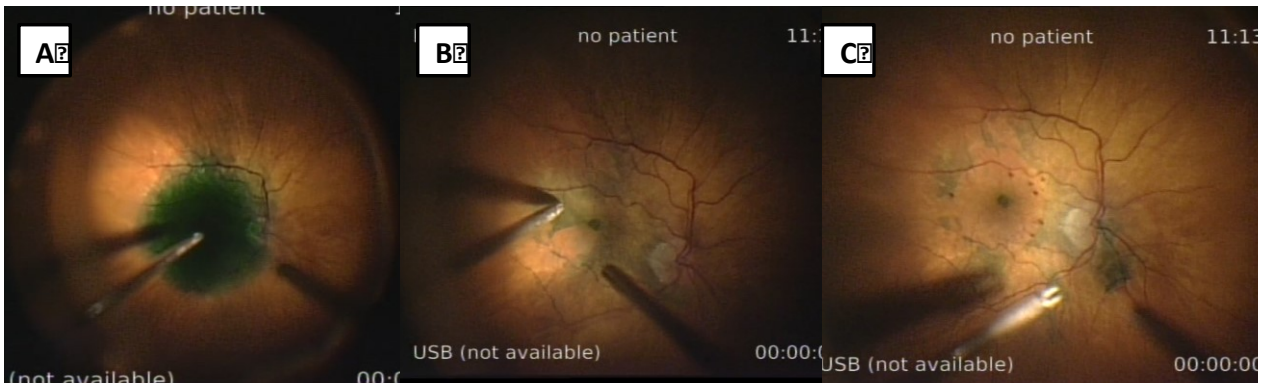

Figure 6. The peeling under Indocyanin Green (ICG) visualization. As a first step (A) ICG is injected onto the macular area with a fluid needle. After a short dwell time the excess ICG is removed via the fluid needle and an endgripping forceps is inserted into the eye instead of the fluid needle (B). By means of mechanically grasping the delicate membranes, that is the epiretinal membrane and the inner limiting membrane. If insufficient staining is achieved with a single staining procedure this might be repeated, similarly after the first peeling a second staining is recommended to detect remaining inner limiting membrane which usually fails to stain where it is covered by an epiretinal membrane.

1.3.1.2.2 Trypan Blue

Trypan blue was developed in 1904 and its initial use was in microscopy. It is part of the azo dye family, which means that it contains an azo (nitrogen double bond) group within its chemical structure. It is also known under the names of Direct Blue 14, Diamine Blue 3B, and Niagara Blue 3B. Most of its effect is on the cell nuclei of severely damaged, dead, or descement membrane stripped endothelial cells. [47] This makes it a good candidate for staining ERMs.

The first reported use of this dye in ophthalmology was in the sixties for staining the ocular surface [51] [52]Its first intraocular use was for staining the anterior lens capsule for improved visualization of the capsular rhexis during cataract surgery,

for which it is still in use today. [53] First toxicological studies of intravitreal Trypan blue injection took place in 2001 in a rabbit model [54] and the dye was subsequently first used for staining ERMs in humans in 2002 [55] . The dye is especially suitable for staining the ERM because it adheres to degenerated cell parts much better than to live tissue or vital cells with a patent cell membrane.

The two concentrations that are currently commercially available are 0.06% (Vision Blue, DORC International, which is most commonly used for staining the anterior capsule in cataract surgery) and 0.15% (Membrane Blue, DORC International, which is most commonly used in the ERM peeling to stain the ERM and the ILM). [56] In this range an excellent safety profile has been reported and because of that most surgeons, at lest in Europe, have adopted the use of Trypan blue. However, only slightly higher concentrations as typically used during dye-assisted vitrectomy (that is 0.2% or more) have caused retinal toxicity in rabbits. [54] While Trypan blue has been successfully used in humans to identify undetected retinal breaks in retinal detachment surgeries, it has been also described to induce RPE changes after a subretinal migration in a human patient after macular hole surgery. [57] [58] Another drawback is that in contrast to ICG Trypan blue stains the ILM much less and as such might also have less of a stiffening effect on the ILM. [59] Figure 7 shows a staining process with Trypan blue.

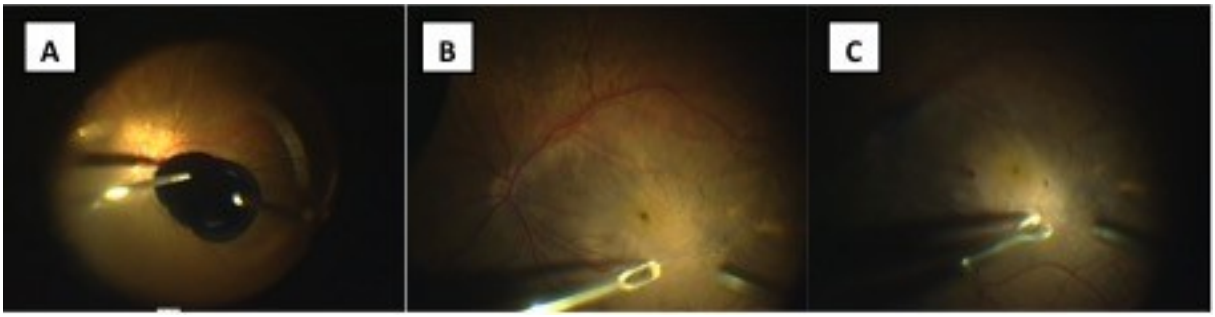

Figure 7. The peeling under Trypan blue visualization. As a first step (A) Trypan blue is injected onto the macular area with a fluid needle. After a short dwell time the excess Trypan blue is removed via the fluid needle and an endgripping forceps is inserted into the eye instead of the fluid needle (B). By means of mechanically grasping the delicate membranes, that is the epiretinal

membrane. In this case the ILM stuck on the retina and a second staining process was performed (not shown). Subsequently the ILM was peeled in a second peeling step (C). Note the slightly poorer staining than with ICG.

1.3.1.2.3 Brilliant Blue

Brilliant blue belongs to the arylmethane dyes, which are derived from methane. Synonymes for Brilliant Blue include Acid Blue and Coomaddie Brilliant Blue. [47] Similar to ICG, the staining agent Brilliant blue has a high affinity to basement membrane components such as the ILM. Compared to the ILM staining, its staining capacity towards the ERM is much lower. This results in a contrast between the poorly stained ERM and the bluish tainted ILM.

However, multiple authors have suggested that the staining capability of brilliant blue for the ILM appears to be lower than the staining capability of ICG. [60] [61] If the staining seems for the surgeon insufficient to safely peel the ILM, it has been shown that the application of the dye in an air filled eye can significantly improve the tissue uptake of the dye and hence improve the contrast. Of note is also that albeit the staining in a fluid filled eye was weaker than in an air filled eye, neither the visual acuity nor the multifocal electroretinography results showed any difference between the two groups. As such it is debatable if the additional step truly is worth while. In the same studies the authors also noted that the ILM seemed stiffer and easier to peel after brilliant blue application under air. The latter behavior is similar to the effect earlier described for ICG. The authors, however, did not measure stiffness in the study and the surgeons were obviously not masked whether the dye had been applied under air or fluid. [43]

Compared to ICG the toxicological profile of Brilliant blue seems to be favorable. Neither in vitro nor in vivo studies of Brilliant blue have noted retinotoxic effects. Even an anti-apoptotic capacity in vitro has been reported. [62]This might be mediated via the antagonism of Brilliant blue to P2RX7, a purinoreceptor for ATP

which when activated seams to trigger cell death and/or the release of inflammatory cytokines such as IL-1ß, IL-6, and TNF-alpha. [63] [64]

However, despite the aforementioned low toxicity a RPE atrophy after subretinal Brilliant Blue in a mouse model and in a small case series has been reported and thus contact between the RPE and the dye should be avoided. [65] [66] Still, since its approval from the European Medicines Agency in 2007 Brilliant blue has, not least because of its favorable side effect profile gained increasing numbers of advocates in the vitreoretinal community. An approval from the United States based Food and Drug Administration (FDA) is still pending, but in 2015 the Pharmacy compounding Advisory Committee of the FDA recommended to put Brilliant Blue on the list of bulk substances that may be used for compounding. That means that albeit not being FDA approved it may be used for vitreoretinal surgery having a similar status as for example Bevacizumab (Avastin®) for the intravitreal anti-vascular endothelial growth factor therapy. [67]

1.3.1.2.4 Principals of Dye toxicity

The potential retinal toxicity of intravitreal dies depends mainly on four factors: concentration, osmolality, retention time in the eye, and illumination time. [56]

Some surgeons have proposed the combination of different dyes such as Trypan blue for the ERM with subsequent ICG for the ILM. [68] [69]One should keep in mind that such approaches not only might increase the risk of retinal toxicity by the agents interaction with each other, but the additional handling can increase the surgery time, which might pose an additional risk for chemo-toxicity and photo-toxicity. This might be aliviated by using a mixture of both dyes in one solution. However, excess time of surgery should be weight against a potential decreased risk of retinal trauma because of better visualization for the surgeon.

1.3.2 Visual outcomes of ERMs

1.3.3 Minimization

The early stages of macular surgery were a revolution for retinal surgery all together. When treating localized pathologies in otherwise healthy retinas, a damage caused by to aggressive techniques such as an excessive light exposure became apparent. As such a major focus today is minimizing trauma to the eye. For the early vitrectomy devices the surgeon had to incise the sclera with a paracenthesis and the instruments were inserted into the eye directly through the resulting scleral tunnel.

Machemer used in his first experiments single port 19-gauge instruments with extremely low cut rates. Such instruments not only required large scleral openings, but also caused significant vitreoretinal traction. Luckily for most surgeons and patients the early indications for vitrectomy were severely damaged eyes with dens vitreous hemorrhage. As such it was often hard to tell how much damage was caused by the original disease and how much by the surgery. It was only later when the instruments became more sophisticated that surgeon became more courageous and started to tackle macular diseases. In such eyes most of the retina is healthy and it became soon apparent that the ocular trauma due to the surgery was significant. Not least the photo toxicity of the light sources used at that time was an issue.

So really the advance of macular surgery triggered a new refinement in the vitreoretinal armamentarium. On step was the development of less aggressive light probes with a cooler less intense light. Another step was the minimization of the instruments and the development of a trocar system through which the instruments are inserted and retracted from the eye.

Until recently trocars were quite uncommon and the standard vitrectomy was a 20-gauge transscleral 3 port approach. Such transscleral tunnels required postoperative closure with sutures, first because of the straight incision (that is perpendicular to the ocular surface), second because of the sheer size of the initial incision made, and third because of additional stretching an tearing of the scleral wound du to the manipulation while moving the instruments in and out of the eye as well as within the eye. The first attempts, half successful, to minimize this trauma was the introduction of much smaller trocar based 25-gauge vitrectomy. [70] [71] However, at that time the materials of the instruments suffered form insufficient stiffness to resist

the torque applied while moving them around in the eye. Surgeon often had difficulties reaching very peripheral lesions and instruments tended to bend during the procedures. Also the pumps in the vitrectomy machines were underpowered to produce enough suction so that at least somewhat comparable flows to the larger gauge instruments could be achieved. Last but not least the cut rates were still in the three digit range. Taken together the surgery was cumbersome and took a long time and as such the initial 25-gauge attempts did not become very popular with most vitreoretinal surgeons and were mostly used for very select cases such as children.

To alleviate some of the problems, which the early 25-gauge system had to face, a compromise between the 20- and 25-gauge instruments was introduced in the first decade of the twenty-first century. [72] [73] In contrast to 20 and 25-gauge these instruments used an angled scleral tunnel and similar to the 25-guage system a trocar-based approach was chosen. This resulted in a self sealing scleral wounds like with the 25 gauge system and the instruments remained sufficiently stiff for comfortable intraocular manipulation.

Also the slightly larger instruments were quicker in terms of aspiration than their 25-gauge predecessors. With less trauma to the eye these systems were as fast as the previous standard, that is the 20-gauge systems, and there was no increase in postoperative complications. Today the 23-gauge 3 port vitrectomy is the most commonly used vitrectomy system. As time went on further refinements were developed; these include valved trocars to reduce vitreous-, fluid-, or gas-loss while inserting and removing the instruments; chandelier light sources to enable bimanual manipulation in the eye; double cutting vitrectomes, which the oscillating blade within the vitrectomy does not only cut when moving down towards the tip of the instrument, but also when moving up, which effectively doubles the cut rate; better pumps in the vitrectomy systems; and stiffer materials for the instruments. All of these features have sparked once again the interest in not only 25-gauge, but also 27-gauge instruments. Many vitrectomy systems that currently hit the market already include instruments or at least the capability for the use of 27-gauge instrumentation and some have such instruments already commercially available. As of now it seems that

this time the smaller instruments are here to stay. Figure 8 shows the various vitreous cutter sizes that are currently in clinical use.

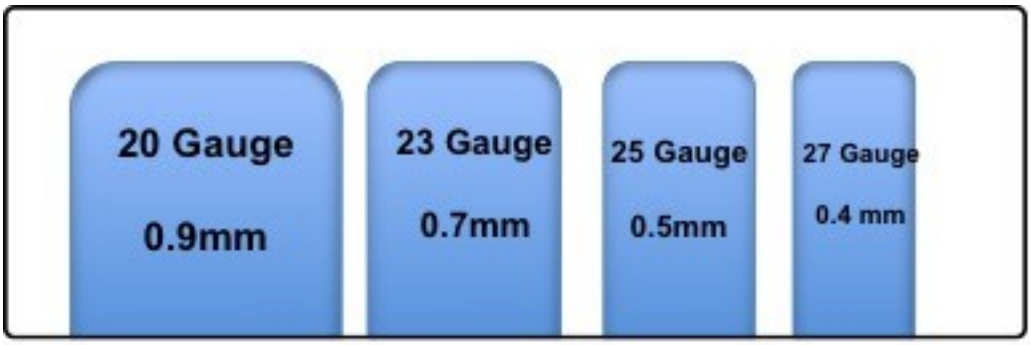

Figure 8. An Example of the various vitreous cutter sizes that are currently in use. The initial 20-gauge vitrectomy system used no trocars and has been widely replaced by the 23-gauge system. Novel developments in rheology and mechanics make small cutters ever more efficient and feasible for routine practice. As such the minimal invasive 25- and 27-gauge vitrectomy cutters have recently started to become more wide spread available.

When changing from the larger sutured scleral tunnel to the smaller sutureless systems, there was a concern regarding higher complication rates, such as endophthalmitis, choroidal detachment, and hypotony. The main reason for this was that an unsutured wound might serve as a portal of entry for germs, which can never be completely eliminated form the eyes surface, and at the same time might leak after the surgery resulting in low intraocular pressure. Especially the 23-guage system, which still is relatively large as compared to the 25-gauge or even 27-guage system, was under suspicion of instable wound closure. It has been, however, shown in a study on rabbit eyes, that given the proper incision technique the postoperative reflux was similar in 23 and 25 gauge sclerotomies. The postoperative leak was very small in straight 25-gauge sclerotomies as well as in angled 23-gauge sclerotomies. However, unsutured 23-guage sclerotomies that were created in a straight fashion exhibited relatively high leakage. [74] Still, the postoperative hypotony rates in eyes that

underwent surgery with a sutureless 23-guage system are higher than those in eyes that underwent surgery with a sutured 20-gauge system. The clinically much more important complication rates, such as endophthalmitis seem not to differ though between the gauge sizes.[75]

1.4 Optical Coherence Tomography

1.4.1 Principals of Optical Coherence Tomography

The first report on the in vivo use of optical coherence tomography (OCT) in a human was published in Science in 1991. [76] Since then OCT has spread through ophthalmology and beyond.

The principal of OCT is a mapping of the reflectivity in a tissue measured by laser interferometry. For that purpose a light beam with a specified spectrum is split into a reference arm and a scanning arm. While the earlier arm is reflected by a mirror within the device, the latter arm is reflected by the tissue that is to be measured. The reflection of these two arms is again unified in the device and the resulting interference signal is recorded by a detector. See figure 9 for a schematic drawing of an OCT device.

Since the OCT scans with light and many ocular structures are essentially constructed to enable light penetration, the OCT and the eye can be considered “a match made in heaven”, to use the words of David Huang, the other of the 1991 publication in Science and one of the scientist leading the way for the ophthalmic applications of the OCT.

Since 1991 the field of in vivo ocular imaging has been rapidly evolving and today we have devices that superceed the original machienes in speed, resolution, automated segmentation algorithms, and recently also functional imaging has been introduced.

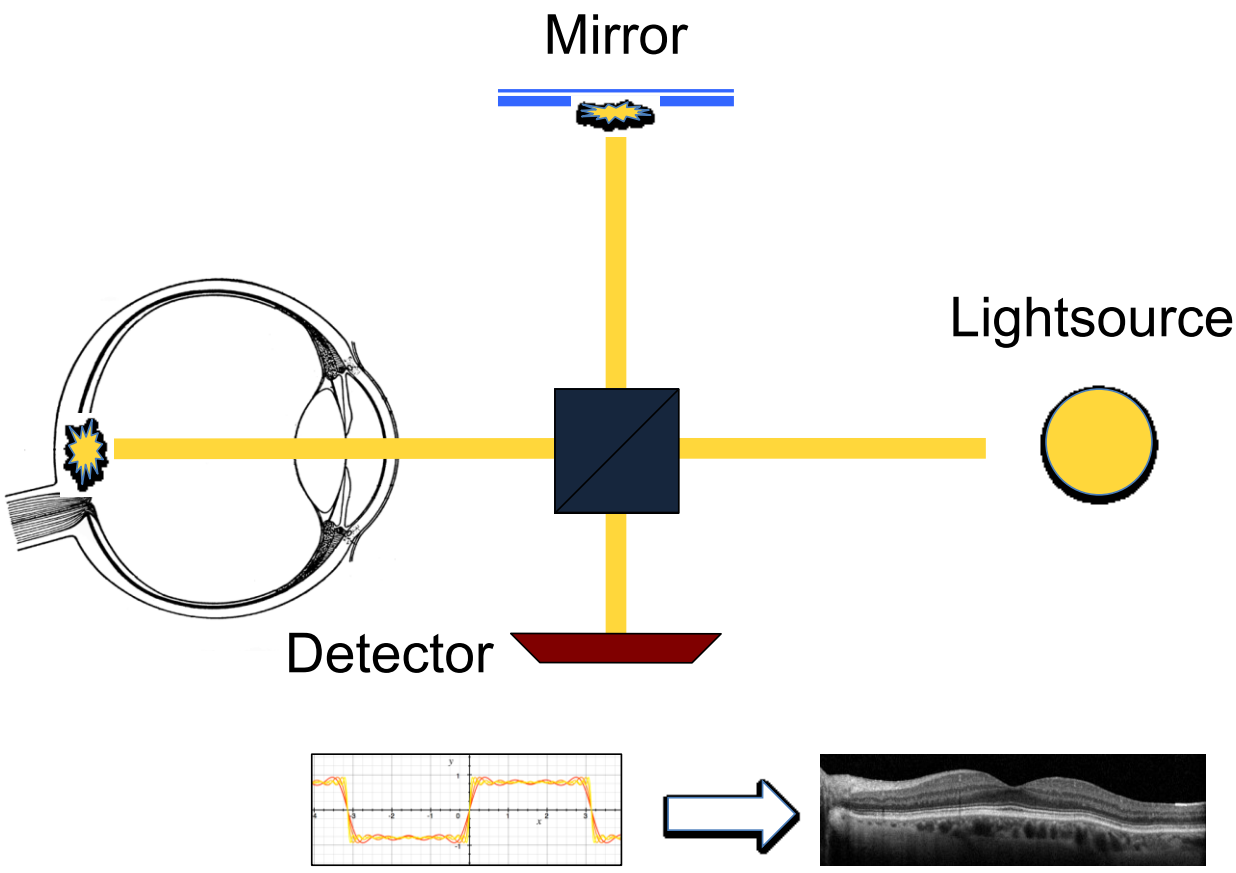

Figure 9.Schematic of an Optical coherence tomograph. The light beam originates at the light source (usually a LED or LASER). It is split into a reference arm, which is reflected by a mirror, and into a scanning arm, which is reflected by the tissue. The two reflected beams interfere with each other, which results in a characteristic pattern. This interference pattern is detected by a detector array and is subsequently analyzed and transformed into a gray scale image where brighter areas represent areas of higher reflective tissue and dark areas represent low reflective tissue. One single A scan only scans the retina from interior to exterior (axial), the combination of multiple of these A scans results in the B scan which analogous to ultrasonography provides an in vivo 2 dimensional cross section through the tissue. Multiple B scans can be rendered for 3 dimensional reconstruction of the tissue reflectivity and might be used for volume calculations.

In the earlier devices the signal was analyzed as a function of time (so called time-domain), that is the reflection intensity at various time points was assessed and correlated with the depth of the signal at this time point. This was possible because in time domain OCTs the reference mirror was moving for each scan back an forth and , thus, determined the scanning depth. This made the calculation of the signal relatively straight forward, however, it also significantly limited the speed of the recording since the mirror had to travel the entire scanning distance for each A-scan. In these devices the limiting factor was the mechanical component of the measurement.

A more modern approach is to work with a stable mirror and analyzing the signal as a function of frequency (so called frequency domain or spectral domain). In these devices the resulting interference pattern needs a mathematical transformation where the complex pattern is split into multiple simpler patterns that are accessible for calculation (Fourier Transformation). This method increases the recording speed around 100 times, mostly due to eliminating any moving parts, but it also causes artifacts. First, the Fourier transformation works with imaginary numbers and results in multiple solutions (at least one positive and one negative one). This results in an image that is mirrored around a center, the zero delay line. There are multiple of these mirror images, but each one fades with increasing distance from the zero delay line. Clinically, this is apparent in mirror artifacts often observed in patients with axial myopia, patients with lesion protruding into the vitreous cavity, or vitreal opacities. (Figure 10 shows examples of such artifacts).

Motion artifacts were mostly observed in the older slower time-domain versions of OCTs. This led to dragging of the image when the patient was not keeping a steady fixation during the imaging. The newer spectral domain devices don’t significantly suffer from this problem for purely anatomical imaging (amplitude imaging). Devices that need to measure the same spat at least twice (leading to at least a double in recording time) and need a high resolution over a broad area still need to minimize such artifacts. The prime example of such OCTs are OCT angiography devices. In these OCTs the signal speckle decorrelation between the

first recording and the second recording is used to detect motion in the retinal tissue. That is if one pixel in the first recording is highly reflective in the first recording, it might be of low reflectivity in the second. As the only moving particles with a significant size to be resolved by current OCT technology in the retina are erythrocytes, the resulting areas of high speckle decorrelation corresponds to the retinal vasculature. This can then be superimposed onto the conventional amplitude based analysis (such as a 3 dimensional cube scan).

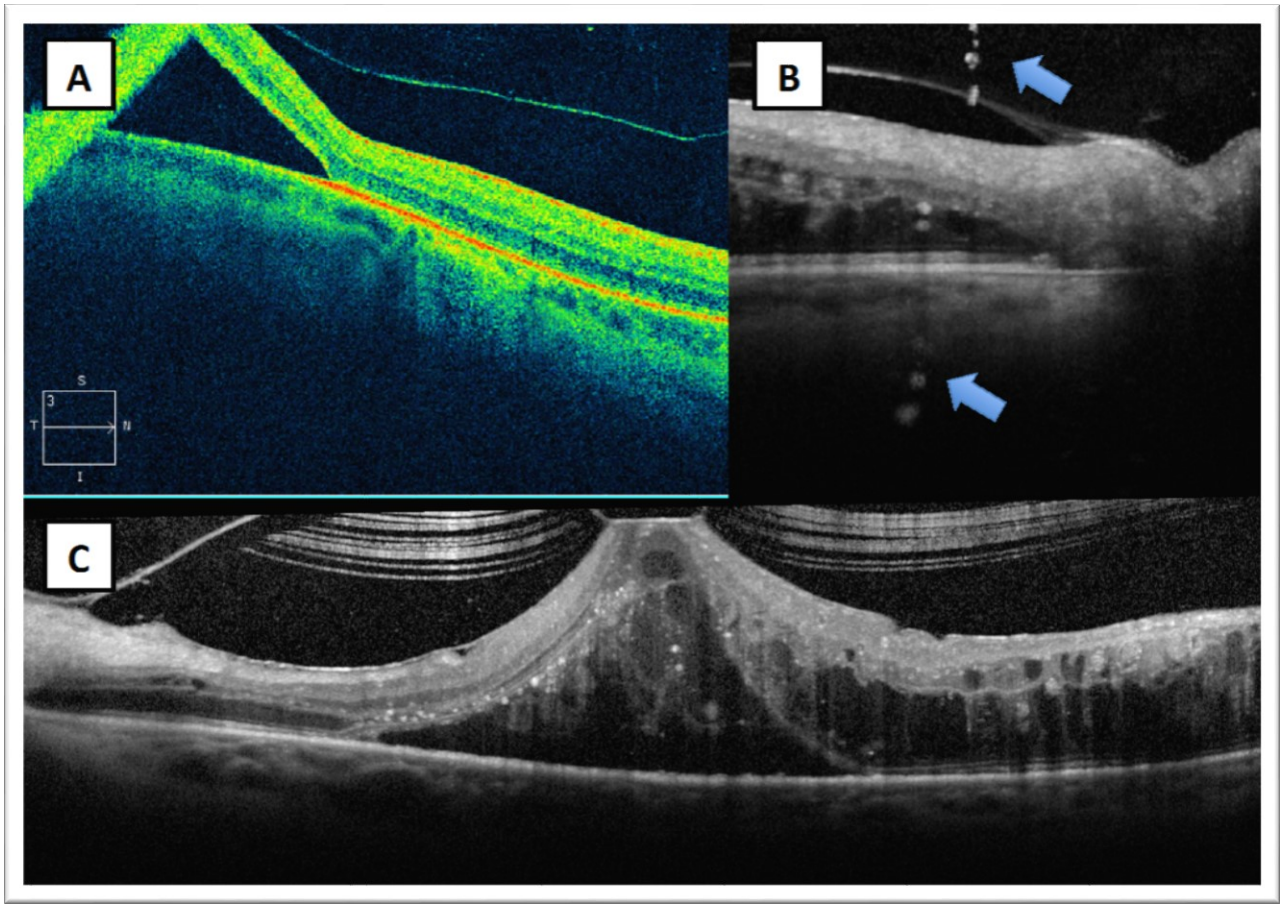

Figure 10. Examples of mirror artefacts on frequency domain optical coherence tomography. (A) shows on the top left corner the detached retina being mirrored downward into the choroid. In reality the retina would in this case continue upward. Note that the mirror image is also of lesser acuteness as the un-mirrored retina to its right. (B) shows vitreous debris that is mirrored down

into the choroid (arrows). Similar to (A) the mirror image is again less sharp. (C) shows on the top the mirrored vitreous cortex. The multilayered appearance in this case is produced by the averaging of the OCT device. That is a single image is composed of up to 100 single scans an overlay of these images is created. However, a slight shift in the relation of the zero delay line to the tissue (such as slight anteroposterior oscillations of the patients head) result in slight shifts of the mirror artifact in relation to the rest of the image, so that an excellent alignment of the un-mirrored image automatically results in a feathered appearance of the mirror artifact.

Second, The calculation accuracy of the image is higher close to the zero delay line. This means that the structures depicted closer to the mathematical mirror appear sharper than those farther away, the clinical implication being to move the image as close as possible to the mirror whilst avoiding mirror artifacts. In current devices the zero delay line is placed on top of the retina (which on OCT is the inner retina) highlighting the vitreoretinal interface. Inversion of the Zero delay line to the bottom of the retina leads to higher resolution of the deeper structures such as the choroid and the sclera. This is the bases of enhanced depth imaging. Figure 11 shows a healthy retina with a conventionally placed zero delay line and a recording in enhanced depth imaging mode.

1.4.1.1 Light sources

Ophthalmologic OCTs need an optical system with a bright light source. The latter is usually a low-coherence super luminescent diode (SLD) or in newer devices a fine tunable laser (swept source). The wavelength of the emitted light is either around 840 nm or 1060 nm. At these values the absorption profile of water is at a relative low (as can be seen in figure 12.). Albeit there are some differences especially at the higher

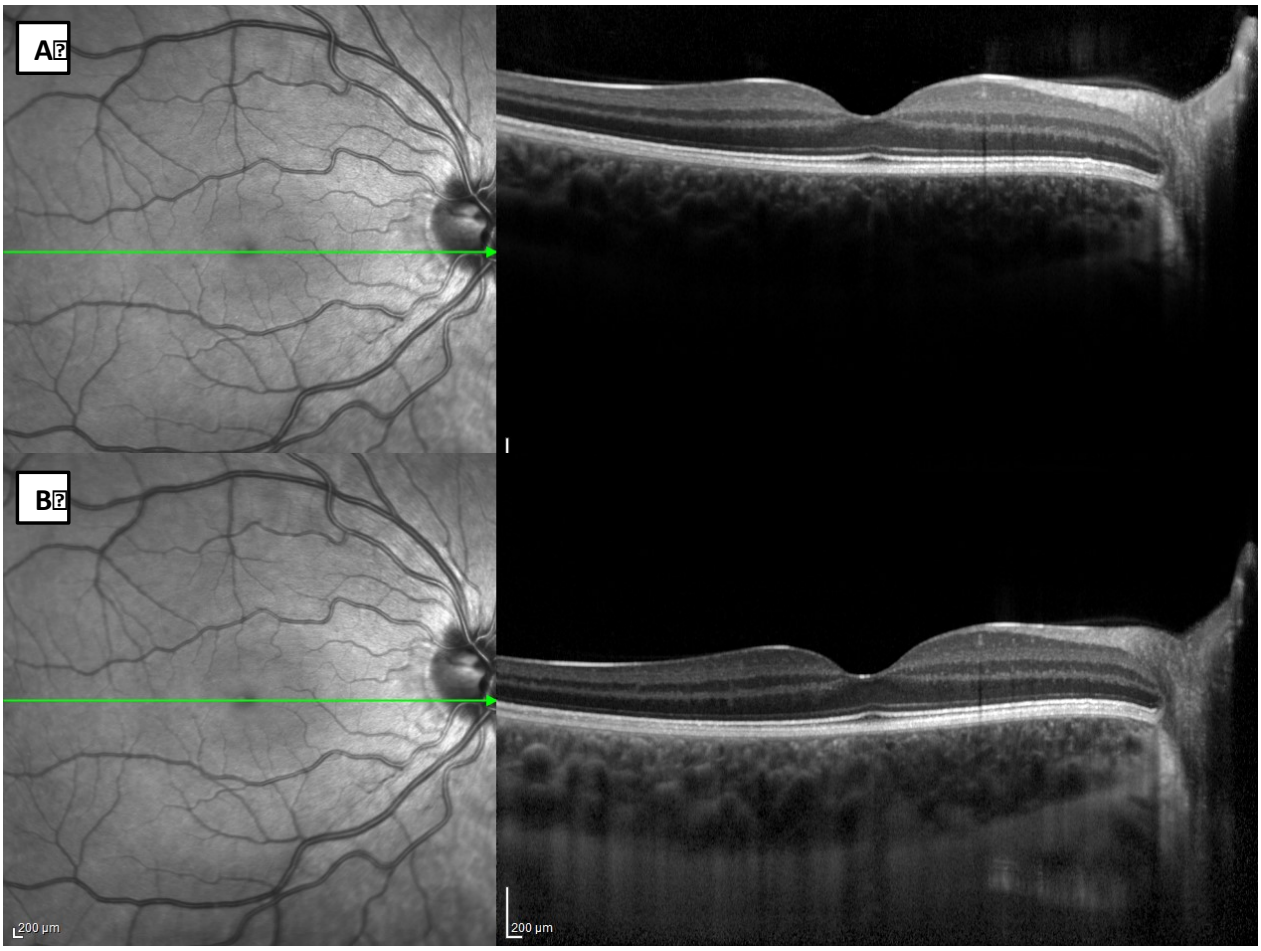

Figure 11. Conventional optical coherence tomography versus enhanced depth imaging. (A) shows a conventional imaging with the zero delay line placed on the top of the image. Compared to enhanced depth imaging (B) the inner retina and the vitreoretinal interface are imaged with a much higher contrast. Conversely in (B) the detailed structures of the choroid an the inner most boarder to the sclera can be appreciated due to the placement of the zero delay line at the bottom of the image. In the nasal inferior boarder a faint mirror artifact of the choroido-scleral interface can be seen.

and lower end of the spectrum, the absorptions spectrum of water can serve as a reasonable approximation of the absorption profile in the eye as the aqueous humor and vitreous consist mainly of water. While the absorption in water increases with an increasing wavelength, higher wavelengths on the other hand exhibit a better tissue

penetration in general. As such efforts for devices with light sources with a good compromise of tissue penetration (meaning high wavelengths) and low water absorption (meaning short wavelengths) are undertaken. This explains the tendency to center newer light sources at the absorption depression around 1060 nm, where the absorption is still higher than at the conventional 840 nm.

This compromise is much less of a problem for OCTs that are developed for the anterior segment. Here the light needs to travel much less aqueous matter in the first place and actually a high absorption in the vitreous is desired to serve as an additional shield for the delicate retinal tissue. In these devices longer wavelengths such as 1300 nm can be applied with high power in a relatively save fashion. This provides excellent tissue penetration (such as the sclera) and keeps the retina save due to the high absorption of the light in the vitreous.

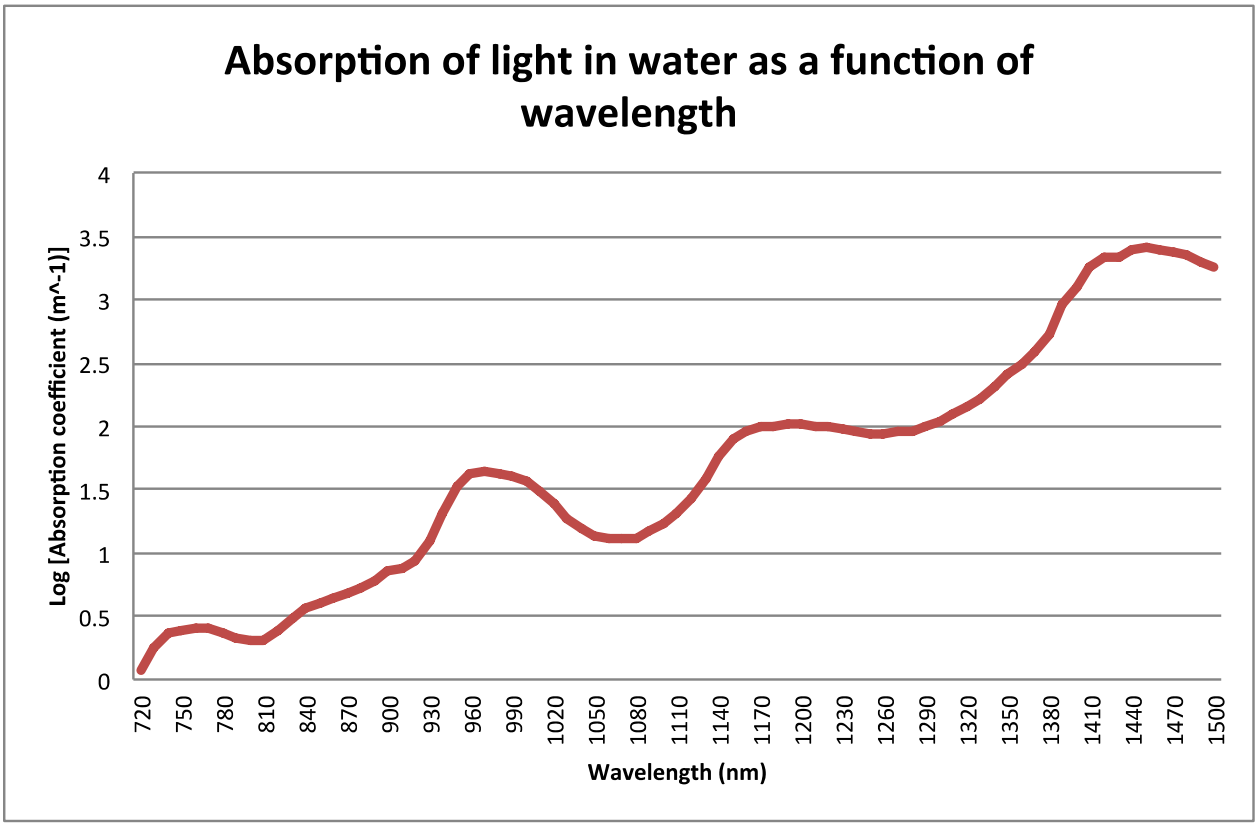

Figure 12. The absorption of light in water increases with the wavelength. A distinct dip can be seen at 1060nm which is exploited in some new optical

coherence devices for retinal imaging. Most devices so far (time-domain and spectral-domain) center their spectra around 840 nm. [77] The data are composed from Smith and Baker (1981) [78] for the values under 800nm, and from Curcio and Petty (1951) for those above 800nm.

A remarkable feature of OCT is the decoupling of the transversal and axial resolution of the device. While the latter is determined by the optical system, the earlier is determined by the light source. The axial resolution of an OCT system dependents on the brevity of the coherence lengths (l_c) which depends on the one hand on the central wavelength (the shorter the higher the resolution, at the cost of tissue penetration) and on the other hand on the bandwidth of the light source's spectrum according to the formula $lc \approx \lambda_0^2/\Delta\lambda$. Where λ_0 is the central wavelength $\Delta\lambda$ is the bandwidth. [79] That means the broader the spectrum the higher the axial resolution. As a reduction of the central wavelength constrains the tissue penetration, the most feasible option to improve the axial resolution is to find light sources with a wider bandwidth. In this regard a shift away from SLD-based towards laser-based systems is under way. Whereas the SLDs currently used in commercial OCTs have a bandwidth around 50 nm, a laser can be tuned one much wider scale (currently around 100 nm). [80] This, however, comes at an increased cost of the light source and the respective detector.

The effective axial resolution of the currently available commercial devices is between 3 to 8 µm. [81] Albeit this is resolves much detail of the retina, such a resolution prohibits a close assessment of the ILM, as a normal ILM is between 2 and 4µm thick at the posterior pole.

As mentioned before the transversal resolution is independent from the axial resolution and depends on the optics of both the device and the patient's eye. The current devices operate with a transversal resolution between 7 to 10 µm. A significant improvement in transversal resolution (down to 1µm) is obtained by implementing adaptive optics in the OCT device. Adaptec optics uses a bendable mirror to correct for aberrations in the optical system. While such a device can

resolve single photoreceptors and RPE cells, its clinical implementation is impeded by an exceedingly cumbersome image acquisition (both for the patient and the technician). In addition to that the area that can be imaged in one scan is very limited to around 4° x 4°. [81] In any case for evaluating ERMs and the ILM a higher axial resolution seems to be the more relevant parameter.

1.4.2 Optical coherence tomography and epiretinal membranes

OCT was a game changer in diagnosing ERMs. This reflects in a much higher prevalence of ERMs in studies using OCT as compared to fundus photography (see epidemiology section).

Previously epiretinal membranes were roughly characterized by the amount of whitish discoloration on the fundus and terms like cellophane retinopathy - signifying a very faint and supposedly thin membrane; macular pucker – signifying a very supposedly thick and white membrane; Further funduscopic calcifications have been proposed ranging from a water silk reflex and a translucent membrane (stage1), over an incipient tortuosity of the retinal vasculature with a translucent membrane (stage 2), to an opaque sheet of tissue (stage 3). [82] From clinical experience, however, often times the funduscopic appearance does not correlate with the membrane appearance measured by OCT, where sometimes relatively prominent membranes are actually relatively thin tissue sheets. Some authors have also proposed an evaluation of the ERM with a scanning laser ophthalmoscope imaging with an argon blue laser. With this imaging technique the authors had found a statistically significant difference concerning the amount of preoperative metamorphopsia between the 3 ERM stages. The, however, did not evaluate the respective correlation between the ERM score and the metamorphopsia. So the degree of relationship between the two parameters remains unknown. [82]

Besides the diagnosis the retinal appearance on the OCT has a plethora of implications for the patient's severity of symptoms and their prognosis with and without treatment. [11,83]

1.4.2.1 The Outer Retina

One field of high interest in this regard, that is concerning the symptom severity, are the outer most layers of the photoreceptors. On optical coherence tomography the photoreceptor layers are defined from the most inner aspect to the most outer aspect as the following: 1.) the outer plexiform layer, which correlates to the synapses of the photoreceptor axons and the bipolar cell dendrites with some intermingling of the horizontal neuronal network consisting of mainly amacrine cells. This layer appears moderately hyperreflective on OCT. 2.) the outer nuclear layer, which correlates to the cell bodies of the photoreceptors. Notably, the inner most cell bodies are mainly of rod origin and the outer most and often somewhat larger cell bodies are more consistently of cone origin. This layer appears relatively hyporeflective on OCT. 3.) the external limiting membrane, which corresponds to the junctional system of the Mueller cells and represents the outer pendant to the inner limiting membrane . This layer appears moderately hyperreflective on OCT and is very thin, in correspondence to its presumed histologic equivalent. 4) the myoid zone, appears hyporeflective on OCT and corresponds to the portion of the outer segments of the photoreceptors that is relatively depleted of mitochondria compared to the subsequent outer layer 5.) the ellipsoid zone, which correlates to the outer segments of the photoreceptors with tightly packed mitochondria. This layer is intensely hyperreflective on OCT. 6.) the interdigitation zone, this layer follows closely to the ellipsoid zone as a second, but slightly less pronounced, hyperreflective layer. It correlates to the overlap of the microvilli of the retinal pigment epithelium and the tips of the photoreceptors. This layer is essential for a correct function of the phagocytic process of the shed outer segment tips by the retinal pigment epithelium. 7.) the most outer layer with the most hyperreflective optical properties is the retinal pigment epithelium, correlating to the cellular monolayer of the respective cells. [84,85] Figure 13 shows a detailed description of the outer layers on the OCT.

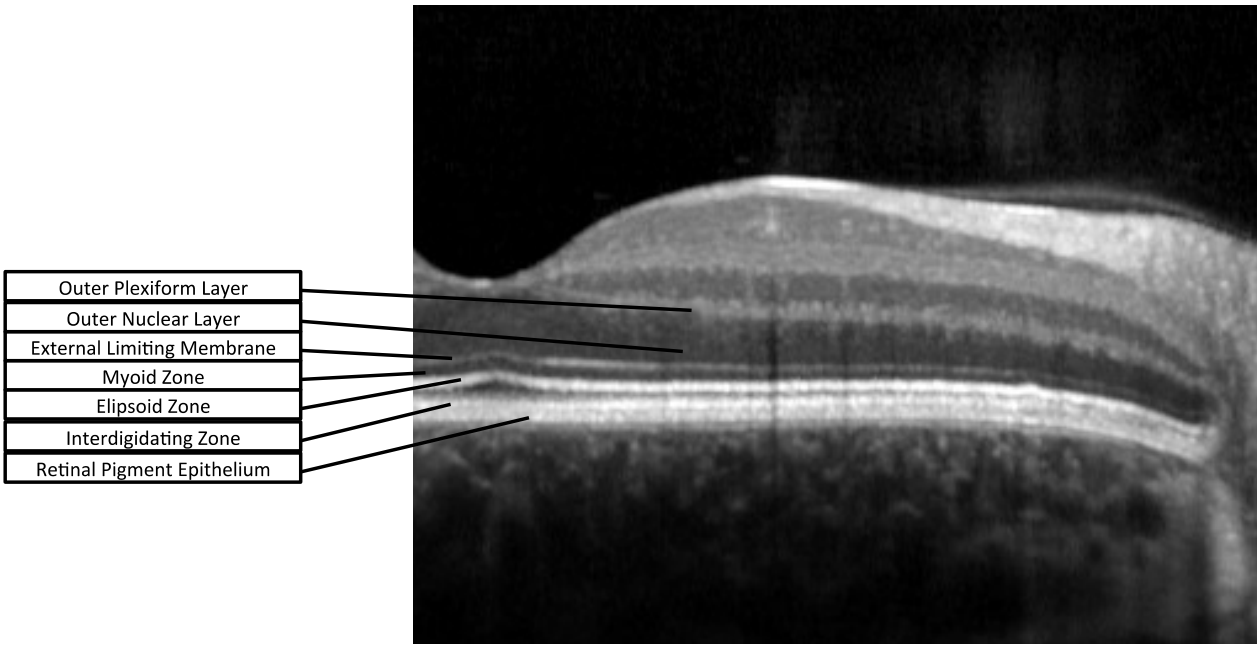

Figure 13. The normal retinal architecture on optical coherence tomography: A detailed description of the layers that make up the retinal photoreceptors and the retinal pigment epithelium. The outer plexiform layer consists of the synapses between the bipolar cell dendrites and the photoreceptor axons. The Henle fibers (not clearly demarcated in this imaging technique) lead to the cell bodies of the photoreceptors (the outer nuclear layer).The are adjacent to a thin hyperreflective line, the external limiting membrane, which is formed by the junctional complex of the Mueller cells. The layers further down are the outer segments of the photoreceptors. The myoid zone represents the segment which is relatively poor in mitochondria as compared to the tightly packed mitochondria of the ellipsoid zone. The tips of the photoreceptors then insert into microvilli of the retinal pigment epithelium which forms the interdigitation zone. Finally the retinal pigment epithelium with its characteristically highly hyperreflective band on the optical coherence tomography can be seen.

Michalewski and coworkers found that patients with a defect in the photoreceptor layer had a significantly worse visual acuity at presentation than those without such a defect. [83] Interestingly such alterations in the photoreceptor layer were more frequently found in patients without any splitting of the retinal layers, or lamellar holes.

It might indicate that a break of the retinal tissue elevates the vertical traction on the outer retinal layers which in turn might guarantee a maintenance of the close special juxtaposition of the photoreceptor tips with the processes of the retinal pigment epithelium. (for a more detailed description and pathophysiologic explanation see the chapter “Physiologic and pathophysiologic aspects of the outer retina”)

Whatever the cause may be, the correlation between alterations in the outer retina with visual acuity remained true whether this were cases with solely a decreased or flattened foveal depression due to their ERM, or whether this were cases with other additional changes in the retinal architecture such as lamellar macular holes, macular pseudo holes, vitreoretinal traction, or retinal cysts. [83]

The latter was confirmed in a study by Schumann and coworkers. [86] In the same paper there was also a significant correlation between a atypical ERM tissue and such an photoreceptor defect in patients with macular pseudo holes and patients with lamellar macular holes. Such atypical epiretinal membranes are membranes that in contrast to the typical, or also called tractional, ERMs show a medium reflectivity on OCT and are much thicker than their more common counterparts. [86]The histologic difference between these two types of membranes, if there is any, is still under discussion. Figure 14 shows an example of a photoreceptor layer defect in a patient with an ERM and Figure 15 three examples of atypical ERMs with and without photoreceptor alterations.

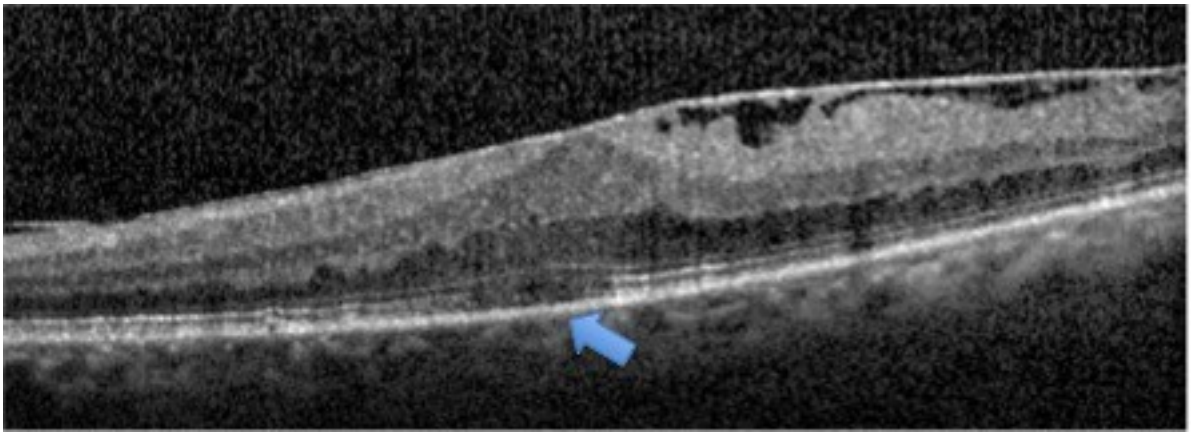

Figure 14. An optical coherence tomogram of an epiretinal membrane (ERM) causing a defect in the photoreceptor layers. The ERM stretches over the entire scan, but seem more prominent on the nasal side (right) where it is also widely elevated form the retinal surface. The foveal depression has been lost. The blue arrow points to the area of a resolution of the interdigitation zone and of the ellipsoid zone. The band of the external limiting membrane seems intact. This correlates with a loss or at least a dysfunction of the outer segments of the photoreceptors. The patient accordingly had a relatively poor visual acuity of 0.3 (Snellen).

Kim and coworkers found in their work on the relationship between the photoreceptor appearance eon OCT and the visual function of patients with ERM that the preoperative integrity correlated highly with the surgical outcome of these patients. A defect in the photoreceptor layer (specifically the ellipsoid zone) indicated a worse preoperative and postoperative visual acuity and less visual gain after the surgery. It was a better prognostic factor than foveal thickness, which did not correlate with the postoperative visual acuity. [87]

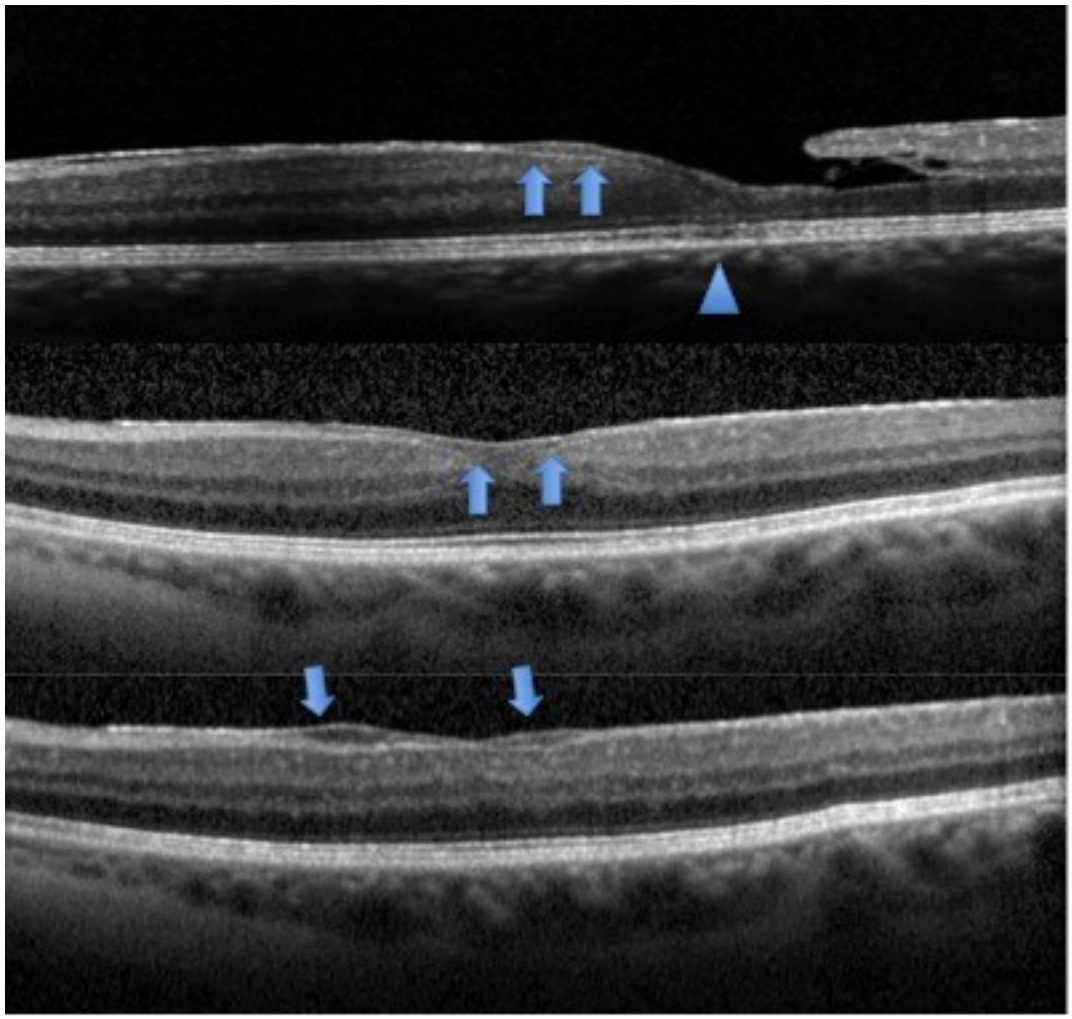

Figure 15. Three examples of an atypical epiretinal membrane. In these optical coherence tomography scans an atypical very thick hyporeflective membrane is apparent (blue arrows). These membranes seem to exalt very little traction on the retinal tissue, which itself looks relatively normal. This contrast them to the more common typical tractional membranes. In the topmost image the atypical ERM is associated with a macular lamellar hole and a slight photoreceptor defect (Arrow head). Here a loss of the interdigitation zone and a attenuation of the ellipsoid layer is apparent.

Shimozono et al described what they termed the cone outer segment line (which is according to todays international consensus termed the interdigitation zone)

together with, what was then a commonly misused term, the inner segment / outer segment junction (or IS/OS) as a prognostic factor for the postoperative visual acuity after one and six months. [88] The misuse of the term inner segment / outer segment junction is actually still widely prevalent today. It most probably originated in a confusion of the histologic correlate in a work by one of the pioneers of the field of optical coherence tomography. In his early works on ultra-high resolution OCT Prof. Drexler used inverted OCT images, that is highly reflective structures appeared dark and vice versa; in such images the ellipsoid zone (as the inner outer segment junction is now called) appears as a relatively prominent dark band in the outer retina. If the histologic correlate would have been the transition form the inner to the outer photoreceptor segments this band would, much less reflection at this band should be encountered.

There are two good reasons why the transition form the outer to inner segments should be hyporeflective on OCT. First, the transition from the photoreceptor segments is much more fuzzy which would unlikely result in such high reflectivity, and second the light reflected at this boundary calculated via the Fresnel equation would be exceedingly low, given the optical properties of the inner and outer segments measured so far are even approximately correct. [85]

1.4.2.1.1 Physiologic and pathophysiologic aspects of the outer retina

From a pathophysiological point of view, the correlation between visual acuity and the outer most retinal bands on the OCT seems reasonable. The outer segments of the photoreceptors are the area where the photo transduction takes place. Thus, most metabolic activity is confined in this area. This requires amongst others an ample supply of nutrients and also an effective mechanism of metabolic waste removal. Such waste accumulates in many ways.

One is the production of metabolic water during the burning of glucose on which the retina relies heavily. As expected the water accumulation is the most in areas of high turnover, which in our case certainly is the macula area and in particular the fovea. This metabolic water adds up to the water that is driven into the retina via

the steady flow from the anterior segment of the eye where aqueous humor is continually produced [89]. Besides water the conversion of glucose into adenosine triphosphate (ATP) not only results also in lactate, which in turn lowers the pH of the tissue. This water and lactate is transported into the subretinal space (that is between the tips of the photoreceptors and the retinal pigment epithelium). [90] Here it must not stay. Like in the rest of the human body, a correct retinal cell function is highly dependent on relatively stable pH values and further an accumulation of water between the retina and the retinal pigment epithelium leads to a loss of the vital nutrient supply for the outer most retinal tissues, which do not receive nutrition from the retinal vasculature.

This is where the retinal pigment epithelium jumps in. The retinal pigment epithelium is a cellular monolayer between the retina and the choroid. Its tight junction in between the cells makes it a barrier for uncontrolled substance diffusion from one side to the other, as such it is the outer blood-retina barrier. The retinal pigment epithelium is not only responsible for the absorption of light, but it serves as a hub between the highly vascularized choroid and the photoreceptors. It is of outmost importance to regulate the retinal pH concentration and elegantly combines this with one of its methods to remove water from the subretinal space at the same time. A plethora of ion channels on both the apical and the basal side of the retinal pigment epithelium actively transport ions from on side to the other and with it pump the water from the subretinal space to the choroid at a rate between 1.4 to 11.0 µL per cm^2. [91,92] Most water is transported via an ATP dependent chloride pump. In addition to that to regulate the pH drop after lactate production, a chloride anion/Bicarbonate exchanger on the basolateral side of the retinal pigment epithelium comes into play. It removes chloride form the retinal pigment epithelial cell to choroid in exchange for bicarbonate which serves as a buffer. [93] [94] This mechanism is exploited for example when azetazolamide (Diamox®) is used to treat cystoid macular edema. Azetazolamide blocks the carboanhydrase, an enzyme that catalyzes the transformation from water and carbon dioxide into bicarbonate and protons. As such it effectively lowers the pH within the retina and the aforementioned mechanisms are triggered. [95] [96]

Another waste product of the visual cycle are the used up discs of the photoreceptors. The outer segments of photoreceptors consist of multiple discs that evolve from membrane outpunchings of the photoreceptor's cell membrane. In the wall of these discs both cones and rods contain their opsin molecules that hold the vitamin A derivate (11-cis retinal). A configuration change in this molecule initiated by a photon hitting it results in the photo-transduction cascade. Subsequently the retinal which is now in its all-trans state needs to be recycled to its 11-cis configuration. [97] This happens in the retinal pigment epithelium. For that purpose each photoreceptor in a circadian fashion sheds its disks, which get subsequently phagocytized by the retinal pigment epithelium. For this to happen a close anatomical relationship between the tips of the photoreceptors and the retinal pigment epithelium is crucial. [98] As mentioned before (see outer retinal anatomy) the retinal pigment epithelium actually produces processes that enclose the photoreceptor tips to guarantee a rapid and efficient removal of disks. [85]

Diseases that impair this relationship and where the photoreceptors are still viable lead to an accumulation of disks within the subretinal space. [99] One prime example of this is central serous chorioretinopathy. In this disease a hyperperfusion of the choroid can lead to leakage of fluid through breaks in the retinal pigment epithelium into the subretinal space. The resulting mechanical disruption of the photoreceptors form the retinal pigment epithelium leads to an outer retinal accumulation of the disks that were originally supposed to be phagocytized. When the subretinal fluid subsides these accumulated disks crunch together in small heaps which can be observed funduscopically as yellow dots. [100] [101] Consequently yellow dots on the fundus of a patient with central serous retinopathy are a sign of improvement. Figure 16 and 17 show OCT examples of central serous chorioretinopathy with an accumulation of unphagocytized shed outer segment disks on the outer retinal surface.

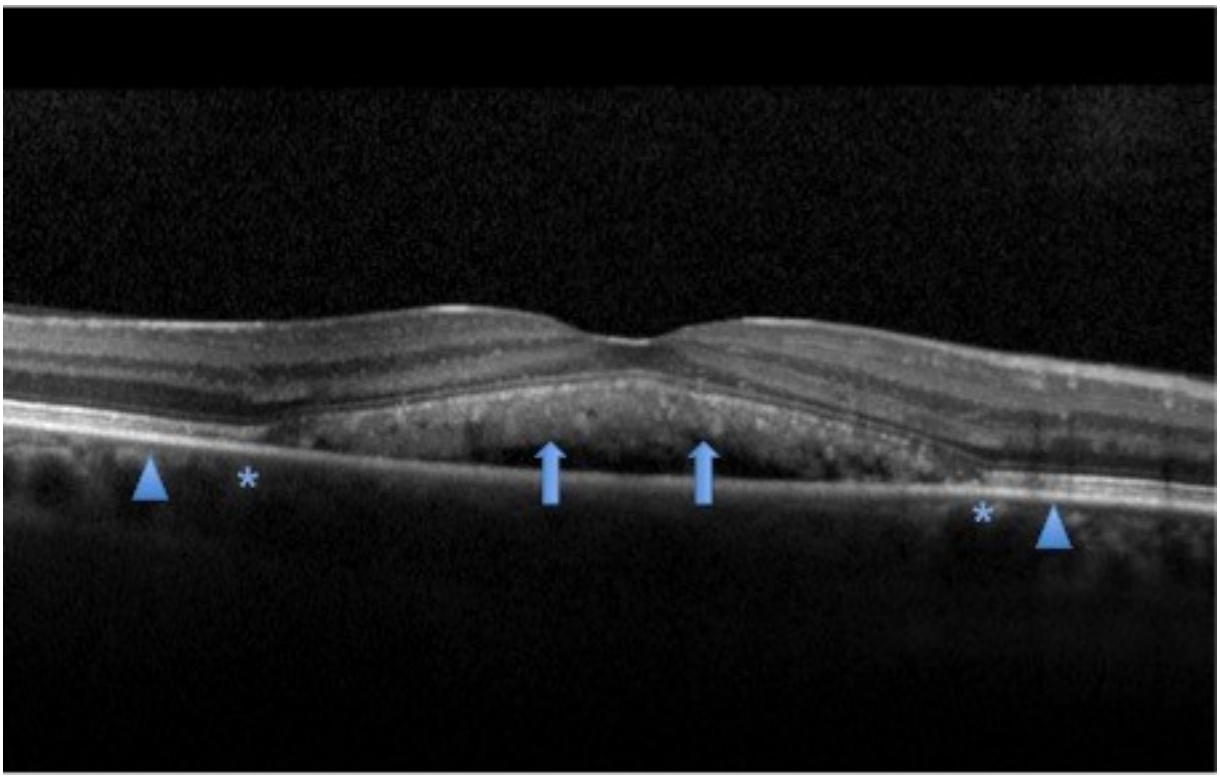

Figure 16. Optical coherence tomography in a patient with acute central serous chorioretinopathy. Because of the special separation of the retinal pigment epithelium and the photoreceptors in this eye, the photoreceptor disk cannot be phagocytized and accumulate on the outer surface of the retina. This reflects in an inhomogeneous mildly hyperreflective debris on OCT (arrows). On both the nasal (right side of the page) and temporal side of the OCT the elevation of the retina from the retinal pigment epithelium is apparently preceded by a loss of the interdigitation zone (the second relatively thin hyperreflective band from the bottom up). Only further inwards at the beginning of the elevation can a disruption of the ellipsoid zone be seen (asterisk). However, the ellipsoid zone does not vanish completely which corresponds to a preservation of the photoreceptors mitochondria. As such good vision is maintained (0.8 in this case).

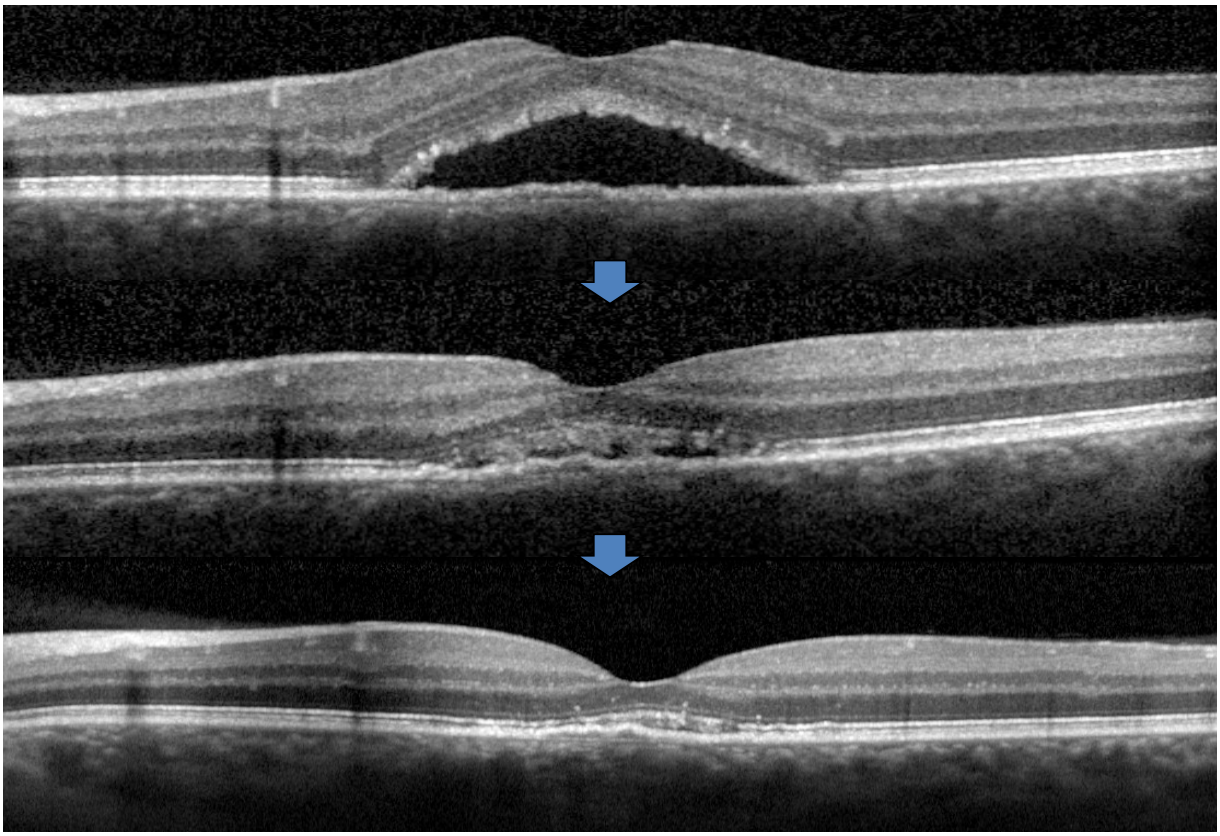

Figure 17. The spontaneous evolution of a patient with central serous chorioretinopathy. In the topmost optical coherence tomography (OCT) image the elevation of the neurosensory retina from the retinal pigment epithelium (RPE) is reflected by the dark triangle shaped area in the center of the scan. On the outer side of the retina a thin layer of granular hyperreflective material representing the shed photoreceptor disks has already accumulated. In time course of the disease the fluid underneath the neuroretina subsides and this debris is again approximated towards the RPE (middle OCT scan), where it eventually is removed via phagocytosis. Still some damage to the photoreceptors might remain. The morphological equivalent being in this case the speckled appearance of the ellipsoid zone in the fovea.

While delayed phagocytosis without a residual pathology is possible, problems may arise. The delay in outer segment disk with its containing retinal break down leads to

a prolonged exposure to oxidative processes. These cause chemical and structural changes in the many components of the photoreceptors and lead to an increase in a waste product called lipofuscin. Lipofuscin is a substance composed of multiple components which often bypass the normal digestion process of the retinal metabolism. As such it is also found in healthy aging eyes in increasing concentration.

One prominent component of lipofuscin is the fluorophore N-retinylidene-N-retinylethanolamine (A2E). [102] While the role of A2E in the retinal autofluorescence is still unresolved, it has important pathogenic capabilities in a plethora of diseases such as age related macular degeneration, Stargardt's disease, and Best's disease.[103] [104] [105] A2E is formed within the retinal pigmentepithlium via cleavage of the phosphatidyl group from N-retinylidene-phosphatidylethanolamine (A2PE). The latter forms most likely in photoreceptor disks through oxidative processes, which occur more frequently if a fast removal of the all trans retinal is impaired. This might be while the disks are still attached on the photoreceptor or when the disks are waiting for phagocytosis in the subretinal space. Figure 18 shows a schematic drawing of this process.

In Stargardt's disease such an impaired removal of the retinal molecule is caused by one of two ways: first and most commonly, a defect in the gene coding for a transmembrane protein called the ATP-binding cassette transporter (ABCA4). This transporter moves the all trans retinal form one side of the disk membrane to the other; second, a defect in the gene (ELOVL4) that encodes for an enzyme that is responsible for the production of very long chain fatty acids. These very long chain fatty acids make up an integral part of the photoreceptors membrane, which have the highest concentration of such long fatty acids in the human body. Here they are responsible for the fluidity of the membrane, which is important for a smooth transport of A2E from one membrane side to the other.

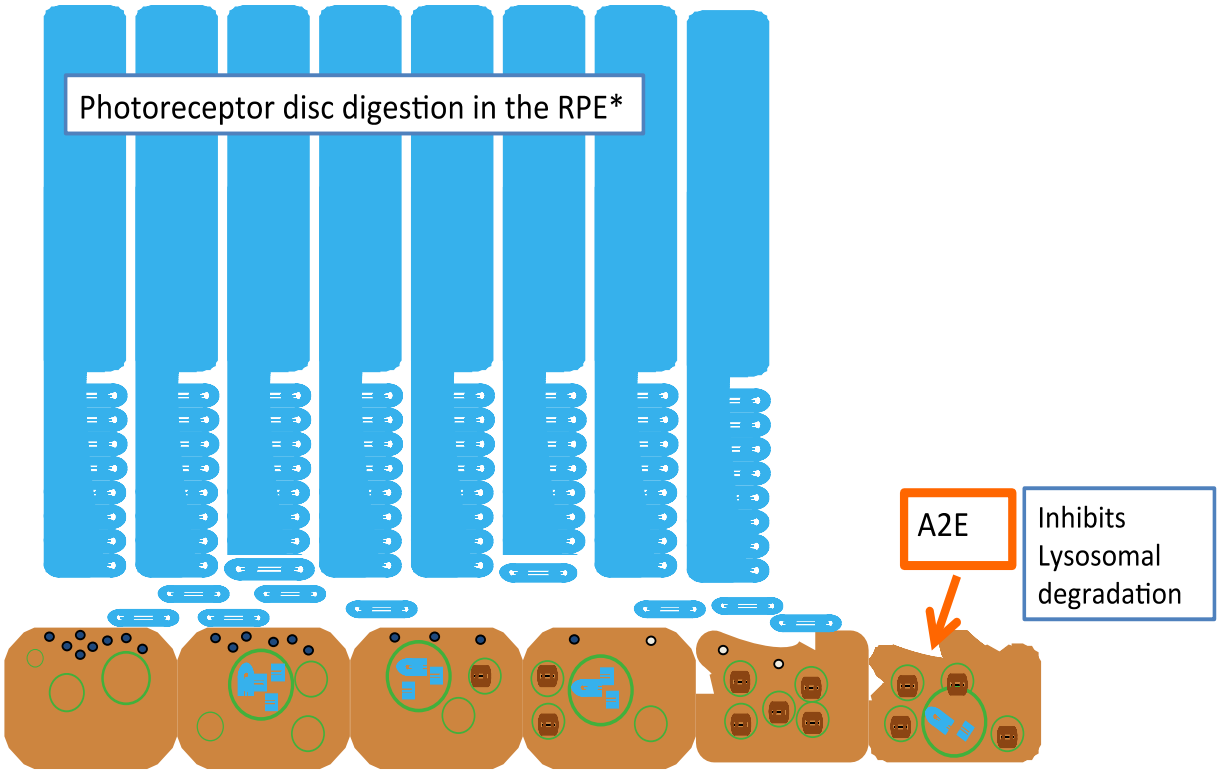

Figure 18. Schematic of the phagocytosis process of the shed photoreceptor disks. Each photoreceptor (blue) renews its complete outer segment within about 3 days by shedding small disks that get phagocytized by the retinal pigment epithelium (brown cells at the bottom of the image; * …. RPE) Within these cells lysosomes (green bubbles) degrade the disks in order to subsequently recover amongst others the contained retinal molecule. However some portion of the retinal might already by oxidized to a less degradable form called N-retinylidene-N-retinylethanolamine (A2E). Over time this A2E accumulates within the RPE cells where it impairs the cells metabolism, leads to a degradation of the apical melanin (black dots in the graphic), and ultimately kills the RPE cell.

A similar mechanism of action, that is an impaired retina to retinal pigment epithelial interface might be true for ERMs. The superficial traction on the inner retina leads to an ever so slight disconnection between the photoreceptor outer segment tips and

the retinal pigment epithelial processes (which was termed the cone outer segment tip line in Shimozono et al [88]). A continuous disruption in this area might first lead to an accumulation of subretinal material, as can be observed form a clinical perspective relatively frequently in patients with ERMs. Persistence of such material for a short time period might be well tolerated, however, a longer persistence might lead to cell damage in the form of RPE loss or photoreceptor damage like loss of the tightly packed mitochondria in the cell. The later corresponds in many diseases to a loss of the ellipsoid zone on the OCT (which was termed the inner segment/ outer segment line in Shimozonos paper [88]). It might be the case that a loss of the mitochondria leads to a not fully recoverable loss of function in the photoreceptors, but other data suggest that a thinner ellipsoid zone, but not the absence thereof, might even indicate more potential for improvement after an ERM peeling. [106]

These factors are not necessarily mutually exclusive. A thinning of the photoreceptor's mitochondrial layer might indicate a state of distress which presumably is alleviated by the ERM peeling. Cells under a higher distress might profit more from a surgery than those in less distress or those where permanent damage (such as a loss of the mitochondria) has already occurred. In accordance with this presumption the authors of the aforementioned study also found that albeit the preoperative visual acuity correlated positively with the postoperative visual acuity, those patients with a worse initial vision improved more than those with a better initial vision. [106]

However, the exact implications of this presumed mechanism are not clear and further studies not least with fundus autofluorescence and volumetric instead of only two-dimensional measurements could prove valuable in this regard.

1.4.2.2 The Inner Retina

Besides the outer most part of the retina, they inner retina also plays a role in evaluating eyes that suffer from ERMs. Figure 19 shows a detailed description of the inner layers on OCT and their anatomical correlates.

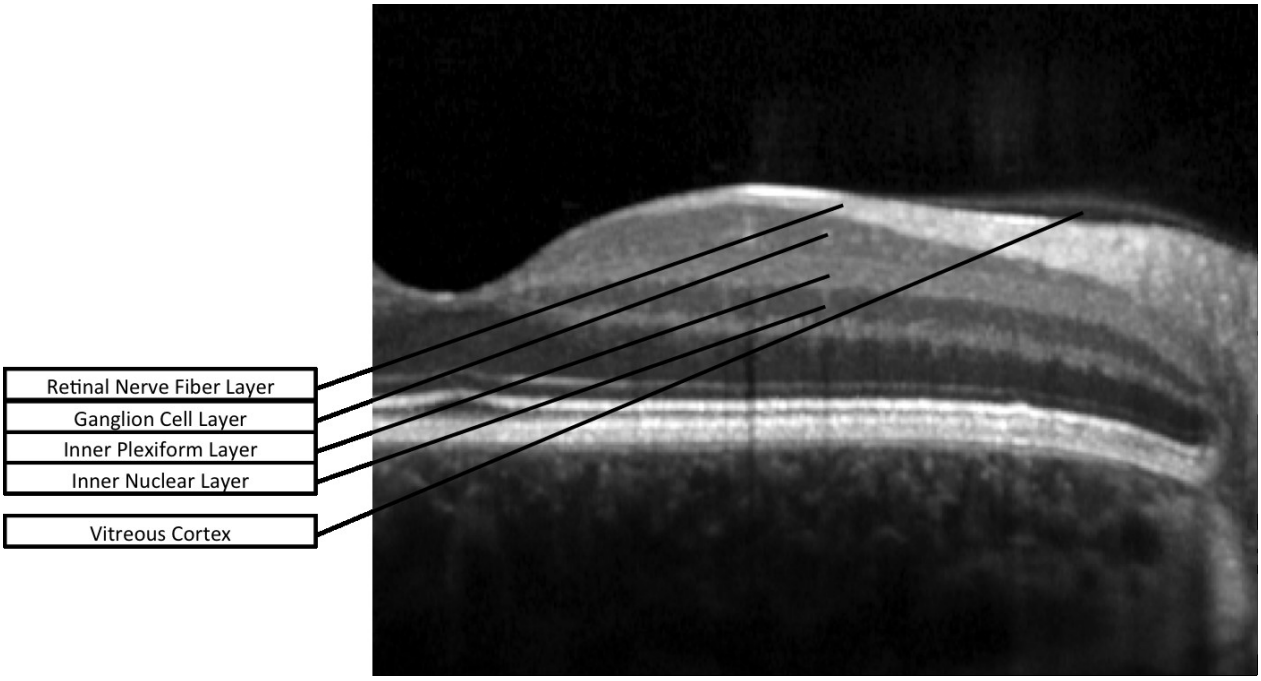

Figure 19. The normal retinal architecture on optical coherence tomography: A detailed description of the layers that make up inner retina and the vitreoretinal interface. From the bottom to the top the cell bodies of the bipolar cells make up the inner nuclear layer. These cells receive their input mainly from the photoreceptors and to a minor extent from the horizontal network in the outer plexiform layer. The bipolar cells synapse with the third neuron the ganglion cell in the inner plexiform layer. These cells have their cell bodies in the ganglion cell layer from where the signal travels in the retinal nerve fibers via the retinal nerve fiber layer to the optic nerve. Sometimes, but not always, can the vitreal cortex be identified on the optical coherence tomogram. However, the absence of vitreous reflection does not always indicate a complete poster vitreous detachment. Note that the inner limiting membrane can not be identified on the image.

Hwang and coworkers found in their work on the macular function in patients with unilateral idiopathic ERMs a significant correlation between the multifocal electroretinogram and the spectral domain optical coherence tomography image. [22] In

their study the patients were divided into two groups. Group 1 comprised patients where the ERM growing over the fovea and was additionally subdivided into group 1a where the outer retina was thickened, group 1b where the outer retina in the fovea was more tented, and group 1c where the inner retina was thickened. Group 2 comprised patients where the fovea was spared. This group did also involve cases with a macular pseudo hole or a macular lamellar hole. (Figure 20, shows exemplary cases of our own patients with the categorizing features used by Hwang et al) The unaffected fellow eyes served as a control.

They included 71 patients and as expected compared to the fellow eyes visual acuity was much worse in eyes with ERMs (BCVA, mean logMAR 0.33 ± 0.23 versus 0.07 ± 0.09) and the central retina was much thicker (453.6 ± 101.5 μm versus 249.9 ± 22.5 μm). This reflected in a lower amplitude in the multifocal electroretinogram. From all eyes those categorized as 1c (fovea involved and thickened inner retina) performed the worst regarding the visual acuity and regarding the multifocal retinography. Unsurprisingly macular pseudo holes showed near normal retinal function, however of note is that eyes with lamellar macular holes showed near normal electroretinograms too. [22] This supports the clinical approach of most experienced surgeons that lamellar macular holes are not necessarily an indication for prompt treatment.

Okamoto and coworkers found in their work on prognostic factors for metamorphopsia after ERM peeling that the inner nuclear layer thickness correlated with the metamorphopsia experienced by ERM patients before and also after their surgery. This remained true 3 and 6 month after the peeling and the authors attributed this effect to a change in the structure of the cells that make up the inner nuclear layer, namely the horizontal cells, the Mueller cells, the bipolar cells, and the amacrine cells.[107] The true mechanism behind this association remains yet to be fully understood.

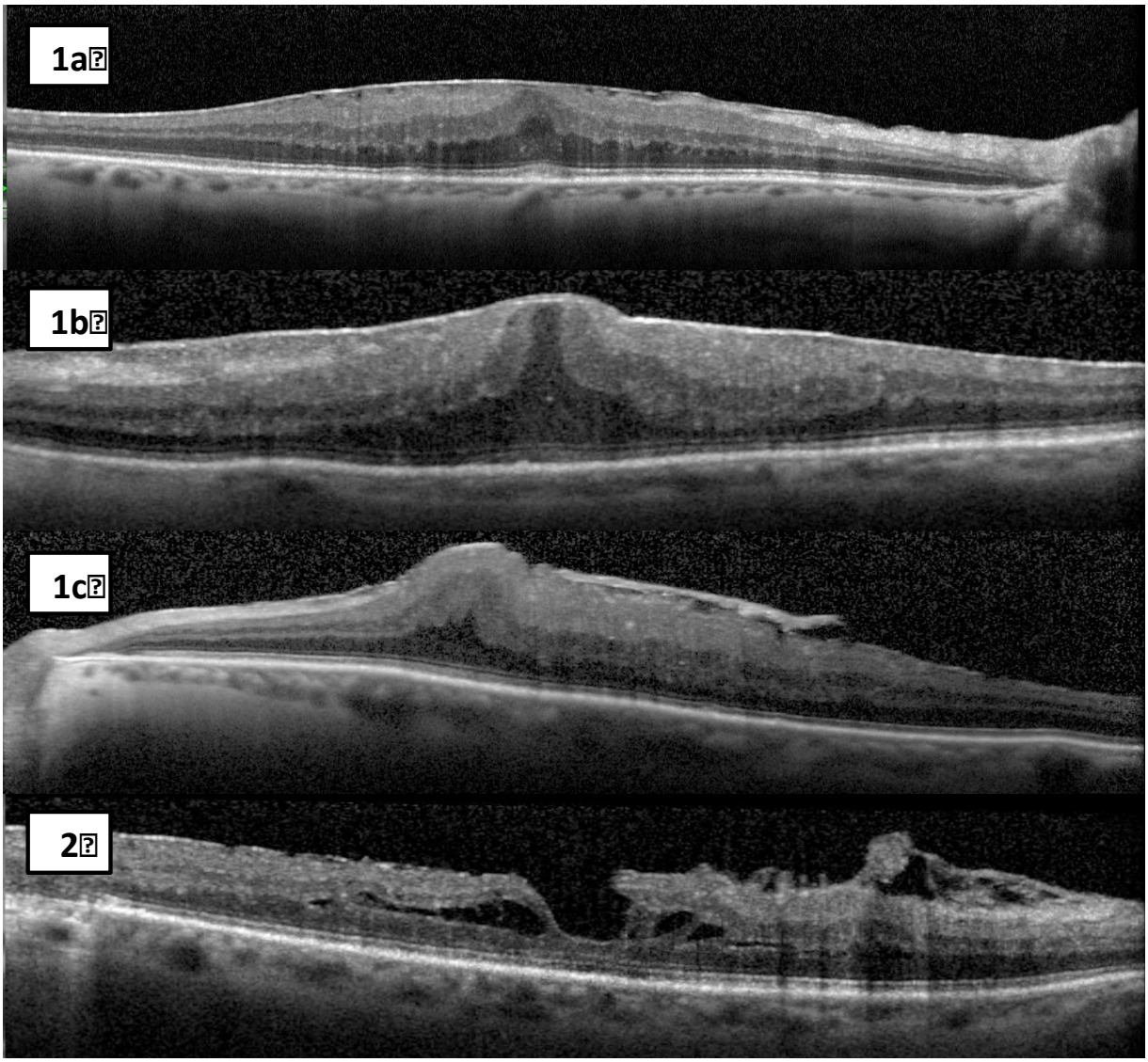

Figure 20. The ERM classification according to Hwang et al. Group 1 was with the ERM involving the fovea and was subsequently subdivided into (1a) with minor changes in the inner retina and some thickening of the outer retina, (1b) with significant tenting of the foveal area, (1c) with significant swelling of the inner retina. Group (2) comprised all patients where the ERM was not covering the fovea. This group did, however, include patients with lamellar holes.

Chung and colleagues found that the anisoconia usually presents as a macropsia in ERM patients and correlates with the thickness of the inner nuclear

layer as well as the thickness of the ganglion cell layer plus the inner plexiform layer on OCT. [11] These finding seem reasonable since concentric traction of the retinal tissue leads to movement of more peripherally interconnected photoreceptors to the center, where they get excited by light rays from objects which would usually have failed to extend into the more peripheral retinal areas. This makes objects appear larger the more contraction the ERM inflicts on the retina.

1.4.2.2.1 Physiologic and pathophysiologic aspects of the inner retina

Similar to the outer retina, it is hardly surprising that structural changes at the level of the inner retina inflict a significant change in vision to the patient. The inner retina is the connection hub of the retina. Here we have connections not only vertically from the photoreceptors over the bipolar cells to the ganglion cells, but we also find the horizontal network via the amacrine cells and the horizontal cells.

The bipolar cells stretch from the outer plexiform layer to the inner plexiform layer. The synapses of the photoreceptors with the bipolar cells are located in the outer plexiform layer. Here the visual signal is split up into two pathways, the ON pathway and the OFF pathway. While the former detects objects that appear brighter than the surroundings, the latter detects objects that appear darker than the surroundings. [108]

The messaging from the photoreceptors to the bipolar cells is actually not entirely straight forward. Besides having ON and OFF subtypes, there are specific bipolar cells for cones and rods, as well as different subtypes of bipolar cells according to the branching pattern of their connections. An especially interesting point is that the only effective neurotransmitter that photoreceptors have to communicate with the bipolar cell is glutamate. [109] Yet, instead of an unspecific activation of the bipolar cell network, this single neurotransmitter evokes specific reactions in only the bipolar cells intended. The modus operandi is via highly specialized glutamate receptors on the bipolar cells themselves. [110-112] [113] As such, instead of only transmitting the signal from the photoreceptors the bipolar neuronal network is an

integral part of the signal processing already at the initial synapses with the photoreceptors. [108]

Still, the signal processing of the bipolar cells is additionally enhanced farther downstream at the level of the inner plexiform layer. Here the bipolar cells synapse with the ganglion cells and the amacrine cells. The amacrine cells are part of the horizontal neuronal network in the retina and connect to other amacrine cells, ganglion cells, other bipolar cells, and sometimes even back to the bipolar cell where it originally got the signal from. Amongst the possible functions of the amacrine cells is a speeding up of the signal organization. [114] [115] Figure 21 shows a schematic drawing of the intricate signaling pathways in the inner plexiform layer.

In the inner plexiform layer the signal ultimately gets passed on to the ganglion cells. These cells are often slightly larger than the preceding neurons and have thicker axons for an onward transmission at a higher speed. Similar to all the other neurons, Ganglion cells are also highly specialized and different types according to there morphology have been identified (alpha, beta, gamma, delta). [116,117] The branching of the alpha and beta ganglion cells increases with eccentricity of their location. That means the farther one moves to the peripheral retina the larger the area that is served by one single ganglion cell. This effectively reduces the resolution with eccentricity. [109,118] The axons of the ganglion cells (around 1.2 million per eye) converge at the optic disc to form the optic nerve. [119]

In addition to the neuronal wiring, we find structural cells, the microglia, in the retina, namely the Mueller cells. They intermingle in between the neuronal network and not only do they provide structural support for the retina, but they are also heavily involved in transducing the retinal signal and in metabolic homeostasis of the retina.

The Mueller cells stretch from the inner limiting membrane, which is made up by their feet and probably some collagen secretion, to the external limiting membrane. The Mueller cell bodies are located in the inner nuclear layer. From a structural point of view, these cells have multiple connections with each other (especially at both limiting membranes) and with the cells and structures around them, like the photoreceptors and the retinal vasculature. After trauma such as retinal detachment, the Mueller cells probably play an important role in the retinal

remodeling , which is indicated by a significant upregulation of type III intermediary filaments such as vimentin and glial fibrillary acidic protein after the induction of a retinal detachment. [120] [108]

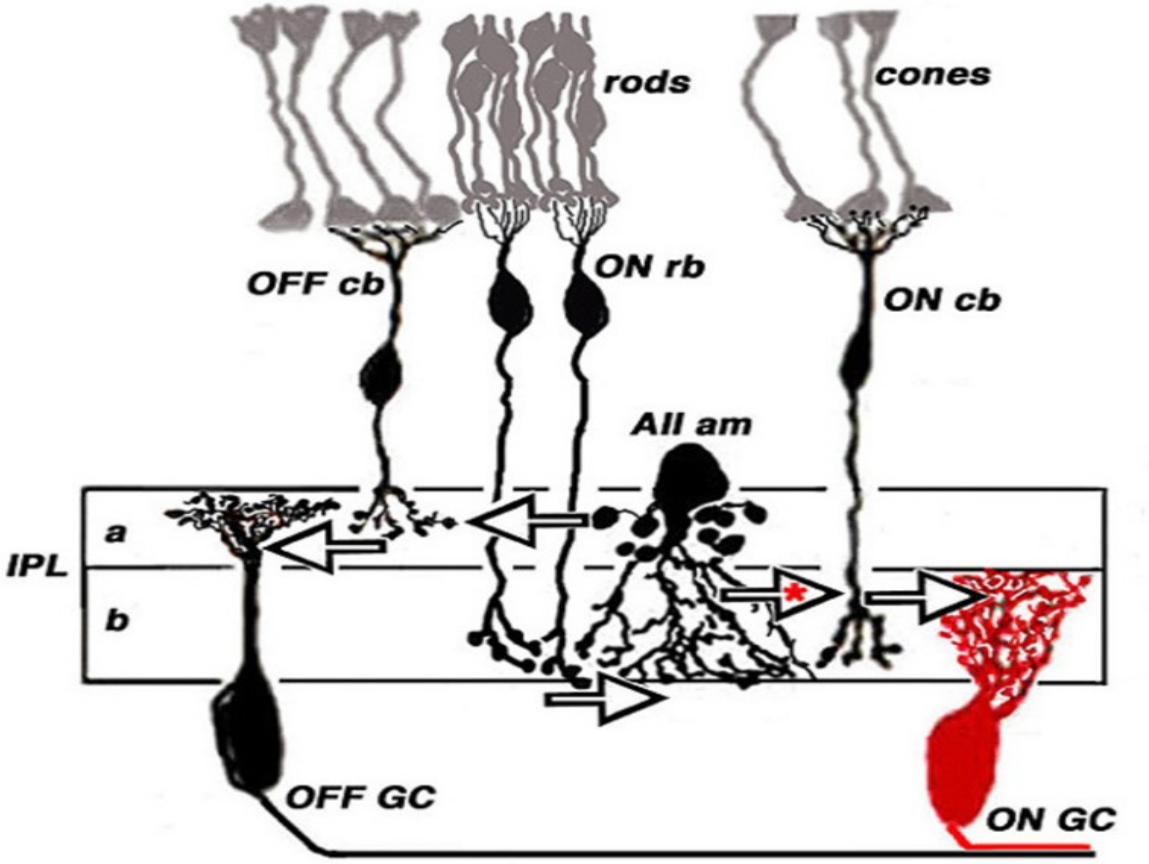

Figure 21. The signaling pathways in the inner plexiform layer (from http://webvision.med.utah.edu/). In the inner plexiform layer (IPL) both the ON and OFF bipolar cells (cone bipolar cell … cb; rod bipolar cell … rb) synapse in the inner plexiform layer with their respective ganglion cells (GC) and amacrine cells (am). The synapses of off bipolar cells are located in the distal part of the pathway (zone a), where as the ON pathway synapses in the proximal b zone. The figure was generously provided under a non-commercial commons license by Nelson and Connaughton and originally adapted from Kolb et al. [108,121]

What is more is, that for the toxicity of tamponades used in a vitrectomy for a retinal detachment the Müller cell function has been implicated as potential explanation. As the Müller cells are responsible for much of the buffering of extracellular potassium in the retina. The potassium in the retina accumulates in an activity dependent manner and higher levels in the inner retina are found during light and higher levels in the subretinal space are observed during darkness. The latter is presumably a result of the photoreceptors dark current. [122] [123] [124] In case of excess extracellular potassium the Mueller cell virtually siphon the potassium in to the vitreous, which represent a large reservoir with ample space for secretion. However, if the vitreous cavity is occupied by a substance with less solubility of potassium, then this ion exchange can be severely impaired leading to a subsequent outer retinal degeneration. [125]

The essential role of the Mueller cells in regulating the retinal ion homoeostasis is also reflected in the fact that it is widely believed that they contribute the mayor part of the b-wave in the electroretinogram. Where a massive depolarization of the Müller cells seems to be triggered by the bipolar cell activity. [126] [127]

As discussed earlier in the chapters for ERM peeling surgery, the adjunct peeling of the ILM, that is the interior endfeet of the Müller cells, is currently the desired approach. In conjunction with the aforementioned important role of the Mueller cells on the retinal metabolism, it begs the question how the ILM peeling might effect parameters such as potassium siphoning. In this regard much additional research is to be conducted.

1.4.2.3 Optical coherence tomography and epiretinal membranes: Conclusions

In summary, the morphology of ERMs is currently best elucidated with OCT. The morphology of ERMs as imaged with OCT correlates with the symptoms of the patients and the outcome of the surgery. In terms of the surgery itself the surgeon

strives for peeling of the ERM as well as the ILM, which is facilitated by the use of intraoperative staining agents, which, however, are in the suspicion of causing to a varying degree retinotoxic damage. As such a preoperative non invasive OCT marker for facilitating the peeling process might alleviate some strain from ERM patients. The aim of the following study was to address this problem.

The following section is being reproduced in large parts identically from the publication of Seidel G. and coworkers “Association of preoperative optical coherence tomography markers with residual inner limiting membrane in epiretinal membrane peeling“ with explicit permission of the respective journal (PLOSone) [128]. In most cases additional graphs have been added, which were omitted in the published manuscript due to journal restrictions. Also some further analysis regarding the postoperative functional and morphological outcomes has been performed. This was omitted from the original manuscript for the sake of brevity and due to some limitations regarding the study design for these parameters. These limitations are discussed in detail in the respective sections. The work constitutes the original work of the author (Seidel G.).

1.5 Association of preoperative optical coherence tomography markers with residual inner limiting membrane in epiretinal membrane peeling

Gerald Seidel, MD[1] Martin Weger, MD[1] Lisa Stadlmüller,[2] Tamara Pichler,[1] Anton Haas, MD[1]

[1] Department of Ophthalmology, Medical University of Graz, Graz/Austria

[2] Institute for Medical Informatics, Statistics and Documentation, Medical University of Graz, Graz/Austria

1.5.1 Abstract

Purpose: To identify preoperative markers on spectral domain optical coherence tomography (SD-OCT) for residual inner limiting membrane (ILM) in epiretinal membrane (ERM) peeling.

Methods: In this retrospective case series the preoperative SD-OCTs from 119 eyes of 119 consecutive patients who underwent surgery for idiopathic ERM by a single surgeon were evaluated for markers predisposing for ILM persistence after ERM

removal. ILM persistence was determined via intraoperative indocyanine green staining. The main outcome measures were correlation of central foveal thickness (CFT), ERM thickness, extent of elevated ERM and retinal folding, intraretinal cysts, and discontinuation of the ERM, with ILM persistence after ERM peeling.
Results: The persistence of the ILM was found in 50.4% (n = 60). After Bonferroni correction for multiple testing, a greater extent of elevated ERM and thicker ERMs were associated with persistence of the ILM ($p < 0.005$). The other parameters showed no statistically significant correlations with the persistence of the ILM ($p \geq 0.005$).
Conclusion: Residual ILM can be found in nearly half of the eyes after ERM peeling. A loose connection between the ERM and the retinal surface predisposes for ILM persistence. Preoperative SD-OCT is helpful in identifying risk markers for the persistence of the ILM in ERM surgery.

1.5.2 Introduction

Epiretinal membranes (ERMs) are avascular tissue sheets that grow on the retinal surface. They consist to varying degrees of glial cells, hyalocytes, fibroblast-like cells, and retinal pigment epithelial cells.[2, 3] ERMs can contract, causing disturbance of the retinal architecture, which may subsequently lead to metamorphopsia and decreased central visual acuity.

The inner limiting membrane (ILM) serves as a scaffold for ERM growth and it has been shown that after removal of only the ERM, glial cells, hyalocytes, and myofibroblasts remain on the ILM.[129] This is thought to be a major factor for ERM recurrences. Recurrence rates of up to 56% have been reported in patients with the ILM left on the retina compared to 9% after additional ILM removal.[33, 34, 35, 36] Thus, when treating ERMs via membrane peeling adjunct removal of the ILM has been advocated.

The ILM, however, remains on the retina in between 50.8 to 64% of cases after ERM peeling.[129, 130] In these cases a second peeling process to remove the ILM

is needed. This study demonstrates predisposing markers on preoperative high-resolution spectral domain optical coherence tomography (SD-OCT) for the persistence of the ILM after ERM removal.

1.5.3 Methods

A retrospective chart evaluation of all patients undergoing ERM peeling at the Medical University of Graz from August 2010 to November 2011 was performed. Exclusion criteria were any previous ocular surgery other than phacoemulsification, a history of uveitis, diabetic retinopathy or maculopathy, macular hole, myopia of more than 6 diopters, lamellar hole, age-related macular degeneration, and history of ocular trauma. One hundred twenty one eyes from 119 consecutive patients with idiopathic ERM met these criteria. From two patients who underwent surgery on both eyes only the first eyes were included, leading to 119 eyes overall. The mean age was 72 ± 8 years, 53% (n = 63) were women, and mean best-corrected visual acuity was logMAR 0.5 ± 0.24 (decimal equivalent of 0.32 median). The study was conducted according to the declaration of Helsinki and was approved by the ethics committee of the Medical University of Graz. All data were collected as part of routine diagnostics and treatment. All patients were diagnosed and treated according to national guidelines and agreements. Data analysis was performed anonymously and in a retrospective fashion. The authors state that individual patient consent was not obtained and hereby confirm that the ethics committee of the Medical University of Graz agreed that individual patient consent was not needed for this study.

All patients underwent 3-port 23-gauge vitrectomy (OS3; Oertli, Berneck, Switzerland) with intraoperative indocyanine green (ICG) staining of the ILM (0.2% solution; ICG-Pulsion, Pulsion Medical Systems AG, Munich, Germany) before and after ERM removal. A single experienced surgeon (A.H.) conducted the surgery in all patients to ensure reproducibility. To maximize the rate of combined removal of the ILM and ERM the peeling was initiated by grasping the stained ILM at the border of the ERM. After primary peeling the macula area was stained a second time with ICG to visualize residual ILM. Any persistence of ILM in the previously peeled area was

defined as residual ILM and peeled in a second step. These cases were termed separate peeling cases, in contrast to combined peeling in case of simultaneous removal of the ERM and ILM. To minimize the potential retinotoxic effect of ICG meticulous attention towards iso-osmolality and minimization of the duration as well as the area of exposure was paid.[131,132] Thus, the dye was washed out immediately after its application on the retina in a fluid filled eye.

SD-OCTs via the 5 line mode of the Cirrus 4000 OCT (Carl Zeiss Meditec, Inc.) were obtained one day before surgery and 7 parameters were assessed: central foveal thickness (CFT), ERM thickness (ERM-Th), ERM elevation, retinal folding, discontinuation of the ERM, and intraretinal cysts. Because of potential erroneous detection by the OCT's integrated algorithms, all parameter were assessed manually by means of the device's inbuilt caliper tool. One technician took all OCTs and two retina specialist performed the parameter assessment. The OCT investigators were not involved in the surgery and blinded regarding intraoperative ILM persistence after ERM peeling.

All data were obtained from the horizontal 6 mm OCT section centered at the fovea. ERM-Th was defined as the thickest part of the ERM within these bounds. Measurement was taken after appropriate zooming. Any non reflective space between the ERM and ILM was defined as ERM elevation. All segments within one scan depicting this feature were added up, consequently leading to a potential distance range from 0 to 6mm. Retinal folds were assessed in a similar fashion. Any interruption in the ERM was defined as discontinuation of the ERM. Any cystoid space in the retina was counted positive for retinal cysts. Figure 1 shows two examples of OCTs depicting dissimilar characteristics and figure XX A-E show an example measurement for each of the seven parameters.

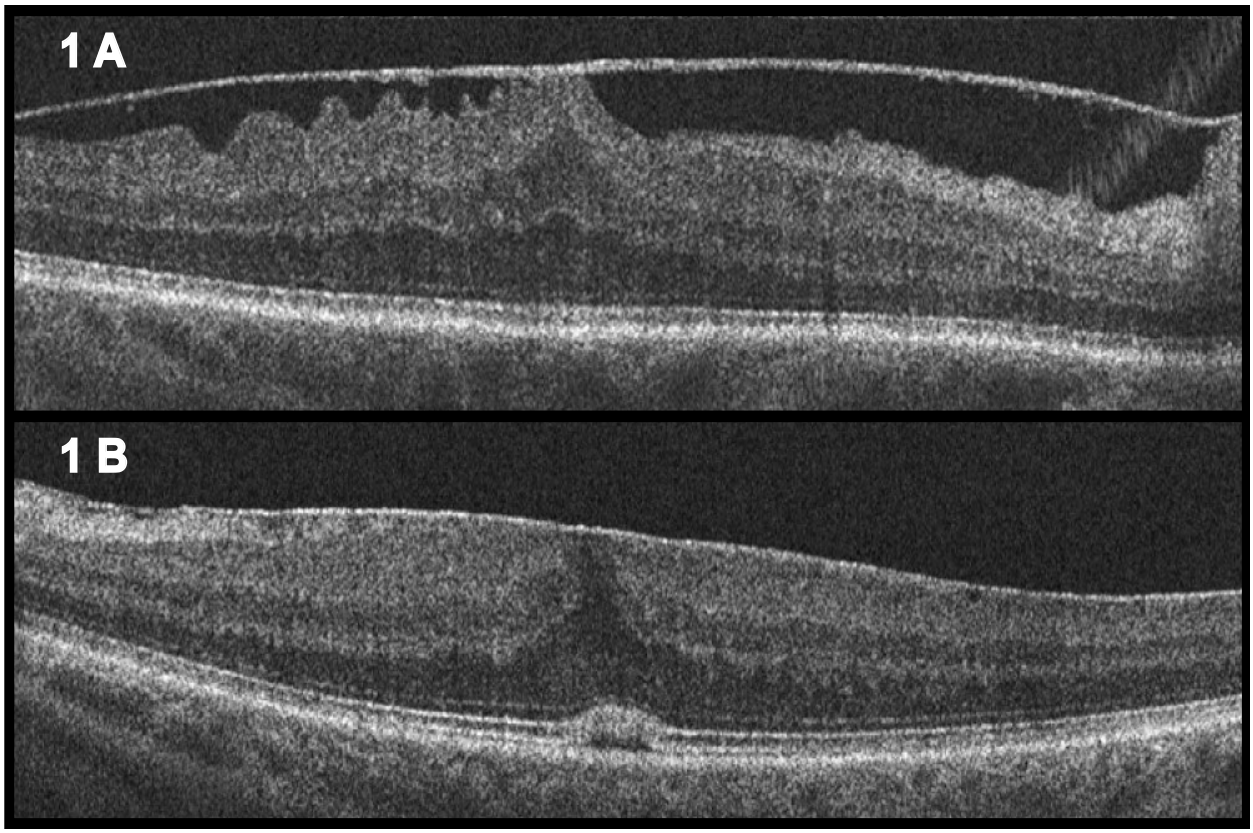

Figure 1. Optical coherence tomography of two eyes with dissimilar characteristics of the epiretinal membrane (ERM):

A shows an almost complete elevation of the ERM and some retinal folds in the temporal segment; 1B shows a diffusely adherent ERM to the retinal surface without elevation and minimal nasal folding;

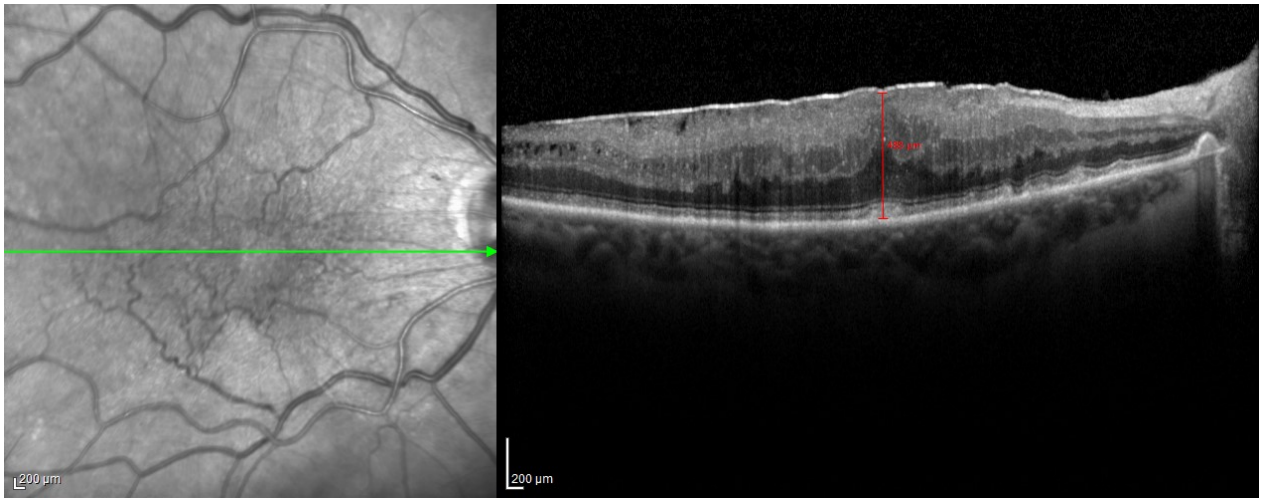

Figure 22. Central foveal thickness measuremnt. The distance form the apex of the retinal pigmenteithelium to inner most surface of the retina including the epiretinal membrane was defined as central foveal thickness. For the measurement the 1 to 1 µm mode was used and the respective measurement line (red) was drawn perpendicular to the retinal pigment epithelium.

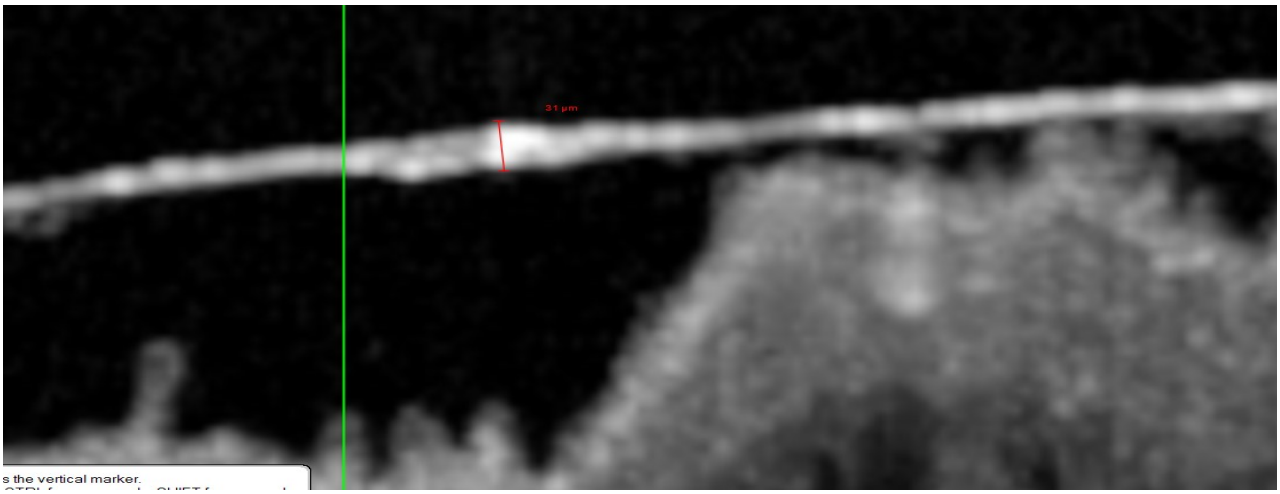

Figure 23. Epiretinal membrane thickness. The Thickness of the epiretinal membrane was determined by the devices inbuilt software under high magnification of the optical coherence tomogram. The thickest component of the membrane was measured as indicated by the red line.

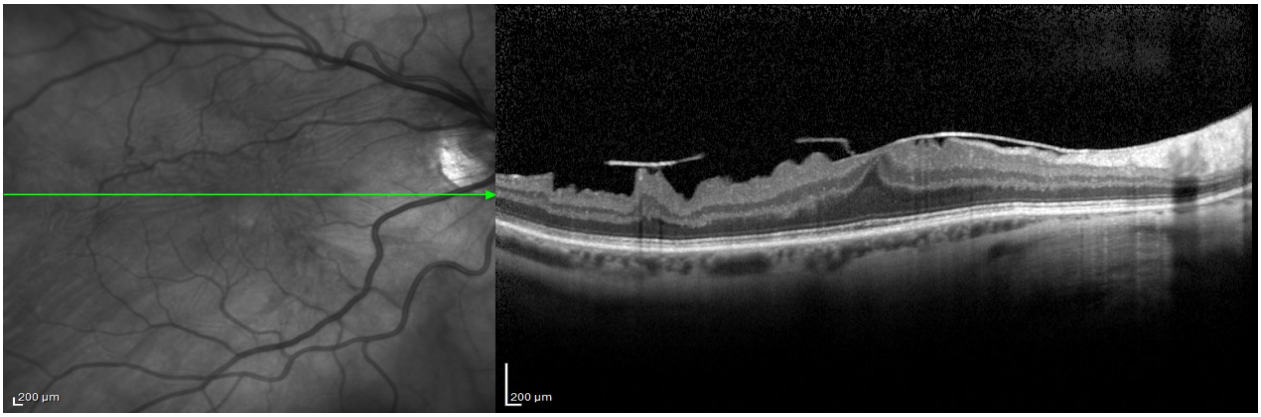

Figure 24. Discontinuation of the epiretinal membrane. The total of all discontinuation over the measured scan was measured.

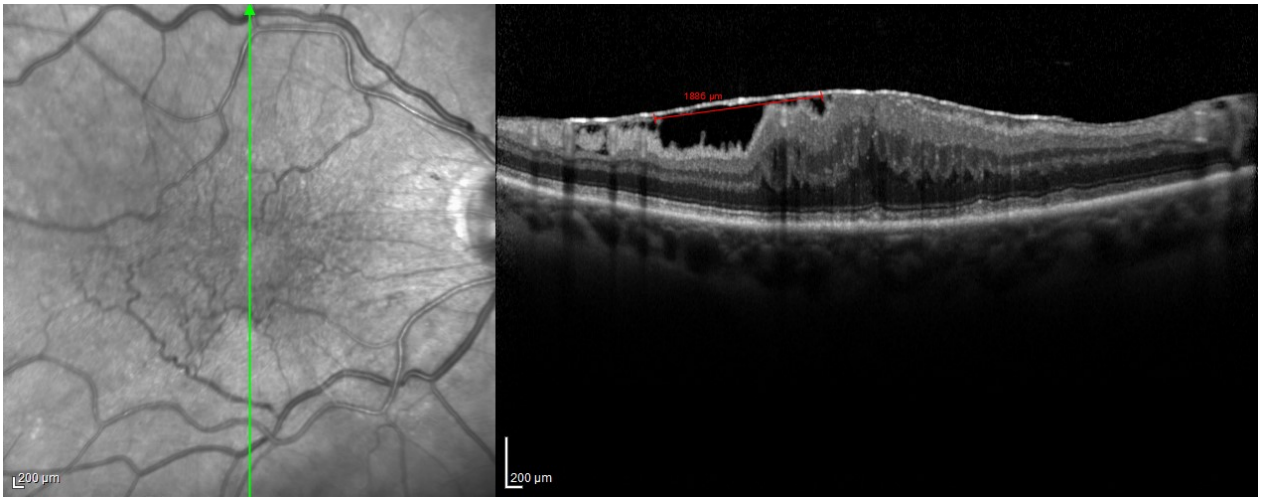

Figure 25. The extend of the elevated epiretinal membrane was measured by means of the device's inbuilt software. The total extend (red line) over the entire scan was added up for the total distance of retinal folding in the scan.

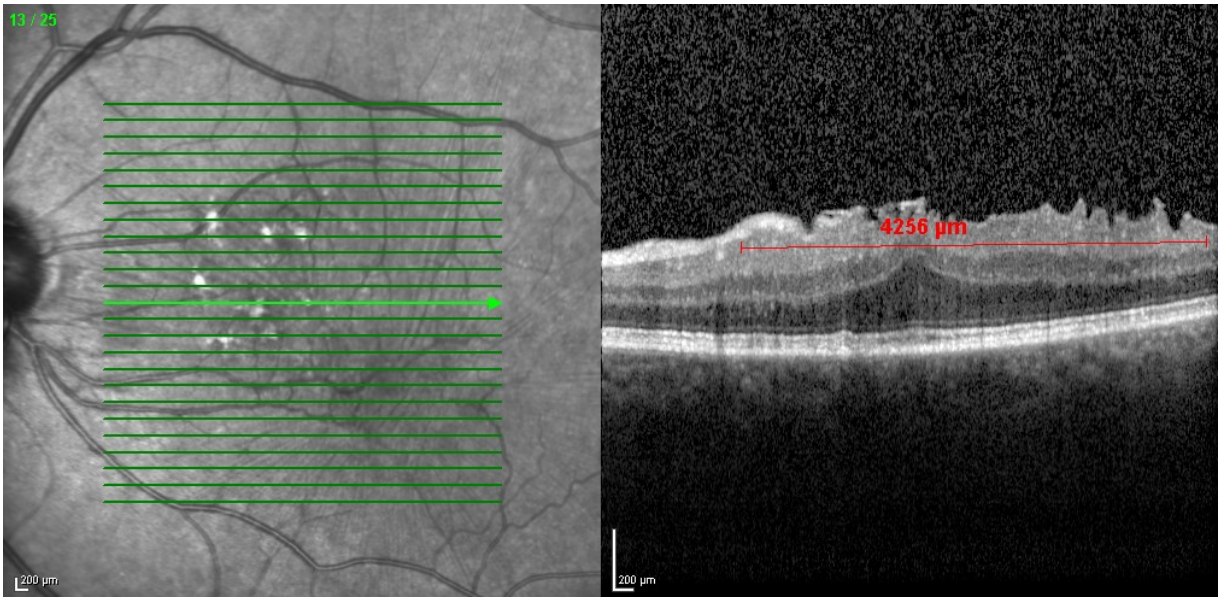

Figure 26. The extend of retinal folding was measured by means of the device's inbuilt software. The total extend (red line) over the entire scan was added up for the total distance of retinal folding in the scan.

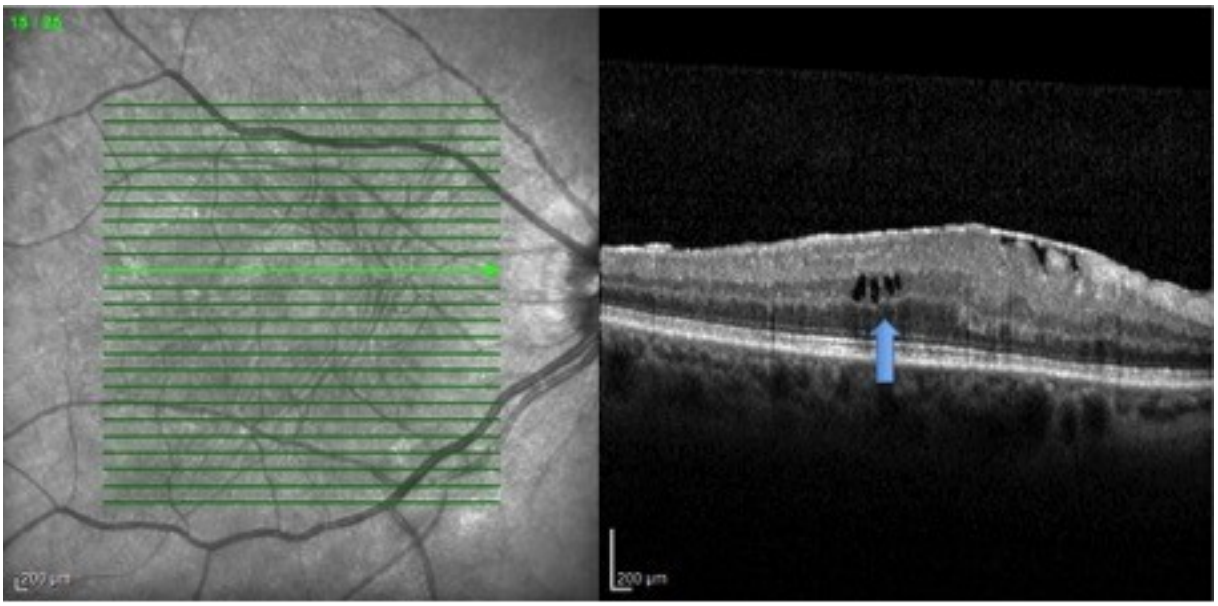

Figure 27. Intraretina cystoid spaces. Any presence of the characteristic hyporeflective round spaces within the retinal alyers, but not between the ERM

and the retina were regarded as intraretinal cystoid spaces and subsequently categorized as positive for intraretinal cysts.

With respect to normal distribution, we used the unpaired t-test or the Mann-Whitney-U test to compare continuous variables. To test categorical variables we used the exact Fisher test and the Pearson chi-quadrat test. Bonferroni correction was used to adjust for multiple testing. Subsequently, a p-value of < 0.005 was considered statistically significant. Analysis was performed with SPSS (Version 20.0 for Windows, SPSS, Inc., Chicago, IL).

1.5.4 Results

The mean age was 72.6 ± 8.4 years and 53% were women. The mean BCVA was 0.5 ± 0.21 logMAR (decimal median 0.32). All 119 eyes underwent uncomplicated ERM peeling. Repeating the ICG staining after complete ERM removal showed persistence of the ILM in 60 out of 119 eyes (50.4%).

To detect predictive factors for combined or separate removal of the ERM and ILM we tested for the following parameters: age, sex, preoperative BCVA, lens status, intraoperative vitreoretinal status, CFT, ERM-Th, ERM elevation, retinal folding, discontinuation of the ERM, and intraretinal cysts.

Sex, age and preoperative BCVA were not correlated with ILM persistence (p > 0.005; data not shown). Out of the 99 phakic patients included into the study 95 had concomitant phacoemulsification and intraocular lens implantation. The status of the lens did not affect ILM peeling (p = 0.626). The vitreous presented intraoperatively detached in 79.8% (n = 95), incompletely detached in 3.3% (n = 4), and completely attached in 16.8% (n = 20) of the cases. The vitreal status did not differ between the combined and the separate peeling group (p = 0.81).

On OCT the mean distance of retinal folding was higher in the separate – than in the combined peeling group (2.5 ± 1.8 and 1.7 ± 1.6, respectively), however, without reaching statistical significance after Bonferroni correction (p = 0.008).

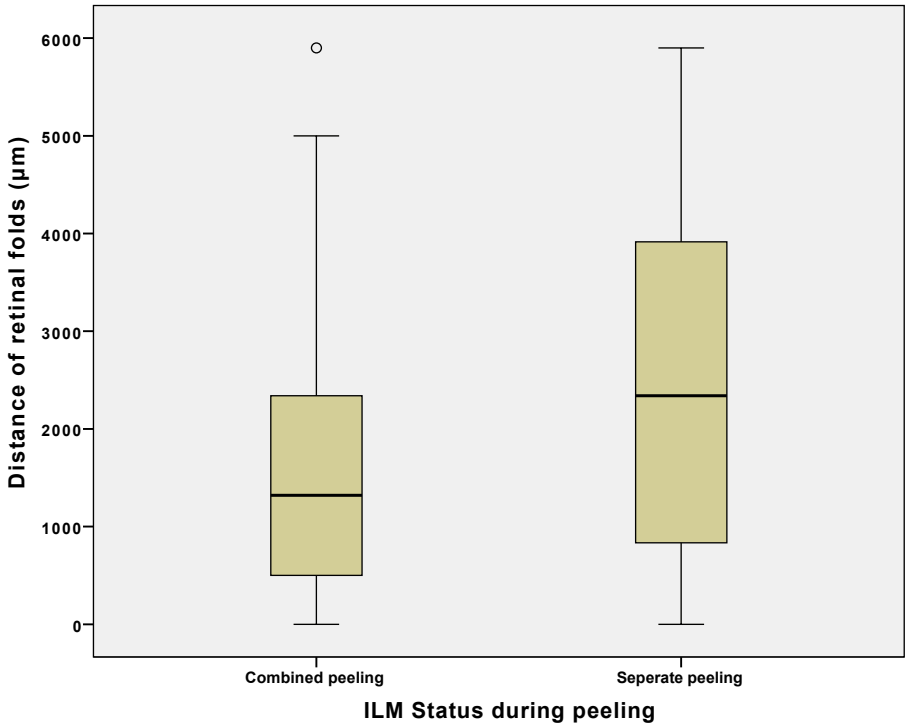

Figure 28. Boxplot of the distance of retinal folding according to separate versus the combined peeling group. While retinal folds were more pronounced in the separate peeling group, this difference did not reach statistical significance.

The mean distance of ERM elevated from the retinal surface was significantly longer in the separate peeling group (1.5 ± 1.5 versus 0.7±1.1 mm; p = 0.001). Figure XX shows boxplots for retinal folding according to the two groups.

ERM-Th was statistically significant higher in the separate peeling (p = 0.002). The mean ERM-Th was 18.9 ± 10.8 µm in cases with persisting ILM and 13.8 ± 3.3 µm in the combined peeling group. A trend towards higher CFT in patients with ILM persistence than in the combined peeling group was observed (511.4 ± 113 and 473.3 ± 102, respectively; p = 0.028).

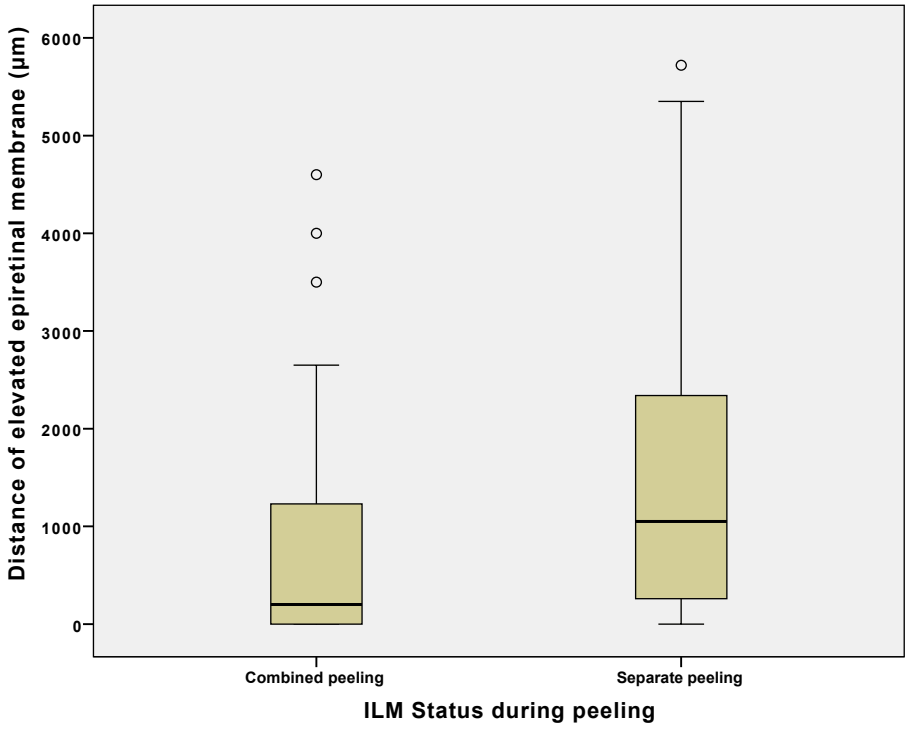

Figure 29. Boxplot of the elevation of the epiretinal membrane according to separate versus the combined peeling group. An elevated epiretinal membrane was significantly more common in the separate peeling group.

The presence of intraretinal cysts did not differ between the two groups (p = 0.632). There was a trend towards discontinuation of the ERM in the separate peeling group (31.7% vs. 15.3%), yet without reaching statistical significance after Bonferroni correction (p = 0.032). Table 1 shows the morphologic parameters for the separate peeling – and for the combined peeling group.

Regarding the preoperative and the postoperative morphological data comparision we evaluated the correlation between the preoperative CRT and the postoperative CRT. There was a significant decrease in the CRT from 491 ± 108 µm to 355 ± 164 µm after the peeling had been performed. This difference was statistically significant (p ≤ 0.0001).

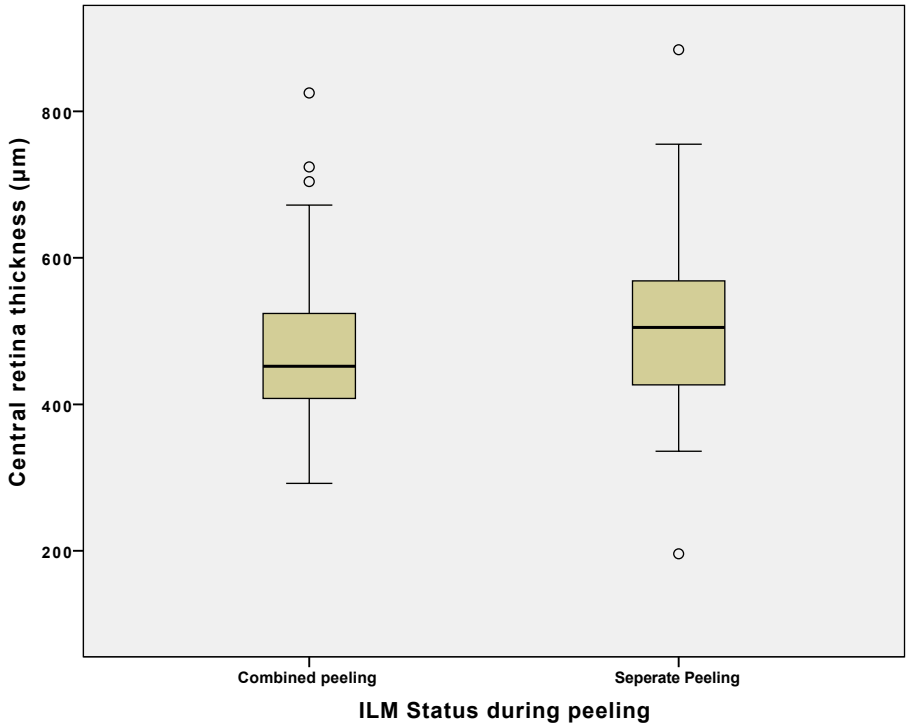

Figure 30. The central retinal thickness according to the intraoperative behavior of the inner limiting membrane (ILM). Central retinal thickness did not differ significantly in between the to ILM peeling groups. As expected the central retinal thickness was however markedly higher than the normal values observed in a healthy population.

These data, however, were not part of the original analysis due to the retrospective nature of this study. The interval between the preoperative optical coherence tomography and the postoperative optical coherence tomography was highly variable and the data for the postoperative evaluation was not available for all the examined patients. As such the amount of the reduction in CRT should be taken with caution, however, the general trend toward a thinning of the retina after the peeling can be

Characteristics of eyes undergoing epiretinal membrane (ERM) peeling

	Combined peeling *n = 59 (49.6%)*	**Separate peeling** *n = 60 (50.4%)*	
Demogrpahic Data			
Sex (female/male)	29/30	35/25	
Age (years)	74.0 ± 7.8	7.1 ± 8.8	
BCVA (logMar)	0.47 ± 0.16	0.54 ± 0.25	
Eyes (right/left)	39/20	28/32	
Analysis Data			P value*
Vitreal status (n (%))			0.801
attached	8 (13.6%)	12 (20.0%)	
incompletely detached	2 (3.4%)	2 (3.4%)	
detached	49 (83.0%)	45 (76.7%)	
Central foveal thickness† (µm)	473.3 ± 101.8	511.4 ± 113.1	0.028
ERM thickness† (µm)	13.8 ± 3.3	18.9 ± 10.8	0.002
Retinal folding† (mm)	1.7 ± 1.6	2.5 ± 1.8	0.008
ERM detachment† (mm)	0.7 ± 1.1	1.5 ± 1.5	0.001
Intraretinal cysts (n [%])	9 (15.2%)	12 (20.0%)	0.632
ERM discontinuity (n [%])	9 (15.2%)	19 (31.7 %)	0.032

Table 1. Characteristics of eyes undergoing epiretinal membrane (ERM) peeling.

*** after Bonferroni correction a p value < 0.005 was considered statistically significant**

† mean ± SD

inferred and is reasonable, given the pathophysiology of the disease and mechanism of the treatment. Figure XX shows a scatter plot of the correlation between the pre- and postoperative CRT.

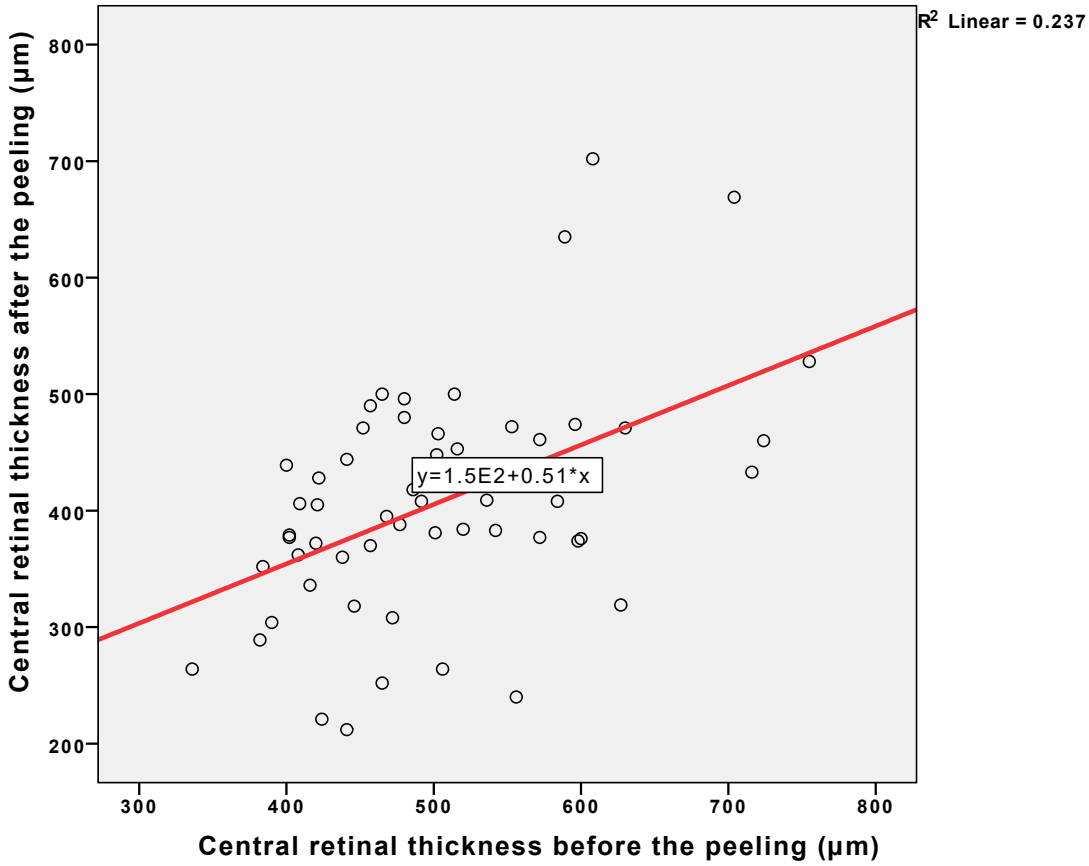

Figure 31. Scatter plot of the preoperative central retinal thickness and the postoperative central retinal thickness as measured by optical coherence tomography. A linear fit was calculated for estimating the correlation for the parameter at the two time points. Unsurprisingly there was a positive correlation, meaning that retinas that were initially thicker tended to remain at

the thicker end of the spectrum after the surgery as well. The only slight upwards slant of the linear fit, however, also indicates that overall there was a reduction in the retinal thickness after the surgery.

As would have been expected the visual acuity before the surgery correlated with the visual acuity 2 days after the surgery. This can be appreciated in Figure xx. However, since the postoperative and to some degree also the preoperative visual acuity measurement was carried out in a non standardized fashion (regarding illumination, refraction, and so on), we refrained form further statistical analysis on this relationship. Of note is that the postoperative visual acuity was already slightly better than the preoperative visual acuity (0.48 ± 0.2 post surgery versus 0.5 ± 0.2 before surgery; $p \leq 0.0001$). As discussed previously this matter needs to be taken with a grain of salt regarding the test setting, but also the type of surgery should be considered. While the visual acuity before and after surgery do correlate with each other, in most studies it is also the case that the visual acuity directly after the peeling is equal or even somewhat lower than the visual acuity at baseline. [6]

This holds true in the case of the epiretinal membrane peeling alone. However, in our study most patients in the examined cohort underwent a cataract extraction in conjunction with their ERM peeling. The visual recovery after an uncomplicated cataract surgery is almost immediate and as such this needs to be taken into account when examining the visual acuity results.

Besides that, the change in visual acuity was small and the clinical significance of the difference, albeit none was predefined, is probably negligible. It needs to be pointed out that the change in visual acuity was also highly dependent on the initial visual acuity. Patients with a worse visual acuity at presentation profited more from the surgery than those with a more favorable visual acuity to begin with. This phenomenon is well known throughout medicine and has been described also for epiretinal membranes. Figure XX shows a scatter plot comparing the change in visual acuity to the visual acuity at baseline.

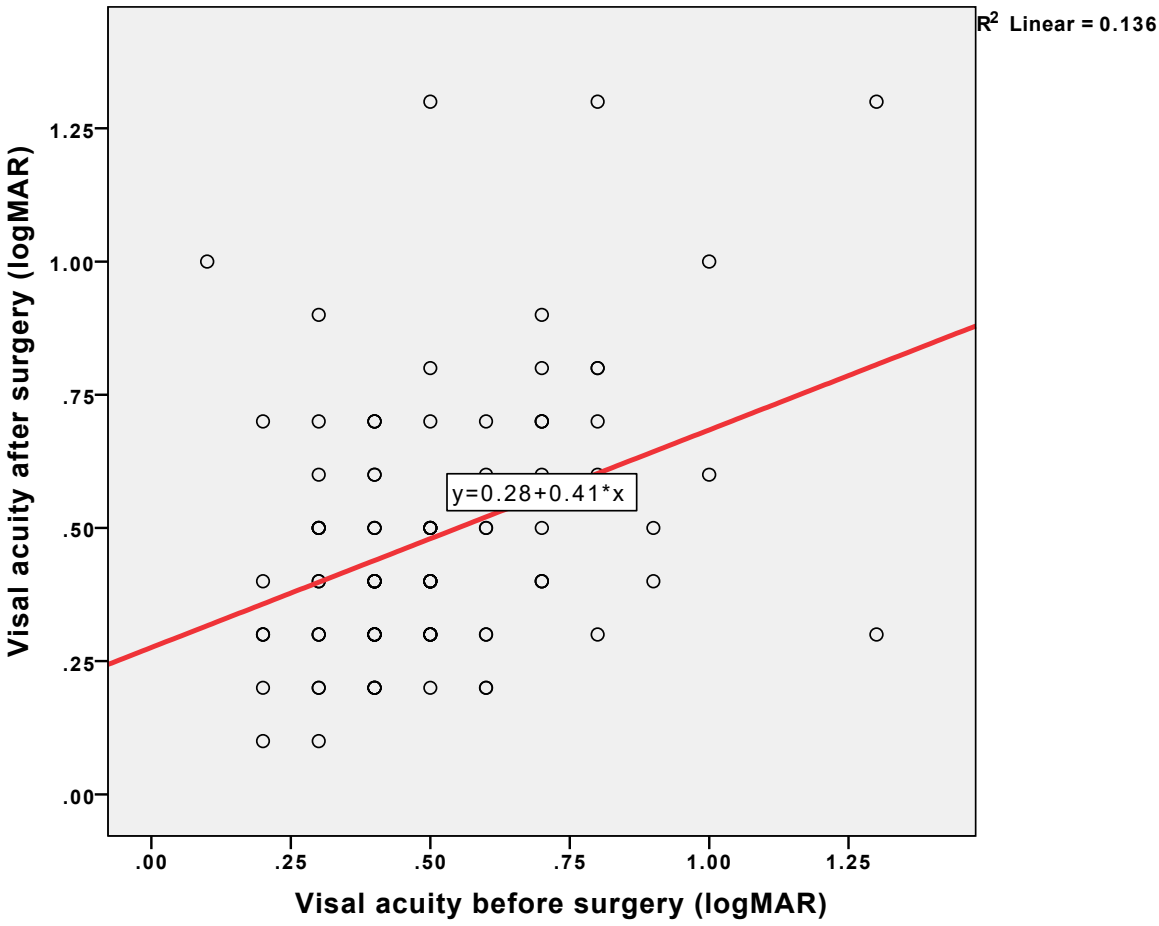

Figure 32. Scatterplot of relationship between the preoperative and the two day postoperative visual acuity. A linear fit was calculated for estimating the correlation between visual acuity at the two time points. There was a positive correlation between the preoperative and the postoperative best corrected visual acuity. The logMAR values for the postoperative visual acuity, however, were generally somewhat lower than those before the surgery indicating some degree of visual improvement after the surgery.

As an additional factor for morphologic evaluation we considered to look at vitreoretinal traction (Figure XX). Since there were, however, only 3 cases of

vitreoretinal traction in the cohort we did not evaluate this parameter because no statistical conclusion could have been made.

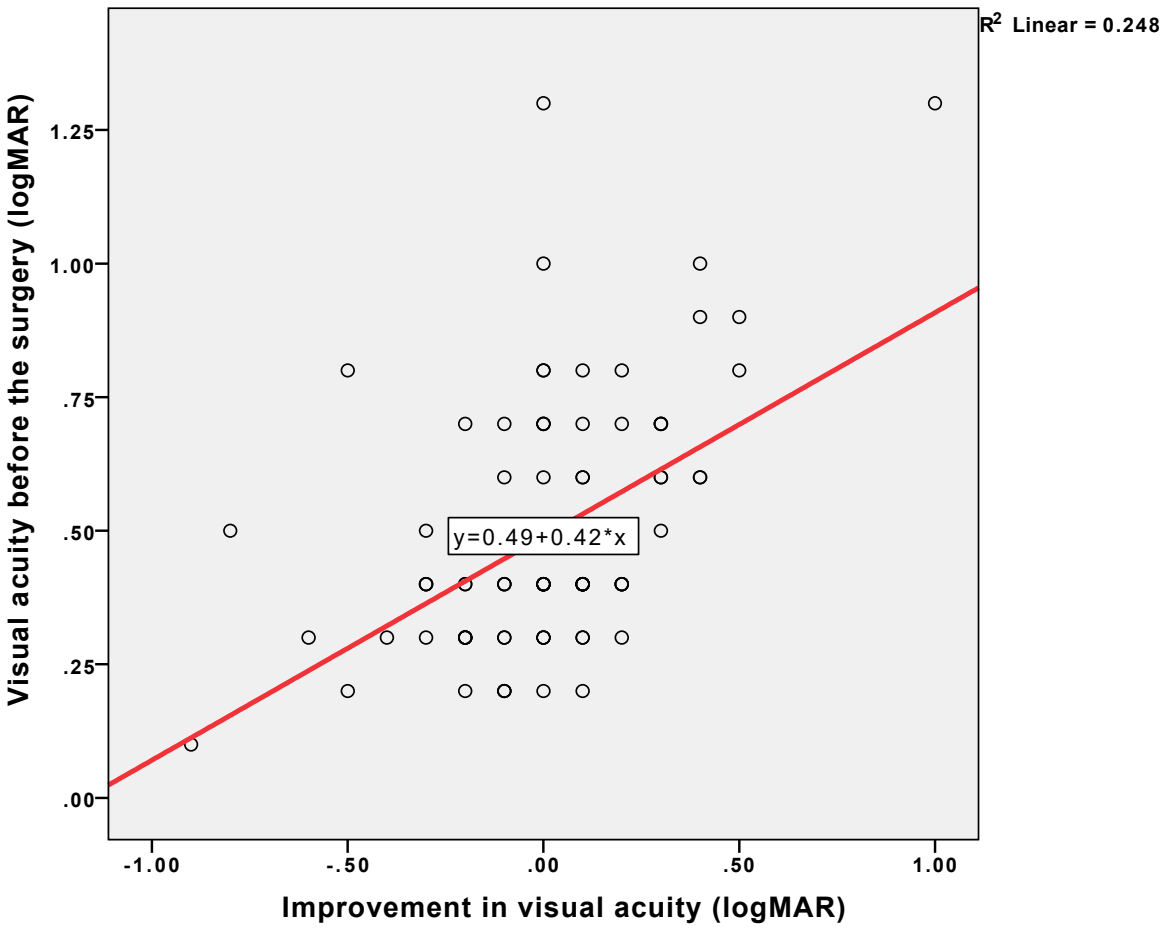

Figure 33. Scatter plot comparing the improvement of visual acuity to the initial visual acuity.A movement on the x axis to the right represents an improvement in visual acuity while a movement up on the y axis represents a worse visual acuity at baseline. The calculated linear fit shows a positive correlation between the improvement after the ERM peeling and an initially lower best corrected visual acuity. Regarding this relationship the same limitations apply as to the other correlations for parameters before and after the surgery. That is the study lacked the design for a standardized postoperative data collection.

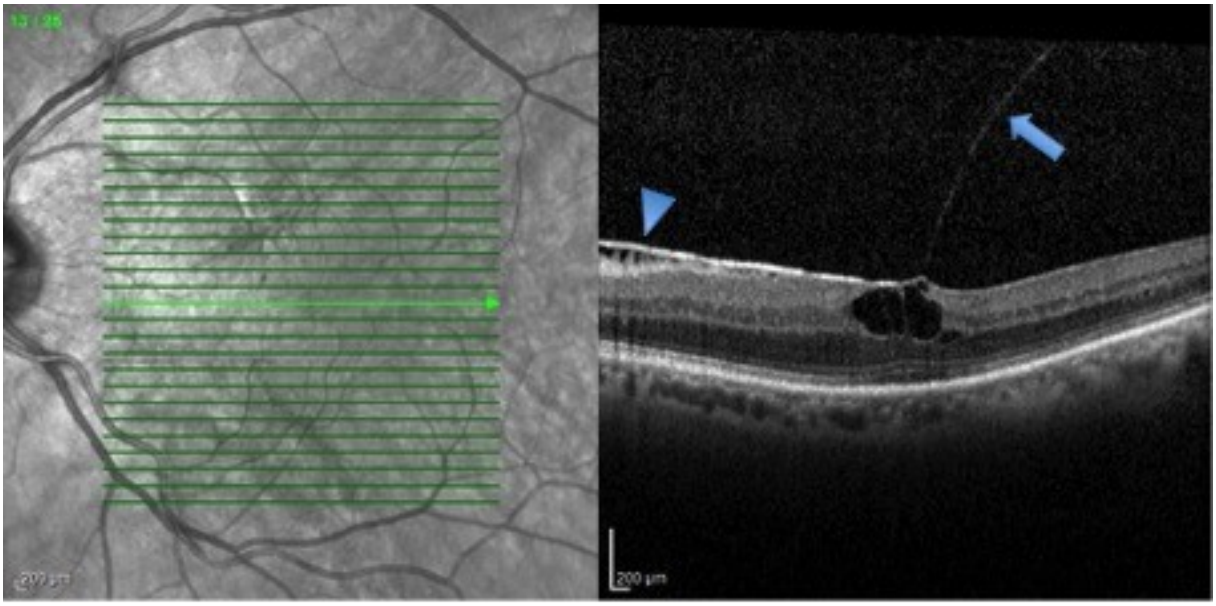

Figure 34. Optical coherence tomography of a vitreo-macular traction syndrome with an epiretinal membrane. The partial posterior vitreal detachment is apparent as a thin line of medium reflectivity within the vitreous cavity (arrow) which leads to the fovea where it often, as in this case, causes the formation of cystoid spaces (hyporeflective intraretinal structures). The nasal macular retina is covered by a much more hyperreflective sheet, which is characteristic of an epiretinal membrane (arrow head). Also some retinal folding can be seen. These membranes sometimes tend to stick firmly to the vitreous cortex and might be peeled with the induction of the posterior vitreous detachment during the surgery or in some cases can even detach from the retinal surface spontaneously rendering a surgical intervention unnecessary. [133]However, the additional peril for the fovea while the traction persists needs to be taken into account when scheduling the surgical intervention and as such observation is not always the optimal choice for such patients. [134]

1.5.5 Discussion

As previously shown, the removal of the ILM is beneficial in ERM peeling.[135] However, the ILM persists on the retina in 50.8 to 64% after ERM peeling.[129,130] Preoperative predictive markers for ILM persistence have not yet been identified. This study shows that a thicker ERM and a loose connection between the ERM and the retina on OCT are associated with ILM persistence in ERM surgery.

Furthermore, our study, which is so far the largest investigating the persistence of the ILM after ERM peeling, confirms incomplete ILM removal in nearly half of the eyes after ERM peeling. To maximize the rate of combined removal we initiated the peeling by grasping the stained ILM at the border of the ERM. Still, our rate of 49.6% was almost identical to the 49.2% reported by Kifuku and coworkers, who had neither performed ICG staining for primary peeling, nor stated any exceptional attention on having primarily grasped the ILM.[129]

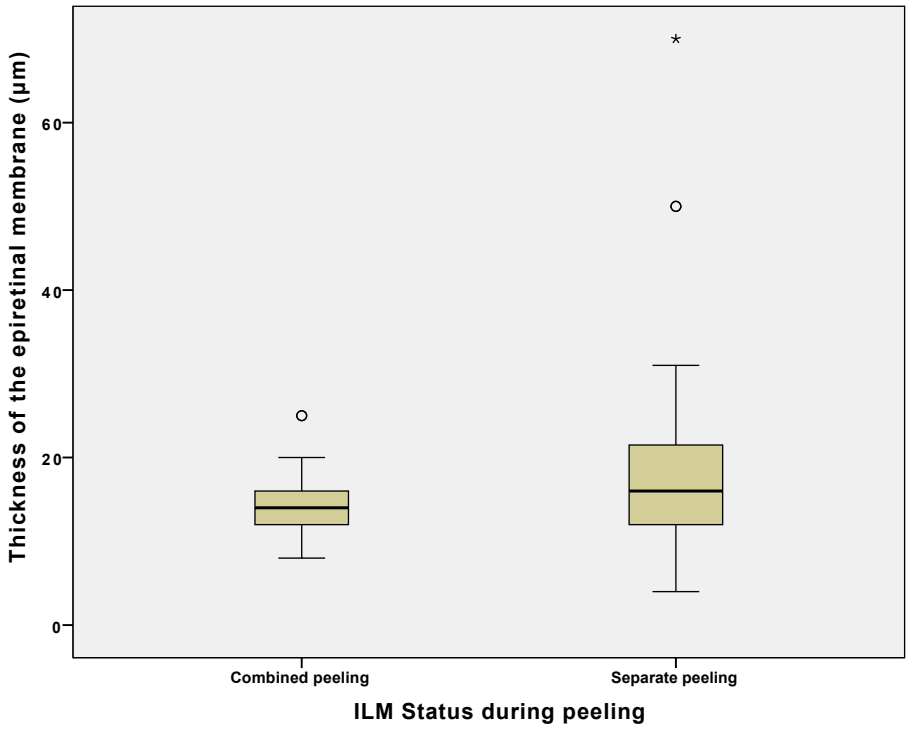

Figure 35. Boxplots for the thickness of the epiretinal membrane according to the peeling groups. The membranes in the separate peeling group were significantly thicker than those in the combined peeling group. However, there

was a higher spread within the thicker group than in the combined group leading to a considerable overlap between both groups.

This study suggests that preoperative OCT findings can indicate the risk of ILM persistence during surgery. Previous studies have already shown that changes on OCT correlate with preoperative BCVA and are of prognostic value concerning postoperative BCVA.[22] [88]

We found 2 markers on OCT showing statistically significant association with persisting ILM: increased ERM-Th and elevation of the ERM from the retina. This supports the idea that a loose connection between the ERM and the ILM increases the risk of residual ILM after peeling. After histologic evaluation of peeled ERM and ILM, it has been proposed that a remaining lamella of the vitreous cortex after aberrant PVD induces a less adhesive ERM by leaving a thin layer of collagen between the ILM and the ERM.[130] Recent literature demonstrated that areas where the ERM was easy to peel were likely to show elevation of the ERM on OCT, whereas membranes with closer adherence to the retinal surface were more difficult to mobilize. [136] [137] In contrast to the aforementioned study, Kim and coworkers concluded that this space between the ERM and the retinal surface rather represents a tissue free zone than an interlayer of collagen Our findings on OCT are consistent with such a predetermined cleavage plane. It would be interesting to combine preoperative OCT and postoperative histology to shed light on the content of this ERM/ILM interlayer.

The present study also suggests that a thicker ERM increases the risk of ILM persistence. Increased rigidity of thicker membranes could account for a weaker adhesion between the ERM and the ILM. Similarly, it has been proposed that the ERM stiffening after ICG staining facilitates the peeling process of the ERM.[138]

One should note that the application of chemical compounds on the retina risks collateral damage. Nevertheless intraocular staining is currently the gold standard for identifying the ILM during surgery, when used uncritically ICG has been shown to be retinotoxic[131,132,138]. The introduction of Trypan Blue (TB) and later

Brillian Blue G (BBG) enhanced the pallet of dyes for surgeons to choose from. [139] [140] Both dies exhibit a better safety profile in vitro and in animal models. [141] TB, however, stains both the ERM and the ILM and is applied under air. BBG is comparable to ICG in its ILM specificity and its ease of use, but shows less discernible contrast than ICG [142,143]. ICG's toxicity depends on its concentration, the duration of staining, and the osmolality of the solution. [138] Subsequently, when using ICG meticulous attention towards exposure minimization is warranted.

Still, considering the impossibility of reliable biomicroscopic detection of persisting ILM, especially in case of small remainders, we recommend a second staining in all cases, since we did not find a marker on OCT to definitely predict simultaneous peeling of the ERM and ILM. There are several potential reasons for the later. First, two-dimensional OCT analysis, as performed in this study, might provide insufficient data. Second, the current axial resolution of OCTs is not capable of detailed imaging of the ILM.[144,145] Concerning the aforementioned issues, further improvement in soft- and hardware of OCTs will provide better resolution and maybe additional algorithms to facilitate a more thorough analysis. This might confine a second staining to preoperatively identified risk groups. However, the sheer absence of a preoperative marker able to definitely predict ILM adherence is possible.

In summary, even when removing the ERM by targeting the ILM, combined removal succeeds in 50% only. A loose connection between the ERM and the retinal surface predisposes for ILM persistence. Preoperative SD-OCT is helpful in identifying risk markers for the persistence of the ILM in ERM surgery.

1.6 References

1. Bu SC, Kuijer R, van der Worp RJ, et al. Immunohistochemical Evaluation of Idiopathic Epiretinal Membranes and In Vitro Studies on the Effect of TGF-beta on Muller Cells. *Invest Ophthalmol Vis Sci.* 2015;56(11):6506-6514.
2. Kampik A, Green WR, Michels RG, Nase PK. Ultrastructural features of progressive idiopathic epiretinal membrane removed by vitreous surgery. *American journal of ophthalmology.* 1980;90(6):797-809.

3. Tari SR, Vidne-Hay O, Greenstein VC, Barile GR, Hood DC, Chang S. Functional and structural measurements for the assessment of internal limiting membrane peeling in idiopathic macular pucker. *Retina.* 2007;27(5):567-572.
4. Okamoto F, Okamoto Y, Hiraoka T, Oshika T. Effect of vitrectomy for epiretinal membrane on visual function and vision-related quality of life. *Am J Ophthalmol.* 2009;147(5):869-874, 874 e861.
5. Okamoto F, Okamoto Y, Fukuda S, Hiraoka T, Oshika T. Vision-related quality of life and visual function after vitrectomy for various vitreoretinal disorders. *Invest Ophthalmol Vis Sci.* 2010;51(2):744-751.
6. Kinoshita T, Imaizumi H, Okushiba U, Miyamoto H, Ogino T, Mitamura Y. Time course of changes in metamorphopsia, visual acuity, and OCT parameters after successful epiretinal membrane surgery. *Invest Ophthalmol Vis Sci.* 2012;53(7):3592-3597.
7. Benegas NM, Egbert J, Engel WK, Kushner BJ. Diplopia secondary to aniseikonia associated with macular disease. *Arch Ophthalmol.* 1999;117(7):896-899.
8. Kushner BJ, Alvares MG, Paysse EA, Brooks SE, Borchert M. Grand rounds #53: A case of small angle strabismus, torsion, aniseikonia and diplopia associated with epiretinal membranes [clincical conference]. *Binocul Vis Strabismus Q.* 1999;14(1):46-51; discussion 51-42.
9. Ugarte M, Williamson TH. Aniseikonia associated with epiretinal membranes. *Br J Ophthalmol.* 2005;89(12):1576-1580.
10. de Wit GC, Muraki CS. Field-dependent aniseikonia associated with an epiretinal membrane a case study. *Ophthalmology.* 2006;113(1):58-62.
11. Chung H, Son G, Hwang DJ, Lee K, Park Y, Sohn J. Relationship Between Vertical and Horizontal Aniseikonia Scores and Vertical and Horizontal OCT Images in Idiopathic Epiretinal Membrane. *Invest Ophthalmol Vis Sci.* 2015;56(11):6542-6548.
12. Arndt C, Rebollo O, Seguinet S, Debruyne P, Caputo G. Quantification of metamorphopsia in patients with epiretinal membranes before and after surgery. *Graefes Arch Clin Exp Ophthalmol.* 2007;245(8):1123-1129.

13. Arimura E, Matsumoto C, Okuyama S, Takada S, Hashimoto S, Shimomura Y. Retinal contraction and metamorphopsia scores in eyes with idiopathic epiretinal membrane. *Invest Ophthalmol Vis Sci.* 2005;46(8):2961-2966.
14. Liu L, Yue S, Wu J, et al. The Prevalence and Distribution of Vitreoretinal Interface Abnormalities among Urban Community Population in China. *J Ophthalmol.* 2015;2015:742686.
15. Klein R, Klein BE, Wang Q, Moss SE. The epidemiology of epiretinal membranes. *Trans Am Ophthalmol Soc.* 1994;92:403-425; discussion 425-430.
16. Stevenson W, Prospero Ponce CM, Agarwal DR, Gelman R, Christoforidis JB. Epiretinal membrane: optical coherence tomography-based diagnosis and classification. *Clin Ophthalmol.* 2016;10:527-534.
17. Fraser-Bell S, Ying-Lai M, Klein R, Varma R, Los Angeles Latino Eye S. Prevalence and associations of epiretinal membranes in latinos: the Los Angeles Latino Eye Study. *Invest Ophthalmol Vis Sci.* 2004;45(6):1732-1736.
18. Sidd RJ, Fine SL, Owens SL, Patz A. Idiopathic preretinal gliosis. *Am J Ophthalmol.* 1982;94(1):44-48.
19. Wise GN. Relationship of idiopathic preretinal macular fibrosis to posterior vitreous detachment. *Am J Ophthalmol.* 1975;79(3):358-362.
20. Hirokawa H, Jalkh AE, Takahashi M, Takahashi M, Trempe CL, Schepens CL. Role of the vitreous in idiopathic preretinal macular fibrosis. *Am J Ophthalmol.* 1986;101(2):166-169.
21. Suh MH, Seo JM, Park KH, Yu HG. Associations between macular findings by optical coherence tomography and visual outcomes after epiretinal membrane removal. *Am J Ophthalmol.* 2009;147(3):473-480 e473.
22. Hwang JU, Sohn J, Moon BG, et al. Assessment of macular function for idiopathic epiretinal membranes classified by spectral-domain optical coherence tomography. *Invest Ophthalmol Vis Sci.* 2012;53(7):3562-3569.
23. Meuer SM, Myers CE, Klein BE, et al. The epidemiology of vitreoretinal interface abnormalities as detected by spectral-domain optical coherence tomography: the beaver dam eye study. *Ophthalmology.* 2015;122(4):787-795.

24. Spaeth GL. Re: Meuer et al.: The epidemiology of vitreoretinal interface abnormalities as detected by spectral-domain optical coherence tomography: the Beaver Dam Eye Study (Ophthalmology 2015;122:787-95). *Ophthalmology.* 2015;122(12):e72.
25. Mitchell P, Smith W, Chey T, Wang JJ, Chang A. Prevalence and associations of epiretinal membranes. The Blue Mountains Eye Study, Australia. *Ophthalmology.* 1997;104(6):1033-1040.
26. Noda Y, Yamazaki S, Kawano M, Goto Y, Otsuka S, Ogura Y. [Prevalence of Epiretinal Membrane Using Optical Coherence Tomography]. *Nippon Ganka Gakkai Zasshi.* 2015;119(7):445-450.
27. Ye H, Zhang Q, Liu X, et al. Prevalence and associations of epiretinal membrane in an elderly urban Chinese population in China: the Jiangning Eye Study. *Br J Ophthalmol.* 2015;99(12):1594-1597.
28. Messner LV, Messner SS. Idiopathic preretinal fibrosis with concurrent cystoid macular edema. *J Am Optom Assoc.* 1987;58(12):976-978.
29. Tsai CY, Hsieh YT, Yang CM. EPIRETINAL MEMBRANE-INDUCED FULL-THICKNESS MACULAR HOLES: The Clinical Features and Surgical Outcomes. *Retina.* 2016.
30. Heegaard S. Morphology of the vitreoretinal border region. *Acta Ophthalmol Scand Suppl.* 1997(222):1-31.
31. Heegaard S, Jensen OA, Prause JU. Structure and composition of the inner limiting membrane of the retina. SEM on frozen resin-cracked and enzyme-digested retinas of Macaca mulatta. *Graefes Arch Clin Exp Ophthalmol.* 1986;224(4):355-360.
32. Joussen AM NG, Coupland SE, et al. Retina and vitreous. In: Naumann GO HL, Kruse FE, et al, ed. *Applied Pathology for Ophthalmic Microsurgeons*. Berlin, Germany: Springer; 2008:306-307.
33. Bovey EH, Uffer S, Achache F. Surgery for epimacular membrane: impact of retinal internal limiting membrane removal on functional outcome. *Retina.* 2004;24(5):728-735.

34. Grewing R, Mester U. Results of surgery for epiretinal membranes and their recurrences. *The British journal of ophthalmology.* 1996;80(4):323-326.
35. Park DW, Dugel PU, Garda J, et al. Macular pucker removal with and without internal limiting membrane peeling: pilot study. *Ophthalmology.* 2003;110(1):62-64.
36. Kwok A, Lai TY, Yuen KS. Epiretinal membrane surgery with or without internal limiting membrane peeling. *Clinical & experimental ophthalmology.* 2005;33(4):379-385.
37. Rahimy E, McCannel CA. IMPACT OF INTERNAL LIMITING MEMBRANE PEELING ON MACULAR HOLE REOPENING: A Systematic Review and Meta-Analysis. *Retina.* 2016;36(4):679-687.
38. Odrobina DC, Michalewska Z, Michalewski J, Nawrocki J. High-speed, high-resolution spectral optical coherence tomography in patients after vitrectomy with internal limiting membrane peeling for proliferative vitreoretinopathy retinal detachment. *Retina.* 2010;30(6):881-886.
39. Nawrocki J, Michalewska Z, Michalewski J. [Vitreous surgery with trypan blue staining of membranes in PVR retinal detachment surgery]. *Klin Monbl Augenheilkd.* 2005;222(7):572-576.
40. Jackson TL, Donachie PH, Sparrow JM, Johnston RL. United Kingdom National Ophthalmology Database Study of Vitreoretinal Surgery: report 1; case mix, complications, and cataract. *Eye (Lond).* 2013;27(5):644-651.
41. Jackson TL, Donachie PH, Williamson TH, Sparrow JM, Johnston RL. THE ROYAL COLLEGE OF OPHTHALMOLOGISTS' NATIONAL OPHTHALMOLOGY DATABASE STUDY OF VITREORETINAL SURGERY: Report 4, Epiretinal Membrane. *Retina.* 2015;35(8):1615-1621.
42. Kumagai K. Introduction of a new method for the preparation of triamcinolone acetonide solution as an aid to visualization of the vitreous and the posterior hyaloid during pars plana vitrectomy. *Retina.* 2003;23(6):881-882.
43. Totan Y, Guler E, Guragac FB, Uzun E, Dogdu E. Brilliant blue G assisted macular surgery: the effect of air infusion on contrast recognisability in internal limiting membrane peeling. *Br J Ophthalmol.* 2015;99(1):75-80.

44. Abrams GW, Topping T, Machemer R. An improved method for practice vitrectomy. *Arch Ophthalmol.* 1978;96(3):521-525.
45. Burk SE, Da Mata AP, Snyder ME, Rosa RH, Jr., Foster RE. Indocyanine green-assisted peeling of the retinal internal limiting membrane. *Ophthalmology.* 2000;107(11):2010-2014.
46. Alander JT, Kaartinen I, Laakso A, et al. A review of indocyanine green fluorescent imaging in surgery. *Int J Biomed Imaging.* 2012;2012:940585.
47. Badaro E, Novais EA, Penha FM, Maia M, Farah ME, Rodrigues EB. Vital dyes in ophthalmology: a chemical perspective. *Curr Eye Res.* 2014;39(7):649-658.
48. Penha FM, Pons M, Costa Ede P, et al. Effect of vital dyes on retinal pigmented epithelial cell viability and apoptosis: implications for chromovitrectomy. *Ophthalmologica.* 2013;230 Suppl 2:41-50.
49. Maia M, Haller JA, Pieramici DJ, et al. Retinal pigment epithelial abnormalities after internal limiting membrane peeling guided by indocyanine green staining. *Retina.* 2004;24(1):157-160.
50. Haritoglou C, Mauell S, Benoit M, et al. Vital dyes increase the rigidity of the internal limiting membrane. *Eye (Lond).* 2013;27(11):1308-1315.
51. Norn MS. Vital staining of the canaliculus lacrimalis and the palpebral border (Marx' line). *Acta Ophthalmol (Copenh).* 1966;44(6):948-959.
52. Norn MS. Trypan blue. Vital staining of cornea and conjunctiva. *Acta Ophthalmol (Copenh).* 1967;45(3):380-389.
53. Melles GR, de Waard PW, Pameyer JH, Houdijn Beekhuis W. Trypan blue capsule staining to visualize the capsulorhexis in cataract surgery. *J Cataract Refract Surg.* 1999;25(1):7-9.
54. Veckeneer M, van Overdam K, Monzer J, et al. Ocular toxicity study of trypan blue injected into the vitreous cavity of rabbit eyes. *Graefes Arch Clin Exp Ophthalmol.* 2001;239(9):698-704.
55. Feron EJ, Veckeneer M, Parys-Van Ginderdeuren R, Van Lommel A, Melles GR, Stalmans P. Trypan blue staining of epiretinal membranes in proliferative vitreoretinopathy. *Arch Ophthalmol.* 2002;120(2):141-144.

56. Hernandez F, Alpizar-Alvarez N, Wu L. Chromovitrectomy: an update. *J Ophthalmic Vis Res.* 2014;9(2):251-259.
57. Jackson TL, Kwan AS, Laidlaw AH, Aylward W. Identification of retinal breaks using subretinal trypan blue injection. *Ophthalmology.* 2007;114(3):587-590.
58. Ghosh S, Issa S, El Ghrably I, Stannard K. Subretinal migration of trypan blue during macular hole and epiretinal membrane peel: an observational case series. Is there a safer method? *Eye (Lond).* 2010;24(11):1724-1727.
59. Mohr A, Bruinsma M, Oellerich S, et al. Dyes for Eyes: hydrodynamics, biocompatibility and efficacy of 'heavy' (dual) dyes for chromovitrectomy. *Ophthalmologica.* 2013;230 Suppl 2:51-58.
60. Henrich PB, Monnier CA, Halfter W, et al. Nanoscale topographic and biomechanical studies of the human internal limiting membrane. *Invest Ophthalmol Vis Sci.* 2012;53(6):2561-2570.
61. Henrich PB, Haritoglou C, Meyer P, et al. Anatomical and functional outcome in brilliant blue G assisted chromovitrectomy. *Acta Ophthalmol.* 2010;88(5):588-593.
62. Bartok M, Tandon R, Alfaro-Espinoza G, Ullrich MS, Gabel D. Reduction of cytotoxicity of benzalkonium chloride and octenidine by Brilliant Blue G. *EXCLI J.* 2015;14:123-132.
63. Nagahama M, Seike S, Shirai H, et al. Role of P2X7 receptor in Clostridium perfringens beta-toxin-mediated cellular injury. *Biochim Biophys Acta.* 2015;1850(11):2159-2167.
64. Clark AK, Staniland AA, Marchand F, Kaan TK, McMahon SB, Malcangio M. P2X7-dependent release of interleukin-1beta and nociception in the spinal cord following lipopolysaccharide. *J Neurosci.* 2010;30(2):573-582.
65. Ueno A, Hisatomi T, Enaida H, et al. Biocompatibility of brilliant blue G in a rat model of subretinal injection. *Retina.* 2007;27(4):499-504.
66. Jindal A, Pathengay A, Mithal K, Chhablani J, Pappuru RR, Flynn HW. Macular toxicity following brilliant blue G-assisted macular hole surgery - a report of three cases. *Nepal J Ophthalmol.* 2014;6(11):98-101.

67. Murray J. Compounding Advisory Committee Meeting June 17-18. 2015; http://www.fda.gov/downloads/advisorycommittees/committeesmeetingmaterials/drugs/pharmacycompoundingadvisorycommittee/ucm455276.pdf. Accessed 30.3., 2016.
68. Stalmans P, Feron EJ, Parys-Van Ginderdeuren R, Van Lommel A, Melles GR, Veckeneer M. Double vital staining using trypan blue and infracyanine green in macular pucker surgery. *Br J Ophthalmol.* 2003;87(6):713-716.
69. Kwok AK, Lai TY, Li WW, Yew DT, Wong VW. Trypan blue- and indocyanine green-assisted epiretinal membrane surgery: clinical and histopathological studies. *Eye (Lond).* 2004;18(9):882-888.
70. Chen JC. Sutureless pars plana vitrectomy through self-sealing sclerotomies. *Arch Ophthalmol.* 1996;114(10):1273-1275.
71. Fujii GY, De Juan E, Jr., Humayun MS, et al. A new 25-gauge instrument system for transconjunctival sutureless vitrectomy surgery. *Ophthalmology.* 2002;109(10):1807-1812; discussion 1813.
72. Hilton GF, Josephberg RG, Halperin LS, et al. Office-based sutureless transconjunctival pars plana vitrectomy. *Retina.* 2002;22(6):725-732.
73. Eckardt C. Transconjunctival sutureless 23-gauge vitrectomy. *Retina.* 2005;25(2):208-211.
74. Singh RP, Bando H, Brasil OF, Williams DR, Kaiser PK. Evaluation of wound closure using different incision techniques with 23-gauge and 25-gauge microincision vitrectomy systems. *Retina.* 2008;28(2):242-248.
75. Haas A, Seidel G, Steinbrugger I, et al. Twenty-three-gauge and 20-gauge vitrectomy in epiretinal membrane surgery. *Retina.* 2010;30(1):112-116.
76. Huang D, Swanson EA, Lin CP, et al. Optical coherence tomography. *Science.* 1991;254(5035):1178-1181.
77. van den Berg TJ, Spekreijse H. Near infrared light absorption in the human eye media. *Vision Res.* 1997;37(2):249-253.
78. Smith RC, Baker KS. Optical properties of the clearest natural waters (200-800 nm). *Appl Opt.* 1981;20(2):177-184.

79. Fuchs S, Rodel C, Blinne A, et al. Nanometer resolution optical coherence tomography using broad bandwidth XUV and soft x-ray radiation. *Sci Rep.* 2016;6:20658.
80. Lim LS, Cheung G, Lee SY. Comparison of spectral domain and swept-source optical coherence tomography in pathological myopia. *Eye (Lond).* 2014;28(4):488-491.
81. Keane PA, Sadda SR. Retinal imaging in the twenty-first century: state of the art and future directions. *Ophthalmology.* 2014;121(12):2489-2500.
82. Matsumoto C, Arimura E, Okuyama S, Takada S, Hashimoto S, Shimomura Y. Quantification of metamorphopsia in patients with epiretinal membranes. *Invest Ophthalmol Vis Sci.* 2003;44(9):4012-4016.
83. Michalewski J, Michalewska Z, Cisiecki S, Nawrocki J. Morphologically functional correlations of macular pathology connected with epiretinal membrane formation in spectral optical coherence tomography (SOCT). *Graefes Arch Clin Exp Ophthalmol.* 2007;245(11):1623-1631.
84. Staurenghi G, Sadda S, Chakravarthy U, Spaide RF, International Nomenclature for Optical Coherence Tomography P. Proposed lexicon for anatomic landmarks in normal posterior segment spectral-domain optical coherence tomography: the IN*OCT consensus. *Ophthalmology.* 2014;121(8):1572-1578.
85. Spaide RF, Curcio CA. Anatomical correlates to the bands seen in the outer retina by optical coherence tomography: literature review and model. *Retina.* 2011;31(8):1609-1619.
86. Schumann RG, Compera D, Schaumberger MM, et al. Epiretinal membrane characteristics correlate with photoreceptor layer defects in lamellar macular holes and macular pseudoholes. *Retina.* 2015;35(4):727-735.
87. Kim HJ, Kang JW, Chung H, Kim HC. Correlation of foveal photoreceptor integrity with visual outcome in idiopathic epiretinal membrane. *Curr Eye Res.* 2014;39(6):626-633.

88. Shimozono M, Oishi A, Hata M, et al. The significance of cone outer segment tips as a prognostic factor in epiretinal membrane surgery. *Am J Ophthalmol.* 2012;153(4):698-704, 704 e691.
89. Marmor MF. Control of subretinal fluid: experimental and clinical studies. *Eye (Lond).* 1990;4 (Pt 2):340-344.
90. Adler AJ, Southwick RE. Distribution of glucose and lactate in the interphotoreceptor matrix. *Ophthalmic Res.* 1992;24(4):243-252.
91. Edelman JL, Miller SS. Epinephrine stimulates fluid absorption across bovine retinal pigment epithelium. *Invest Ophthalmol Vis Sci.* 1991;32(12):3033-3040.
92. Tsuboi S. Measurement of the volume flow and hydraulic conductivity across the isolated dog retinal pigment epithelium. *Invest Ophthalmol Vis Sci.* 1987;28(11):1776-1782.
93. Joseph DP, Miller SS. Apical and basal membrane ion transport mechanisms in bovine retinal pigment epithelium. *J Physiol.* 1991;435:439-463.
94. Linsenmeier RA, Padnick-Silver L. Metabolic dependence of photoreceptors on the choroid in the normal and detached retina. *Invest Ophthalmol Vis Sci.* 2000;41(10):3117-3123.
95. Liew G, Moore AT, Webster AR, Michaelides M. Efficacy and prognostic factors of response to carbonic anhydrase inhibitors in management of cystoid macular edema in retinitis pigmentosa. *Invest Ophthalmol Vis Sci.* 2015;56(3):1531-1536.
96. Wolfensberger TJ, Dmitriev AV, Govardovskii VI. Inhibition of membrane-bound carbonic anhydrase decreases subretinal pH and volume. *Doc Ophthalmol.* 1999;97(3-4):261-271.
97. Mannu GS. Retinal phototransduction. *Neurosciences (Riyadh).* 2014;19(4):275-280.
98. Adler Lt, Boyer NP, Chen C, Ablonczy Z, Crouch RK, Koutalos Y. The 11-cis Retinal Origins of Lipofuscin in the Retina. *Prog Mol Biol Transl Sci.* 2015;134:e1-12.
99. Spaide RF, Noble K, Morgan A, Freund KB. Vitelliform macular dystrophy. *Ophthalmology.* 2006;113(8):1392-1400.

100. Spaide RF, Klancnik JM, Jr. Fundus autofluorescence and central serous chorioretinopathy. *Ophthalmology.* 2005;112(5):825-833.
101. Zhang P, Wang HY, Zhang ZF, et al. Fundus autofluorescence in central serous chorioretinopathy: association with spectral-domain optical coherence tomography and fluorescein angiography. *Int J Ophthalmol.* 2015;8(5):1003-1007.
102. Sparrow JR, Parish CA, Hashimoto M, Nakanishi K. A2E, a lipofuscin fluorophore, in human retinal pigmented epithelial cells in culture. *Invest Ophthalmol Vis Sci.* 1999;40(12):2988-2995.
103. Mata NL, Weng J, Travis GH. Biosynthesis of a major lipofuscin fluorophore in mice and humans with ABCR-mediated retinal and macular degeneration. *Proc Natl Acad Sci U S A.* 2000;97(13):7154-7159.
104. Wu Y, Fishkin NE, Pande A, Pande J, Sparrow JR. Novel lipofuscin bisretinoids prominent in human retina and in a model of recessive Stargardt disease. *J Biol Chem.* 2009;284(30):20155-20166.
105. Zhang J, Bai Y, Huang L, et al. Protective effect of autophagy on human retinal pigment epithelial cells against lipofuscin fluorophore A2E: implications for age-related macular degeneration. *Cell Death Dis.* 2015;6:e1972.
106. Sheales MP, Kingston ZS, Essex RW. Associations between preoperative OCT parameters and visual outcome 3 months postoperatively in patients undergoing vitrectomy for idiopathic epiretinal membrane. *Graefes Arch Clin Exp Ophthalmol.* 2016.
107. Okamoto F, Sugiura Y, Okamoto Y, Hiraoka T, Oshika T. Inner Nuclear Layer Thickness as a Prognostic Factor for Metamorphopsia after Epiretinal Membrane Surgery. *Retina.* 2015;35(10):2107-2114.
108. Nelson R, Connaughton V. Bipolar Cell Pathways in the Vertebrate Retina. In: Kolb H, Fernandez E, Nelson R, eds. *Webvision: The Organization of the Retina and Visual System*. Salt Lake City (UT)1995.
109. Kolb H. Neurotransmitters in the Retina. In: Kolb H, Fernandez E, Nelson R, eds. *Webvision: The Organization of the Retina and Visual System*. Salt Lake City (UT)1995.

110. Kolb H. Roles of Amacrine Cells. In: Kolb H, Fernandez E, Nelson R, eds. *Webvision: The Organization of the Retina and Visual System*. Salt Lake City (UT)1995.
111. Slaughter MM, Miller RF. 2-amino-4-phosphonobutyric acid: a new pharmacological tool for retina research. *Science.* 1981;211(4478):182-185.
112. Dacheux RF, Miller RF. Photoreceptor-bipolar cell transmission in the perfused retina eyecup of the mudpuppy. *Science.* 1976;191(4230):963-964.
113. Awatramani GB, Slaughter MM. Intensity-dependent, rapid activation of presynaptic metabotropic glutamate receptors at a central synapse. *J Neurosci.* 2001;21(2):741-749.
114. Ford K, Feller M. Formation of Early Retinal Circuits in the Inner-Plexiform Layer. In: Kolb H, Fernandez E, Nelson R, eds. *Webvision: The Organization of the Retina and Visual System*. Salt Lake City (UT)1995.
115. Farsaii M, Connaughton VP. AII Amacrine Cells. In: Kolb H, Fernandez E, Nelson R, eds. *Webvision: The Organization of the Retina and Visual System*. Salt Lake City (UT)1995.
116. Kolb H, Nelson R, Mariani A. Amacrine cells, bipolar cells and ganglion cells of the cat retina: a Golgi study. *Vision Res.* 1981;21(7):1081-1114.
117. Levick WR, Cleland BG. Receptive fields of cat retinal ganglion cells having slowly conducting axons. *Brain Res.* 1974;74(1):156-160.
118. Sterling P, Freed MA, Smith RG. Architecture of rod and cone circuits to the on-beta ganglion cell. *J Neurosci.* 1988;8(2):623-642.
119. Medeiros FA, Zangwill LM, Anderson DR, et al. Estimating the rate of retinal ganglion cell loss in glaucoma. *Am J Ophthalmol.* 2012;154(5):814-824 e811.
120. Guerin CJ, Anderson DH, Fisher SK. Changes in intermediate filament immunolabeling occur in response to retinal detachment and reattachment in primates. *Invest Ophthalmol Vis Sci.* 1990;31(8):1474-1482.
121. Kolb H, Famiglietti EV. Rod and cone pathways in the inner plexiform layer of cat retina. *Science.* 1974;186(4158):47-49.
122. Newman EA. Distribution of potassium conductance in mammalian Muller (glial) cells: a comparative study. *J Neurosci.* 1987;7(8):2423-2432.

123. Newman EA, Frambach DA, Odette LL. Control of extracellular potassium levels by retinal glial cell K+ siphoning. *Science.* 1984;225(4667):1174-1175.
124. Karwoski CJ, Lu HK, Newman EA. Spatial buffering of light-evoked potassium increases by retinal Muller (glial) cells. *Science.* 1989;244(4904):578-580.
125. Winter M, Eberhardt W, Scholz C, Reichenbach A. Failure of potassium siphoning by Muller cells: a new hypothesis of perfluorocarbon liquid-induced retinopathy. *Invest Ophthalmol Vis Sci.* 2000;41(1):256-261.
126. Miller RF, Dowling JE. Intracellular responses of the Muller (glial) cells of mudpuppy retina: their relation to b-wave of the electroretinogram. *J Neurophysiol.* 1970;33(3):323-341.
127. Rager G. The cellular origin of the b-wave in the electroretinogram -- a developmental approach. *J Comp Neurol.* 1979;188(2):225-244.
128. Seidel G, Weger M, Stadlmuller L, Pichler T, Haas A. Association of preoperative optical coherence tomography markers with residual inner limiting membrane in epiretinal membrane peeling. *PLoS One.* 2013;8(6):e66217.
129. Kifuku K, Hata Y, Kohno RI, et al. Residual internal limiting membrane in epiretinal membrane surgery. *The British journal of ophthalmology.* 2009;93(8):1016-1019.
130. Gandorfer A, Haritoglou C, Scheler R, Schumann R, Zhao F, Kampik A. Residual cellular proliferation on the internal limiting membrane in macular pucker surgery. *Retina.* 2012;32(3):477-485.
131. Gandorfer A, Haritoglou C, Gass CA, Ulbig MW, Kampik A. Indocyanine green-assisted peeling of the internal limiting membrane may cause retinal damage. *American journal of ophthalmology.* 2001;132(3):431-433.
132. Gandorfer A, Haritoglou C, Gandorfer A, Kampik A. Retinal damage from indocyanine green in experimental macular surgery. *Investigative ophthalmology & visual science.* 2003;44(1):316-323.
133. Pierru A, Heligon JP, Gendron G, Paques M, Baudouin C. [Spontaneous separation of epiretinal membrane: Reports of 3 cases]. *J Fr Ophtalmol.* 2016;39(1):20-25.

134. Ota A, Tanaka Y, Toyoda F, et al. Relationship between variations in posterior vitreous detachment and visual prognosis in idiopathic epiretinal membranes. *Clin Ophthalmol.* 2016;10:7-11.
135. Abdelkader E, Lois N. Internal limiting membrane peeling in vitreo-retinal surgery. *Survey of ophthalmology.* 2008;53(4):368-396.
136. Hattenbach LO, Hohn F, Fulle G, Mirshahi A. [Preoperative assessment of topographic features in macular pucker using high-definition optical coherence tomography]. *Klinische Monatsblatter fur Augenheilkunde.* 2009;226(8):649-653.
137. Kim JS, Chhablani J, Chan CK, et al. Retinal adherence and fibrillary surface changes correlate with surgical difficulty of epiretinal membrane removal. *American journal of ophthalmology.* 2012;153(4):692-697, 697 e691-692.
138. Gandorfer A, Haritoglou C, Kampik A. Toxicity of indocyanine green in vitreoretinal surgery. *Developments in ophthalmology.* 2008;42:69-81.
139. Li K, Wong D, Hiscott P, Stanga P, Groenewald C, McGalliard J. Trypan blue staining of internal limiting membrane and epiretinal membrane during vitrectomy: visual results and histopathological findings. *The British journal of ophthalmology.* 2003;87(2):216-219.
140. Enaida H, Hisatomi T, Hata Y, et al. Brilliant blue G selectively stains the internal limiting membrane/brilliant blue G-assisted membrane peeling. *Retina.* 2006;26(6):631-636.
141. Ooi YL, Khang TF, Naidu M, Fong KC. The structural effect of intravitreal Brilliant blue G and Indocyanine green in rats eyes. *Eye (Lond).* 2013;27(3):425-431.
142. Shukla D, Kalliath J, Neelakantan N, Naresh KB, Ramasamy K. A comparison of brilliant blue G, trypan blue, and indocyanine green dyes to assist internal limiting membrane peeling during macular hole surgery. *Retina.* 2011;31(10):2021-2025.
143. Henrich PB, Priglinger SG, Haritoglou C, et al. Quantification of Contrast Recognizability during Brilliant Blue G- and Indocyanine Green-Assisted Chromovitrectomy. *Investigative ophthalmology & visual science.* 2011;52(7):4345-4349.

144. Naumann GOH, Holbach LM, Kruse FE. *Applied pathology for ophthalmic microsurgeons.* Berlin ; New York: Springer; 2008.
145. Kiernan DF, Mieler WF, Hariprasad SM. Spectral-domain optical coherence tomography: a comparison of modern high-resolution retinal imaging systems. *American journal of ophthalmology.* 2010;149(1):18-31.